

FORM 652

N66-19006

(ACCESSION NUMBER)

(THRU)

188

(PAGES)

(CODE)

CL 70913

(NASA CR OR TMX OR AD NUMBER)

07

(CATEGORY)

# BANDWIDTH COMPRESSION TECHNIQUES FOR METEOROLOGICAL SATELLITE PICTURES

Prepared for:

NATIONAL AERONAUTICS AND SPACE ADMINISTRATION  
GODDARD SPACE FLIGHT CENTER  
GREENBELT, MARYLAND

CONTRACT NO. NAS5-3706

STANFORD RESEARCH INSTITUTE

MENLO PARK, CALIFORNIA



**TANFORD RESEARCH INSTITUTE**

**MENLO PARK, CALIFORNIA**



May 1965

*Final Report*

*Covering the Period 1 March 1964 to 1 May 1965*

## **BANDWIDTH COMPRESSION TECHNIQUES FOR METEOROLOGICAL SATELLITE PICTURES**

*Prepared for:*

NATIONAL AERONAUTICS AND SPACE ADMINISTRATION  
GODDARD SPACE FLIGHT CENTER  
GREENBELT, MARYLAND 20771

CONTRACT NAS5-3706

By: E. D. JONES      A. MACOVSKI      D. W. MASTERS  
S. M. SEREBRENY      R. G. HADFIELD      E. J. WEIGMAN

*SRI Project 4872*

*Approved:* P. J. RICE, MANAGER  
PHYSICAL ELECTRONICS LABORATORY

J. D. NOE, EXECUTIVE DIRECTOR  
ENGINEERING SCIENCES AND INDUSTRIAL DEVELOPMENT

Copy No. **18**

## ABSTRACT

---

A selection of TIROS and Nimbus satellite cloud pictures were processed to reduce the bandwidth required for transmission. Several analog processing methods were studied, each aimed at a 9:1 bandwidth reduction ratio. A detailed technical description of the several processes is given, together with the cloud photographs that resulted. A possible implementation of a real-time operational system is included. A discussion of noise considerations, errors, analog logic techniques, and a comparison of the evolved bandwidth reduction system with other approaches is appended.

It is concluded that the bandwidth compression schemes described here retain meteorologically significant features decidedly better than a system based on simple low-pass spatial filtering (averaging).

## CONTENTS

---

ABSTRACT . . . . .	iii
LIST OF ILLUSTRATIONS . . . . .	vii
LIST OF TABLES . . . . .	ix
PERSONNEL . . . . .	xi
SUMMARY . . . . .	xiii
I INTRODUCTION . . . . .	1
II CONTRACT OBJECTIVES . . . . .	5
III BRIEF SYSTEM DESCRIPTION . . . . .	7
A. Scanning Techniques . . . . .	7
B. Bandwidth-Compression Algorithms . . . . .	8
C. Selection of the Optimum Algorithm . . . . .	9
IV NIMBUS PHOTOGRAPHS . . . . .	11
V TIROS PHOTOGRAPHS . . . . .	39
VI DETAILED TECHNICAL DESCRIPTION . . . . .	111
A. Scanner . . . . .	111
B. The Input System . . . . .	113
C. The Output System . . . . .	114
D. Bandwidth Compaction Algorithms . . . . .	116
1. Conventional Averaging . . . . .	117
2. Selection of Blackest Element . . . . .	117
3. Selection of Whitest Element . . . . .	120
4. Combination of Blackest and Whitest Enhancement . . . . .	120
5. Selection of Second Blackest or Whitest . . . . .	121
6. Line Structure Enhancement . . . . .	122
7. Peripheral Cancellation . . . . .	123
E. Test Charts . . . . .	127

## CONTENTS (Concluded)

VII	CONCLUSIONS . . . . .	135
	A. General . . . . .	135
	B. Errors . . . . .	135
VIII	A POSSIBLE IMPLEMENTATION OF AN OPERATIONAL SYSTEM . . . . .	139
Appendix A	NOISE CONSIDERATIONS . . . . .	145
Appendix B	ANALOG LOGIC . . . . .	151
Appendix C	COMPARISON WITH OTHER BANDWIDTH COMPRESSION SYSTEMS . .	163
REFERENCES	. . . . .	169

## ILLUSTRATIONS

---

Fig. 1	Cellular Patterns of Cumulus Clouds . . . . .	18
Fig. 2	Dendritic Patterns of Snow Cover . . . . .	22
Fig. 3	Pack Ice and Cloud Cover in Lines and Sheets . . . . .	26
Fig. 4	Cloud Clusters, Vortex Pattern, and Convective Clouds .	30
Fig. 5	Cloud Cells and Lines . . . . .	34
Fig. 6	Distribution of Photographic Examples . . . . .	37
Fig. 7	Extratropical Cyclone A . . . . .	44
Fig. 8	Extratropical Cyclone B . . . . .	48
Fig. 9	Tropical Cyclone . . . . .	52
Fig. 10	Secondary Cyclonic Circulations . . . . .	56
Fig. 11	Small-Scale Cyclone . . . . .	60
Fig. 12	Clouds Compared with Ice . . . . .	64
Fig. 13	Frontal Band--Snow-Covered Mountains . . . . .	68
Fig. 14	Frontal System A . . . . .	72
Fig. 15	Frontal System B . . . . .	76
Fig. 16	Lee Wave Clouds . . . . .	80
Fig. 17	Cirrus Clouds . . . . .	84
Fig. 18	Cellular Patterns--Ice and Snow . . . . .	88
Fig. 19	Coastal Stratus . . . . .	92
Fig. 20	Cumulonimbus with Cirrus Plumes . . . . .	96
Fig. 21	Eddies Induced by Islands . . . . .	100
Fig. 22	Cloud "Streets" . . . . .	104
Fig. 23	Air Mass Convective Clouds . . . . .	108
Fig. 24	Nimbus Scanner . . . . .	112
Fig. 25	Simplified Block Diagram of System . . . . .	113
Fig. 26	Delay-Line Sensing Array . . . . .	115
Fig. 27	Selection of Blackest Element . . . . .	118
Fig. 28	Block Diagram of Combining Circuit . . . . .	119

## ILLUSTRATIONS (Concluded)

Fig. 29	Block Diagram of Blackest-plus-Whitest Circuit . . . . .	121
Fig. 30	One-Dimensional Distribution of Light . . . . .	123
Fig. 31	Matrix Array of Photocells . . . . .	125
Fig. 32	Intensity Distribution for a Feature That Occurs Between Scanning Lines . . . . .	125
Fig. 33	Original of Test Chart No. 1 . . . . .	128
Fig. 34	Test Chart No. 1 Reduced 9:1 by Simple Averaging . . . . .	130
Fig. 35	Test Chart No. 2 Reduced 9:1 by Peripheral Cancellation. . . . .	131
Fig. 36	Original of Test Chart No. 2 . . . . .	132
Fig. 37	Test Chart No. 2 Reduced 9:1 by Simple Averaging . . . . .	133
Fig. 38	Test Chart No. 2 Reduced 9:1 by Peripheral Cancellation. . . . .	134
Fig. 39	On-Line Bandwidth-Reduction System . . . . .	141
Fig. B-1	Circuit for Averaging . . . . .	154
Fig. B-2	Circuit for Selecting Blackest Element . . . . .	154
Fig. B-3	Circuit for Selecting Whitest Element . . . . .	155
Fig. B-4	Circuit for Selecting Second Blackest Element . . . . .	156
Fig. B-5	Circuit for Selecting Blackest Line . . . . .	158
Fig. B-6	Nonlinear Comparison Circuit for Black . . . . .	159
Fig. B-7	Nonlinear Comparison Circuit for White . . . . .	159
Fig. B-8	Circuits for Selection of Peripherally-Corrected Black and White Signals . . . . .	161
Fig. B-9	Black-White Combining Circuit . . . . .	162

## TABLES

---

Table I	Evaluation of Significant Pictorial Features After Processing . . . . .	13
Table II	Distribution of Meteorologically Significant Features in Photographic Examples . . . . .	41



## PERSONNEL

---

The Stanford Research Institute staff members who performed the investigation and reported its results here are:

Earle D. Jones, Project Leader, Research Engineer,  
Physical Electronics Laboratory

Albert Macovski, Senior Research Engineer,  
Physical Electronics Laboratory

David W. Masters, Research Engineer,  
Systems Engineering Laboratory

Sidney M. Serebreny, Head, Atmospheric Analysis Group,  
Aerophysics Laboratory

Rex G. Hadfield, Research Meteorologist,  
Aerophysics Laboratory

Eldon J. Wiegman, Research Meteorologist,  
Aerophysics Laboratory

## SUMMARY

---

### A. General

It was the object of the investigation reported here to study techniques by which the bandwidth required to transmit meteorological satellite cloud pictures could be reduced. The over-riding consideration in the evaluation of the evolved techniques is retention of information deemed to be of meteorological importance.

The work described here commenced with the design and construction of an electro-mechanical scanning system. In principle of operation, the scanner samples a square array of picture elements of an original satellite cloud picture. Based on the information from the sensor matrix, a single printout signal is derived. The primary sensory array was a  $3 \times 3$  matrix producing a bandwidth reduction of 9:1. It is very important to note that this bandwidth reduction is based on the original analog signal bandwidth.

The pictures included were selected by meteorologists and include a wide geographical distribution, a variety of camera angles, both NIMBUS and TIROS pictures, and most important, a very large variety of features believed to be of meteorological significance. Five NIMBUS pictures were selected and seven photographs of each are included. The original is presented first, followed by six pictures representing six different bandwidth compression algorithms. All of these six are reduced 9:1 in bandwidth. Seventeen TIROS pictures were selected with three pictures of each situation. The three include one original, one bandwidth reduced 9:1 by simple averaging, and one reduced 9:1 by the best processing technique.

A detailed description of the system is given in Sec. VI and a possible operational version is described in Sec. VII.

The appendix contains a brief discussion of the effects of noise in the system under study, the analog logic employed, the circuits used and a discussion of some other methods of bandwidth compression.

## B. Conclusions

The two major conclusions of the investigation performed under this contract are:

1. That the picture processing techniques described here are decidedly better than simple averaging for reducing the bandwidth required for picture transmission. The value of the resulting picture is measured by the retention of features as interpreted by a group of experienced meteorologists.
2. That there exists a best processing algorithm for all pictures. The best pictures result when detail contrast is preserved for all areas of the picture. Although it is possible to tailor a specific processing technique to a particular picture and optimize the technique for that picture, such a system would require a library of switchable algorithms and a trained man to visually monitor the incoming pictures and make selections of the algorithm.

## I INTRODUCTION

### A. Background

This report describes the result of the investigation performed under Contract NAS 5-3706 during the period March 2, 1964, through April 1, 1965. The primary purpose of the investigation was to demonstrate techniques capable of permitting more efficient transmission of satellite-gathered cloud pictures. The required bandwidth for transmission of pictures is proportional to the amount of information transmitted per unit time. It follows that in sending pictures over a reduced bandwidth transmission line in a given amount of time, information will necessarily be lost or redundant information removed. A goal of this study was to attempt to preserve information that appeared important meteorologically.

As to the degree of bandwidth compaction, it was felt, initially, that savings of only 2:1 or 3:1 would not warrant extensive effort. All of the techniques studied during the course of the research were aimed primarily at 10:1 bandwidth reduction. It is necessary to understand the nature of such a large reduction in bandwidth. A 10:1 reduction removes from the data stream 90 percent of the original number of picture elements. This is, of course, a drastic reduction. It cannot be expected that a picture useful for all purposes can be maintained after this type of processing. What is hoped is that by taking advantage of the high resolution available in the original picture, a lower resolution picture can be synthesized that will retain those meteorologically significant features.

### B. Information Requirements

To obtain picture coverage of the entire earth, a polar orbiting vehicle is required. Ground stations to command and acquire data from these vehicles must be located at high latitudes in order to communicate with the satellite for a large percentage of the total number of orbits.

Since the majority of the users of the data are located in temperate latitudes, a long communication path exists between acquisition site and user.

It is therefore important to make efficient use of the long-line communication link, since this is a complex and costly facility.

### C. The Nimbus Configuration

It is possible to estimate the information capacity of the Fairbanks to Washington link using the Nimbus constants, namely, 33 picture triplets per orbit, 14 orbits per day and  $800 \times 800$  or  $6.4 \times 10^5$  picture elements per picture. Allowing two picture elements per cycle of bandwidth, the long-line bandwidth must be 5.1 kc.

$$\frac{(3)(33)(14)(6.4 \times 10^5)}{(2)(24)(3600)} = 5.1 \times 10^3 \text{ cps.}$$

A number of factors combine to make the bandwidth of the Nimbus system appreciably greater than the number shown above. One of these is the overlap regions in the high latitudes, which demand that a portion of the area of the earth be transmitted during more than one orbit. This factor is approximately 1.6 for the Nimbus orbit. Another factor is the percentage of the orbit time allotted for picture transmission. The requirements for sending other data over the long-lines such as radiation information, and the requirements for transmitting the most-recently-acquired northern hemisphere pictures relatively quickly, both demand that no more than one-third of the orbit time be used for picture transmission. These two factors combine to provide a total baseband video bandwidth for all three Nimbus cameras of approximately 24-kc, which is almost six times the value computed for the minimum required bandwidth. The communications bandwidth used to transmit this information via FM is about three times the baseband video bandwidth. The three camera signals thus required all of one, and half of another standard 48-kc Telpak channel. This amount of bandwidth on a continuous basis is very costly. In addition, future improvements--such as a higher

resolution camera (electrostatic tape system) and multiple satellite systems--will greatly aggravate the bandwidth problem. A further consideration is the distribution of picture information after arrival at a central point. The existing communications facilities to points requiring weather data are inadequate for this amount of bandwidth. Thus any efforts toward solving the transmission problem from the northern acquisition site to Washington are also pertinent to the final data-distribution problem.

## II CONTRACT OBJECTIVES

The purpose of this research was to investigate the application of various data systems and techniques to the processing, handling, and transmission of meteorological satellite data. More specifically, the object of this effort was to evolve techniques for reducing the bandwidth required to transmit meteorological satellite pictures while retaining features deemed to be of meteorological importance. A further objective was to define meteorologically significant features in this context.

### III BRIEF SYSTEM DESCRIPTION

#### A. Scanning Techniques

Several possible configurations were studied whereby information could be derived from a cloud picture, processed and used to print out a picture through a transmission link of reduced bandwidth. Factors considered included the need for good resolution, accurate grey scale reproduction (linearity), sufficient total number of lines for a Nimbus picture, and, of course, minimum cost and complexity of equipment. The scanner was required to derive a multiplicity of video signals simultaneously, representative of an array of picture elements on the input photograph. For reasons of simplicity, systems were favored that required no electrical information storage capability. Flying-spot scanner approaches were ruled out because of the difficulty of scanning an array of elements. Facsimile scanners using electrically-addressed, direct-writing papers were ruled out because of the very poor rendition of grey scale--an important factor in cloud pictures. The approach that seemed most desirable and which was implemented was similar to one used for color separation for graphic arts work. Figures 24 and 25 show a photograph and block diagram of the scanner. This type of scanner uses an input drum rigidly connected coaxially with an output drum. An original is affixed to the input drum, a sheet of film is attached to the output drum. A photo sensor is provided to receive light from the input copy. Its field of view is adjusted to meet the resolution demands. A light source capable of being modulated is arranged to expose the output film. Its field of illumination is also tailored to the requirements of resolution. In the simplest configuration, the video signal from the photo sensor would be used to modulate the output light source. Under these conditions, an output picture would be produced identical with the input picture.

The SRI scanner was constructed in this fashion, except that an array of photo sensors was employed. It was felt that a bandwidth reduction of the order of 10:1 would be desirable. For this reason, the first



efforts were made with an array of  $3 \times 3$  photo sensors. Each sensor was adjusted to view one separate resolution elements of the original copy. That is, the total field of view of the nine photo sensors included a square array whose dimensions were three scanning lines by three picture elements along the line. In such a system nine simultaneous video signals are made available.

#### B. Bandwidth-Compression Algorithms

In the operation of the system, the nine video signals are processed to produce a single printout signal. During the course of the work, several different processing techniques were evolved. These ranged in complexity from simple averaging to highly nonlinear combinations. Section VI-D discusses each of these processing approaches in detail. The pictures in Sec. IV show the results of several of the different algorithms studied. The algorithms are listed below with a brief description.

Simple Averaging--In this technique, the nine signals are resistively summed and divided down to produce an output signal proportional to the average of the nine input signals.

Selection of the Blackest Element--This approach causes the output signal to be equal to the blackest of the nine input signals.

Selection of the Whitest Element--This approach causes the output signal to be equal to the whitest of the nine input signals.

Blackest plus Whitest--With this technique the two operations immediately above are performed, then the two derived signals are averaged.

Line Enhancement--The output is caused to follow the average of the nine input signals except in areas where three input elements along a line are alike and different from the other six. This technique can be used to enhance either black lines or white lines.

Detail Contrast Enhancement with Peripheral Correction--This technique, which proved to be the best of the group studied, differs fundamentally from the others. With this system a matrix of  $5 \times 5$  input

elements are scanned. The bandwidth reduction ratio is still 9:1 since the extra peripheral sensors are only used to make corrections on the nine interior elements.

### C. Selection of the Optimum Algorithm

Of the several processing techniques implemented and tested, the detail contrast enhancement with peripheral correction produced by far the most useful results. The implementation of this algorithm had practical limitations and the full peripheral correction was not employed. A matrix of  $4 \times 5$  signals was used and the effects of the limited aperture can be noticed. It is felt that the optimum processing method will include full peripheral cancellation with perhaps more sophisticated processing within the corrected  $3 \times 3$  interior array.

The value of a particular algorithm is determined by a meteorologist's evaluation of the resulting degradation of meteorologically important features. In all cases, it appears that significant improvements can be effected over simple averaging for bandwidth compaction.

**BLANK PAGE**

#### IV NIMBUS PHOTOGRAPHS

In this section, five photographic frames of the Nimbus I satellite are used to examine the various effects on cloud patterns that result from the six processing methods previously described. The location of the selected frames taken from Orbit 313 is shown in Fig. 6. These five frames were chosen because they contained a typical spectrum of cloud patterns, sizes, textures and grey scales that are of meteorological significance. By virtue of this spectrum it is felt that the frames provide a particularly comprehensive test of the capabilities of the processing system.

The effect of each process on cloud patterns was investigated in terms of alteration or retention of:

Scale--Element size and separation between elements

Texture--Clouds, cloud edges and multi-layered cloud fields

Brightness--variation of grey scale in clouds as well as contrast between clouds and open areas

Pattern--Cloud sheets or large masses, bands, lines (streets) cells, multi-layered cloud systems and terrain-induced patterns such as dendritic snow patterns on mountains, mountain crest clouds, mountain wave cloud, etc.

Terrain--Lakes, rivers, coastlines, mountains, deserts, snow and ice.

A tabulation of the effects of each process on the foregoing is shown in Table I.

The overall results of these five test examples show that large cloud areas are preserved by all processes, though with some loss of brilliance. Major loss, however, may occur in small cloud elements. The white enhancement method results in a merging of closely spaced cloud elements into a cluster of sheet, which may be interpreted as different pattern. With black enhancement, the pattern is retained at the expense

of slightly underestimating the cloud element sizes. A pronounced rectilinear edging to clouds occurs in all processes to some degree. In most processes the black-and-white contrast is heightened over that of the original, thereby obscuring the darker grey tones of cloud or land. In some cases this could result in a definite pattern change that might lead to misinterpretation of significant meteorological elements. The averaged, line enhancement and peripheral cancellation methods retain more of the quality of the original photograph than the other processes and of these the peripheral cancellation method most closely approximates the qualities of the original.

The tradeoff between transmission time and data quality was investigated. This included a study of the advisability of transmitting a gridded picture having degraded resolution in fast time as a part of the general problem of the interaction between data compression, quality, and timeliness. It was concluded that any further reduction of picture quality beyond that obtained when the bandwidth was reduced 9:1 by the peripheral cancellation method was not warranted, since this process reduces the bandwidth sufficiently to allow transmission over ordinary phone bandwidth lines and retains most of the pictorial quality necessary for meteorological interpretation. Any further bandwidth reduction would result in reduced quality pictures with very little or no decrease in transmission time.

The format of each case in this section includes

- (1) a foldout, which contains the original photograph accompanied by a brief description of the principal meteorological features, and the effects of the processes on these features; and
- (2) a foldout showing the resulting photographs using the peripheral cancellation and conventional averaging methods.

The former process best reproduces the original and the latter process (conventional averaging) is one with which the reader is apt to be most familiar. The remaining four processes are presented together in reduced size, since they were merely experimental steps in arriving at the peripheral cancellation method.

## EVALUATION O

Technique Features	Peripheral Cancellation	Averaging
A. Scale		
1. Element Size	Little change	Little change
2. Spacing	Little change	Little change
B. Texture		
1. Appearance	Close to original. Slight rectilinear effect	Grey: Out of focus
2. Cloud Edge	Close to original	Soft, indistinct
3. Transparency (Multi-layered clouds)	Close to original	Recognizable
C. Brightness		
1. Black and White Contrast	Good--greyed in tone	Slightly greater
2. Grey-scale in Cloud	Fair	Retained but subdued
D. Pattern		
1. Cloud Sheets	Retained	Retained
2. Bands	Retained	Retained
3. Lines	Retained	Retained
4. Cells	Retained	Retained
5. Multi-layered Clouds	Retained--distinct	Retained--indistinct
6. Terrain induced	Retained--distinct	Retained--indistinct
E. Terrain		
1. Lakes and rivers	Retained--distinct	Retained--indistinct
2. Mountains	Retained--distinct	Retained--indistinct
3. Deserts	Retained	Retained
4. Snow and ice	Retained	Retained

Table I  
F SIGNIFICANT PICTORIAL FEATURES AFTER PROCESSING

Black and White Enhancement	Blackest
Decreased	Decreased
Enlarged	Enlarged
Altered, rectilinear effect	Altered, rectilinear
Hard; rectilinear	Hard; rectilinear
Not distinguishable	Barely distinguishable
Extremely strong	Strong
Absent	Absent
Retained	Retained
Retained; spacings exaggerated	Bright bands only retained
Retained; spacings exaggerated	Bright lines only retained
Retained; spacings exaggerated	Retains bright cells only--altered
Not distinct	Little retention
Retained; pronounced rectilinear effect on edge	Retained; pronounced rectilinear effect on edge
Retained--but enlarged in size	Retained--indistinct
Obscured	Obscured
Retained--brightness approaches cirrus cloud	Barely retained
Retained	Retained

Line Enhancement	Whitest
Decreased	Enlarged
Enlarged	Decreased
Fairly close to original. Slight rectilinear effect	Altered, rectilinear effect
Soft; rectilinear	Soft; rectilinear
Recognizable	Not distinguishable
Moderately greater	Extremely strong
Retained but subdued	Absent
Retained	Retained
Retained; striations in clouds exaggerated	Retained; bright clouds exaggerated
Retained; spacing exaggerated	Retained; bright clouds exaggerated
Retained; spacing exaggerated	Retained; bright cells exaggerated
Retained--indistinct	Not distinct
Retained--indistinct	Retained; pronounced rectilinear effect on edge
Retained--slightly enlarged in size	Depends on size; small scale obliterated
Retained--indistinct	Obscured
Retained--subdued	Retained--brightness approaches cirrus cloud
Retained	Retained



Throughout the text the processes have been referred to by number as follows:

1. peripheral cancellation
2. conventional averaging
3. black and white enhancement
4. black enhancement
5. line enhancement
6. white enhancement

**BLANK PAGE**

## FIG. 1 CELLULAR PATTERNS OF CUMULUS CLOUDS

LOCATION - Over the broad plateaus of the State of Para, Brazil.

PRINCIPAL PATTERN FEATURES - Cellular structure, rowed patterns, transparent upper cloud sheet.

This frame presents a classic view of the varying rowed cloud patterns and sizes that can be associated with cumulus activity due to midday heating. Note the interference patterns at the juncture of Areas III and IV. Some of this is due to terrain features. The broad, heavy cloudiness (Area II) is composed of cumulus or swelling cumulus. The clustering and brightness suggests showery precipitation. Of particular importance is the existence of thin cirrus cloud (bottom of Area I) through which can be seen the underlying small cumulus, aligned in rows.

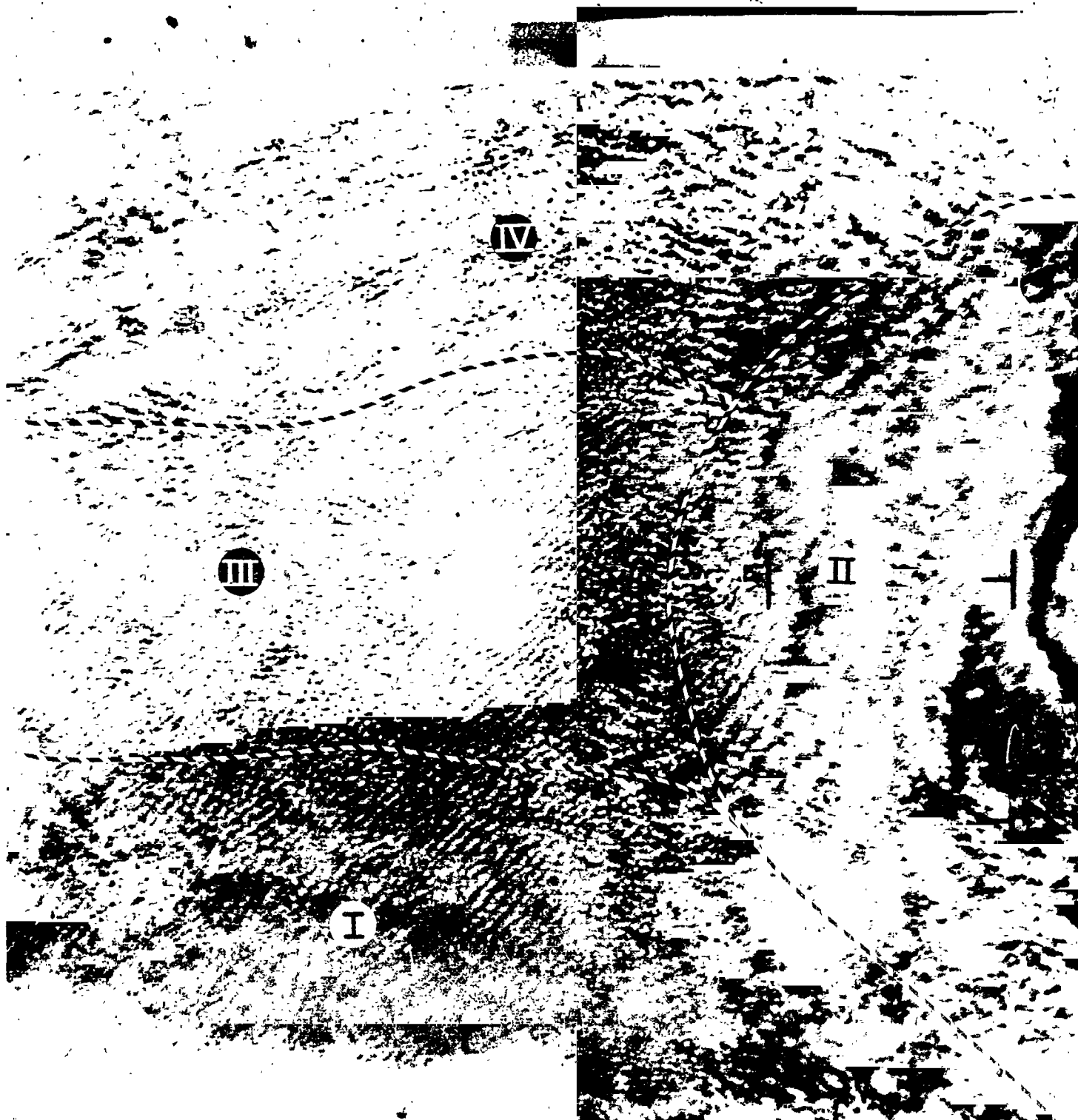
SUMMARY - In Area I the filmy, transparent cirrus cloud and underlying rows of small cumulus are melded into an opaque bright sheet (characteristic of alto-stratus) by processes 2, 3, 4 and 6. The transparency is well retained by Processes 1 and 5 and the small cloud rows are reproduced best by Process 1.

The basic pattern of Area II is retained through all the processes. Although the cloud forms are somewhat indistinct in Processes 2, 3, and 4, no interpretative problems would result. Serious distortion occurs in Process 6 due to exaggerated cloud sizes, loss of texture and merging of elements. Again, Processes 5 and 1 best preserve the character of the original, with Process 1 being the more preferable.

The pattern in Area III consists of small cumulus in crisscross rows (left) and single rows (right). This interpretation could not be ascertained from Processes 2 through 5. Processes 4 and 5 completely obliterate the elements, and Processes 2 and 3 make the elements indistinct or exaggerated. Process 1 retains most, though not all, of the pattern but allows for an interpretation most closely approximating that of the original.

Area IV contains large cloud elements arranged in long rows. Serious interpretative problems result from Processes 4 and 5, which obliterate the small clouds and destroys the pattern. Process 3 exaggerates the elements size and texture but the long rows are visible. Useful interpretations could be made from Processes 2 and 5, though the elements are indistinct. Process 1 approximates that of the original, although an increase in brightness of the clouds would be more desirable.

NAME	ORBIT	FRAME	NASA	TIME		
2	0313	35	2	5	1	1
		TAPE	DATE	HOURS	MIN	SEC
						3 9



(a) Unprocessed Nimbus original: Orbit 0313, Frame 35, Camera 2

2

IN	ORIG	FRAME	DATA	TIME
2	0 3 1 3	3 5	2 6 2	5 1 2 3 9
		TIME	DATA	HOURS MIN SEC



FIG. 1

(b) Bandwidth reduced 9:1 with peripheral cancellation

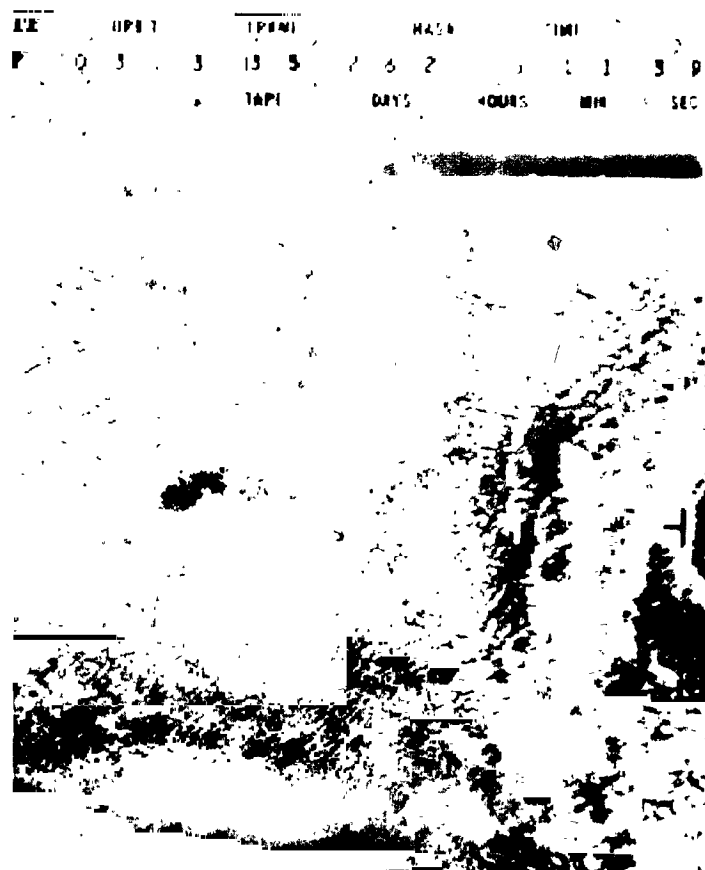


(c) Bandwidth reduced 9:1 with conventional averaging

3  
BLACK AND WHITE  
ENHANCEMENT  
METHOD



5  
LINE ENHANCEMENT  
METHOD



(d) Bandwidth reduced 9:1 with other experimental processing techniques

[illegible]

ORBIT	PERIOD	WASA	TIME
0 3 1 3	3 8	2 6 2	5 1 1 3 9
TYPE 4	DATA	WASA	WASA

2



## FIG. 2 DENDRITIC PATTERNS OF SNOW COVER

LOCATION - Central Argentina, through the states of Newquen and La Pampa.

PRINCIPAL PATTERN FEATURES - Dendritic snow pattern, terrain, and large cloud mass.

The white dendritic pattern (Area I), which characterizes snow on the Andes, has sharp black and white contrast, hard edges and a smooth and untextured appearance. Area II ranges in brightness from dark grey to light grey, rather streaky, typical of terrain. The white blobs at IIA are salt beds (Salina Grande). IIB (black area) is a 9,613-ft mountain peak with clouds on the eastern slope. The dark spot at IIC is due, partly, to light soil types and partly to solar reflection. The right portion of the frame (Area III) shows an extensive cloud mass (rather bright, hard-edged) with rifts or striations appearing in the upper portion. The herringbone or banded cloud patterns reflect wave conditions occurring as a result of wind over hilly terrain.

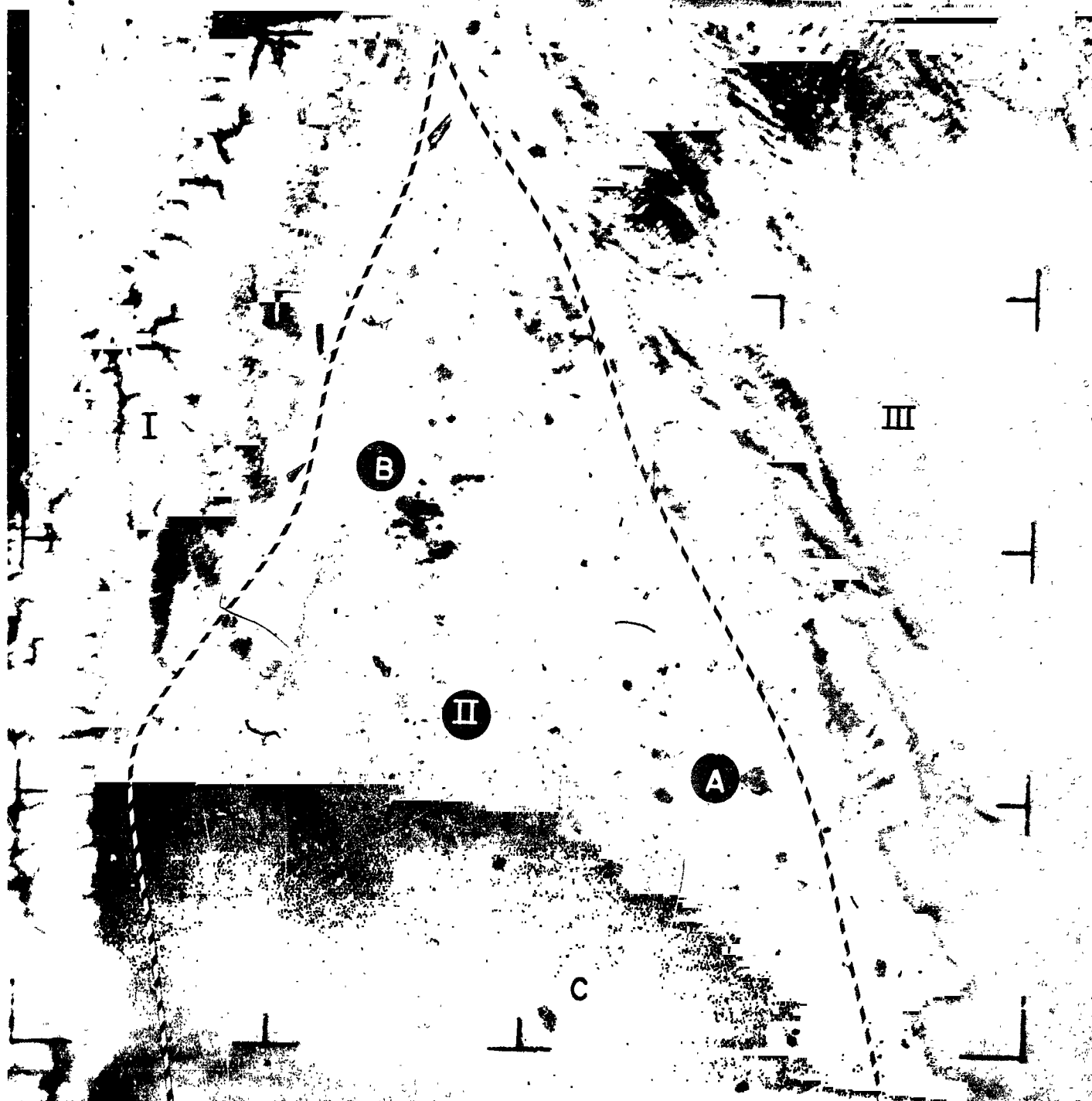
SUMMARY - The dendritic pattern (Area I) is recognizable through all five processings. While Processes 2 and 6 tend to merge the white areas, in no instance would the pattern be confused with that of cloud.

Serious interpretive shortcomings are noticed in the processing of Area II. In Processes 2, 3, 4, and 5, the light soils at the bottom of the frame appear in a manner that could lead to a misinterpretation as cirrus cloud. This tendency is not as marked in Process 6 and least apparent in Process 1. The terrain (mountains and lakes) in the center of the frame is too dark, compared to the original, in all six processes, making interpretation difficult.

The cloud sheet in Area III is retained in all processes. However, details of cells, cloud streets and striations in the cloud sheet are merged too much in Processes 3 and 4, and less so in 2, 5 and 6 and least in 1.

Statements concerning cloud type and organization would be most valid when based on Processes 1 and 5. Without question, Process 1 best retains most of the detail necessary for meteorological interpretation.

AM:	ORBIT				FRAME		NASA		TIME				
2	0	3	1	3	1	0	2	6	2	6	1	0	1
	TAPE				DAYS		HOURS		MIN		SEC		



(a) Unprocessed Nimbus original: Orbit 0313, Frame 10, Camera 2

AMP					HASD					TIME				
2	0	3	1	3	1	0	2	5	2	6	4	1	0	
TAPE					DAYS					HOURS				

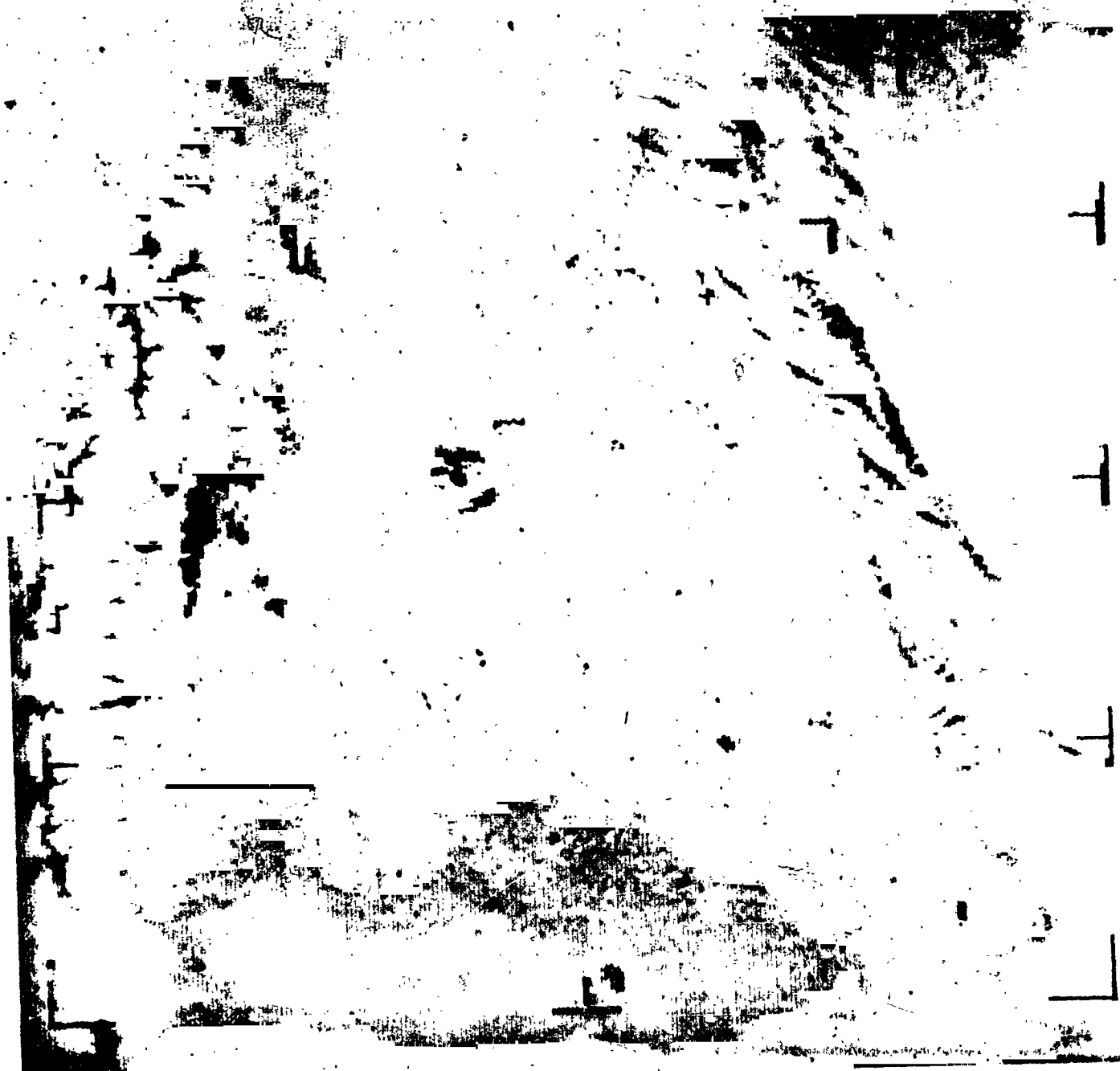
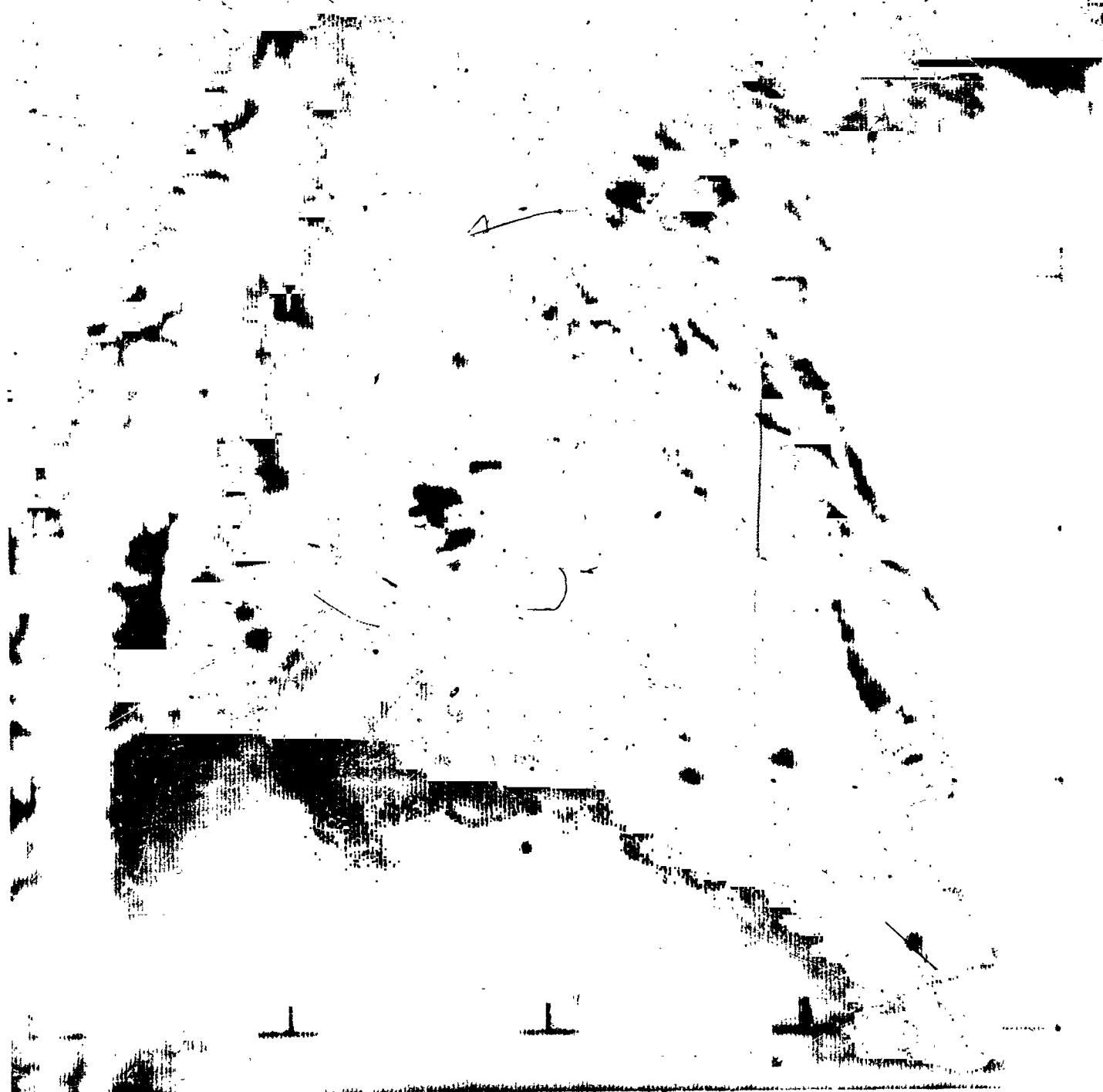


FIG. 2

(b) Bandwidth reduced 9:1 with peripheral cancellation

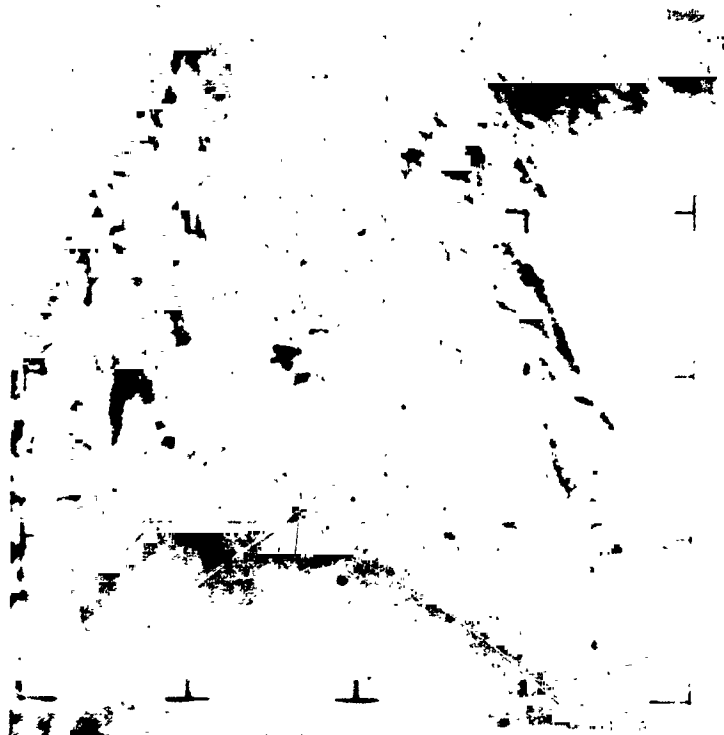
TIME	ORBIT	FRAME	NASA	TIME
2	0 5 1 3	1 0	2 6 2	5 4 1 0 1
		TAPE	DAYS	HOURS MIN SEC



(c) Bandwidth reduced 9:1 with conventional averaging

EXP	ORBIT	FRAME	NASA	TIME
2	0 3 3	1 0	2 6 2	5 4 1 0 1
		TAPE	DAYS	HOURS MIN SEC

3  
BLACK AND WHITE  
ENHANCEMENT  
METHOD



EXP	ORBIT	FRAME	NASA	TIME
2	0 3 3	1 0	2 6 2	5 4 1 0 1
		TAPE	DAYS	HOURS MIN SEC

5  
LINE ENHANCEMENT  
METHOD



(d) Bandwidth reduced 9:1 with other experimental processing techniques

4  
BLACK ENHANCEMENT  
METHOD



6  
WHITE ENHANCEMENT  
METHOD



### FIG. 3 PACK ICE AND CLOUD COVER IN LINES AND SHEETS

LOCATION - Off South Sandwich Islands, southeast of Argentina between 54°S and 60°S, 30°W to 10°W.

PRINCIPAL PATTERN FEATURES - Cloud lines and streets, large cloud sheets, pack ice.

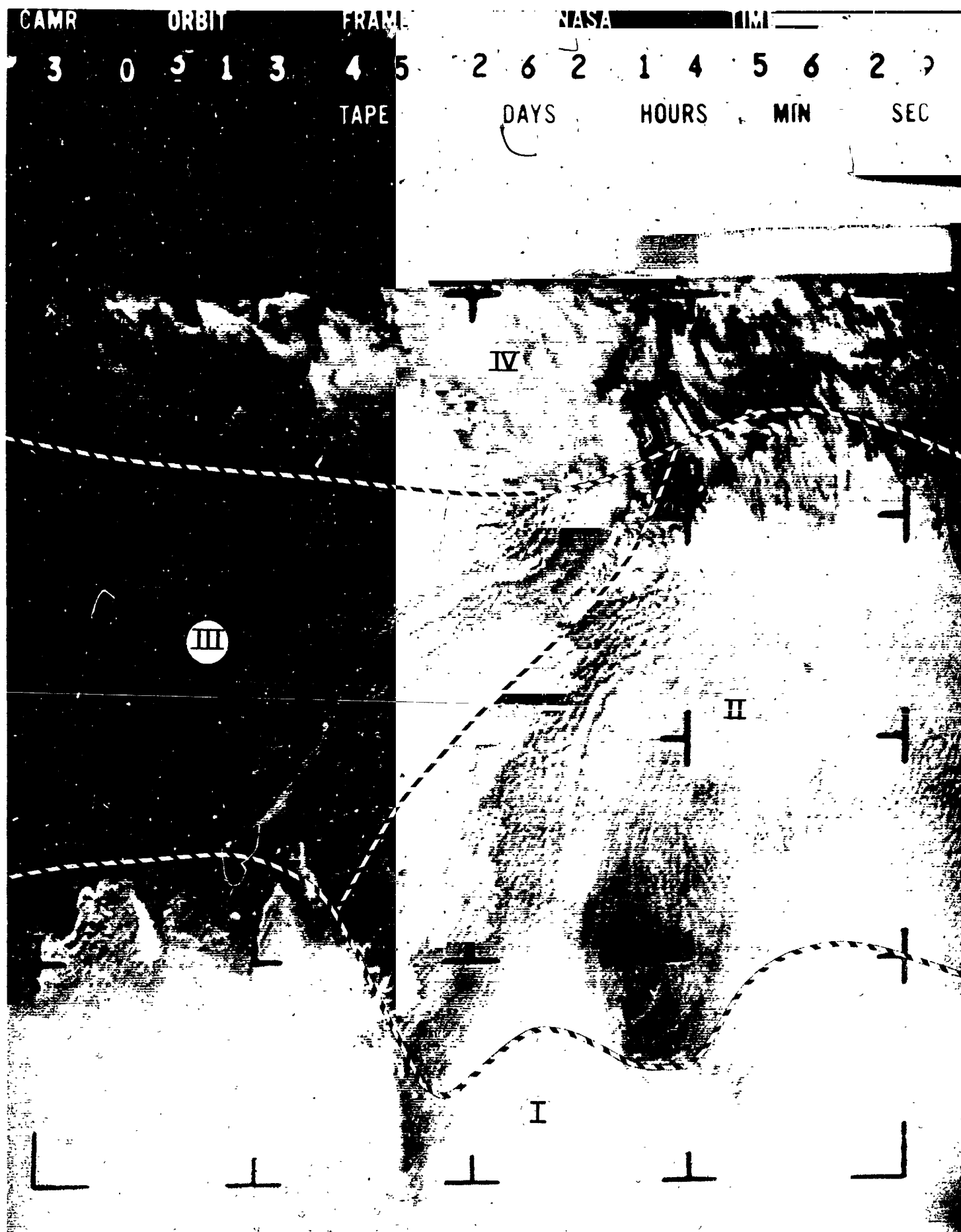
The featureless pattern of Area I is pack ice extending northward from Antarctica. Small detached elements on the periphery of the sheet probably are drift ice. The dominant cloud patterns in the frame are the clearly defined rows of small cell-like cumulus clouds (Area III) which change into a vast sheet of rowed clouds (Area II). The small size of the individual elements suggest limited vertical development due to stable conditions in lower atmosphere. Note that these clouds seem to start from the bright, featureless mass of Area I. The broad patterned, heavy appearing, clouds in Area IV are sheets of strato-cumulus, with the brighter elements representing cumulus buildups.

SUMMARY - The featureless pattern of pack ice (Area I) is unchanged by any of the processes. Small-scale elements along the periphery on the left are definitely rendered indistinct or obscured by Processes 2 and 6. They are most visible in Processes 1 and 5, particularly Process 1. There is a slight rectilinear effect to the elements but it does not affect the interpretive ability.

Area II is subject to possible interpretive errors through processing. In Processes 2, 3, and 6, the cellular structure is obscured and the elements tend to be merged into an undifferentiated sheet, similar to strato-cumulus. Process 5 retains some of the cellular and rowed characteristics but not over all of the area. Process 1 preserves most of the pattern but it too tends to merge more of the elements than is desirable.

Area III suffers badly through the various processes. In Processes 2, 3, and 4 the very small and faintest elements are obliterated and the remainder melded in a smooth sheet with no cellular characteristics. Process 5 approaches the original but the cellular structure is indistinct. Process 6 exaggerates the cloud sizes into large clumps. Process 1 fails to retain the fine-scale grey pattern.

Area IV, because of its large size and brightness, is recognizable in all processes. Detail of cloud edges (except in Process 6) seems to be preserved sufficiently so that no misinterpretation could result. Processes 1 and 5 and particularly Process 1, preserve all the pattern characteristics the best.



(a) Unprocessed Nimbus original: Orbit 0313, Frame 45, Camera 3



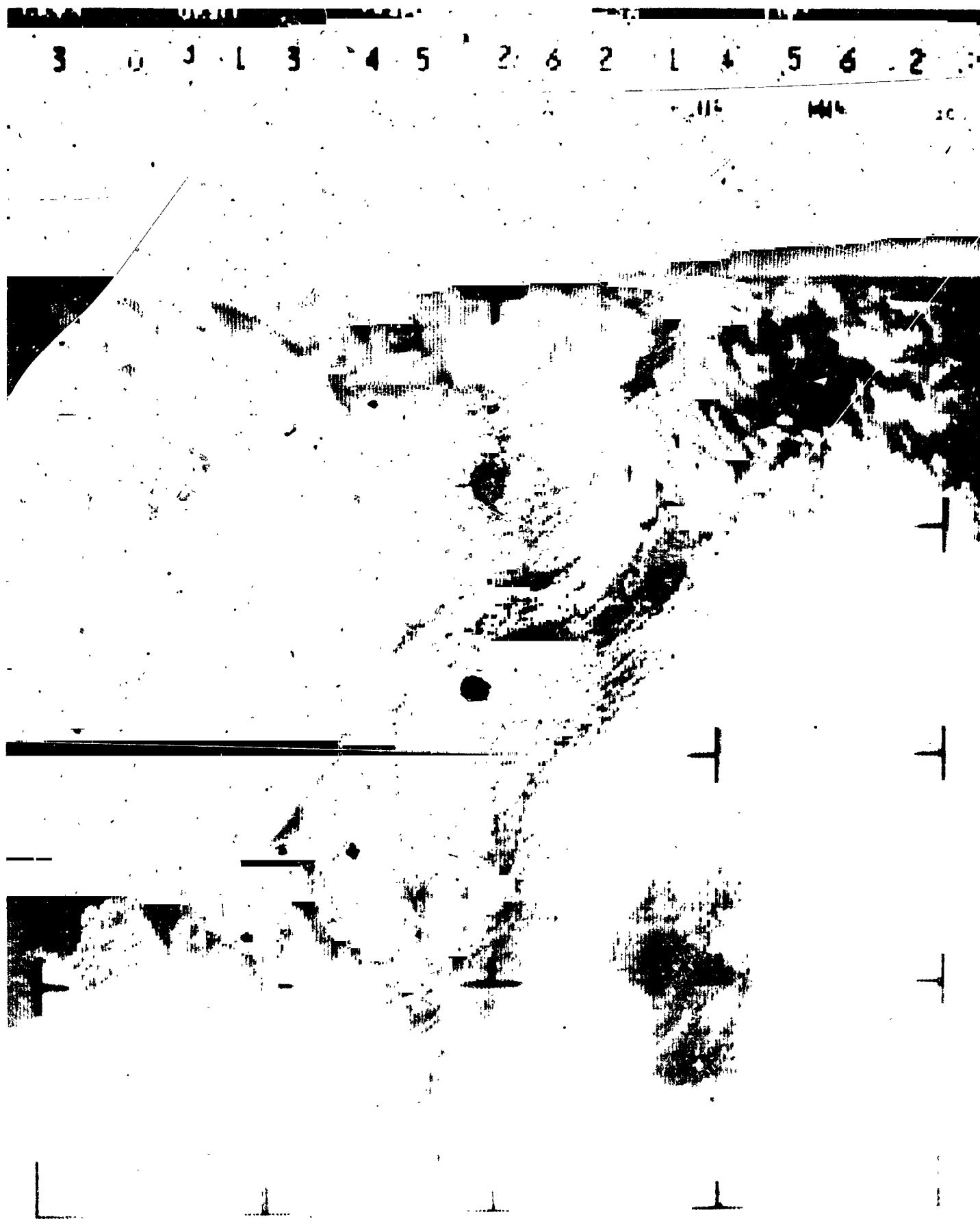


FIG. 3

(b) Bandwidth reduced 9:1 with peripheral cancellation



(c) Bandwidth reduced 9:1 with conventional averaging

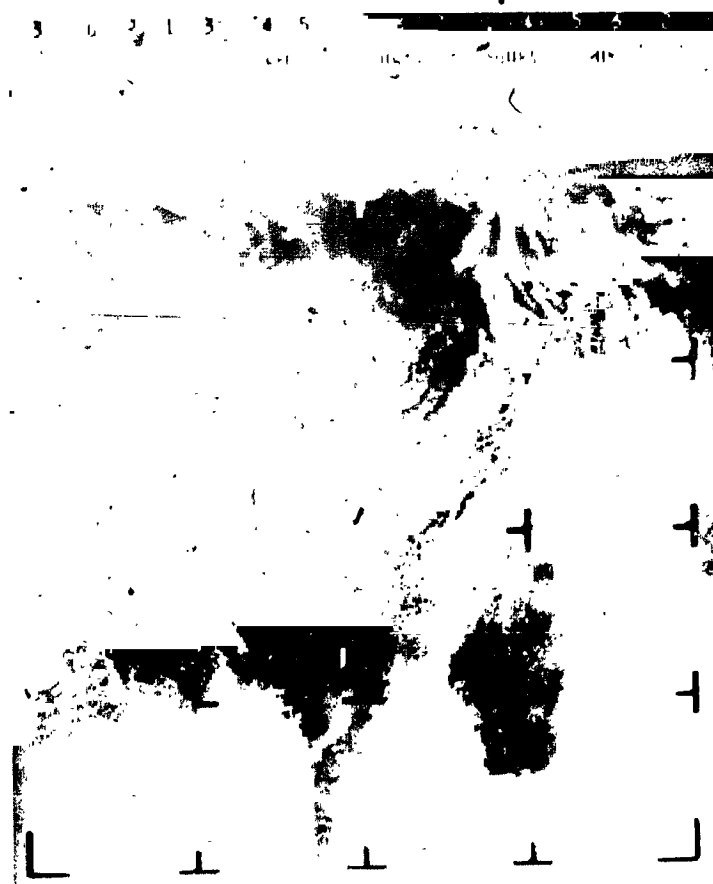
3

BLACK AND WHITE  
ENHANCEMENT  
METHOD



5

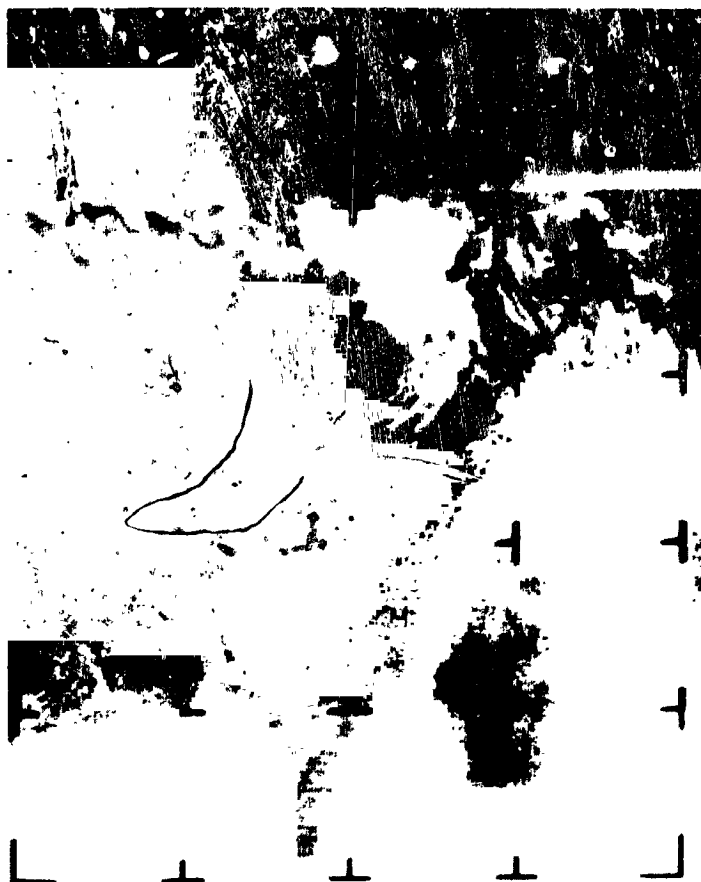
LINE ENHANCEMENT  
METHOD



(d) Bandwidth reduced 9:1 with other experimental processing techniques

4

BLACK ENHANCEMENT  
METHOD



3 0 9 1 8 . 4 5 2 6 2 1 4 5 6 2 7  
TIME DAYS HOURS MIN SEC

6

WHITE ENHANCEMENT  
METHOD



#### FIG. 4 CLOUD CLUSTERS, VORTEX PATTERN, AND CONVECTIVE CLOUDS

LOCATION - East of Falkland Island, between 32°W and 18°W; 54°S and 46°S.

PRINCIPLE PATTERN FEATURES - Vortex pattern, cloud clusters, convective development.

The frame presents a rather chaotic mixture of cloud forms, textures and brightness scales. Area I is very white, even to the extent of obscuring textural details. Some small cloud lines are visible, melding into the large white cluster. These latter elements appear to be composed of cumulus of substantial vertical development, probably with precipitation, along with alto-stratus and/or cirrus clouds. A vortex cloud pattern is apparent just to left of center of the frame Area II. The cloud forms are comprised of small, globular elements, closely spaced, and arranged in a series of rows or streets indicative of cumulus activity. Area III contains grey to grey-white cloud masses, rather broken in coverage, and is comprised of larger cloud elements than in the vortex. The edges are sharp and grey with the interior white and globular, suggesting strato-cumulus decks interspersed with swelling cumulus. The grey, wispy cloud patterns suggest upper level clouds.

SUMMARY - The cloud masses in Area I remain recognizable in all processes. Hard cloud edges and the bright centers seen on the original are subdued in Processes 2 and 6. Processes 3, 4, and 5 alter the detail by introducing rectilinear effects. Process 1 preserves the detail satisfactorily, although the clouds are of diminished brightness compared to the original.

In Area II, the small cumulus cells and lines are merged by Process 2 and 6 to the point of making them appear as stratocumulus bands. In Processes 3, 4 and 5 their true character is also not distinct, although they probably would not be misinterpreted. Process 1 preserves the detail but the low brightness does not highlight the fact that cumulus clouds are present.

The wispy, filmy grey appearance in Area III is a key interpretive feature to recognizing upper clouds. It is lost or altered in all processes except Process 1, though even in it the brightness is considerably diminished over that on the original. The cloud pattern at the upper right of Area III is retained in Processes 1, 2, and 5. Processes 3 and 4 interpret these as thin lines whereas Process 6 tends to merge the elements and make them appear "lumpy". Process 6 best preserves the pattern, but the brightness is subdued.



(a) Unprocessed Nimbus original: Orbit 0313, Frame 44, Camera 3

3 0 5 1 3 4 4 2 5 2 1 4 5 8 0 3  
HEURE MIN SEC

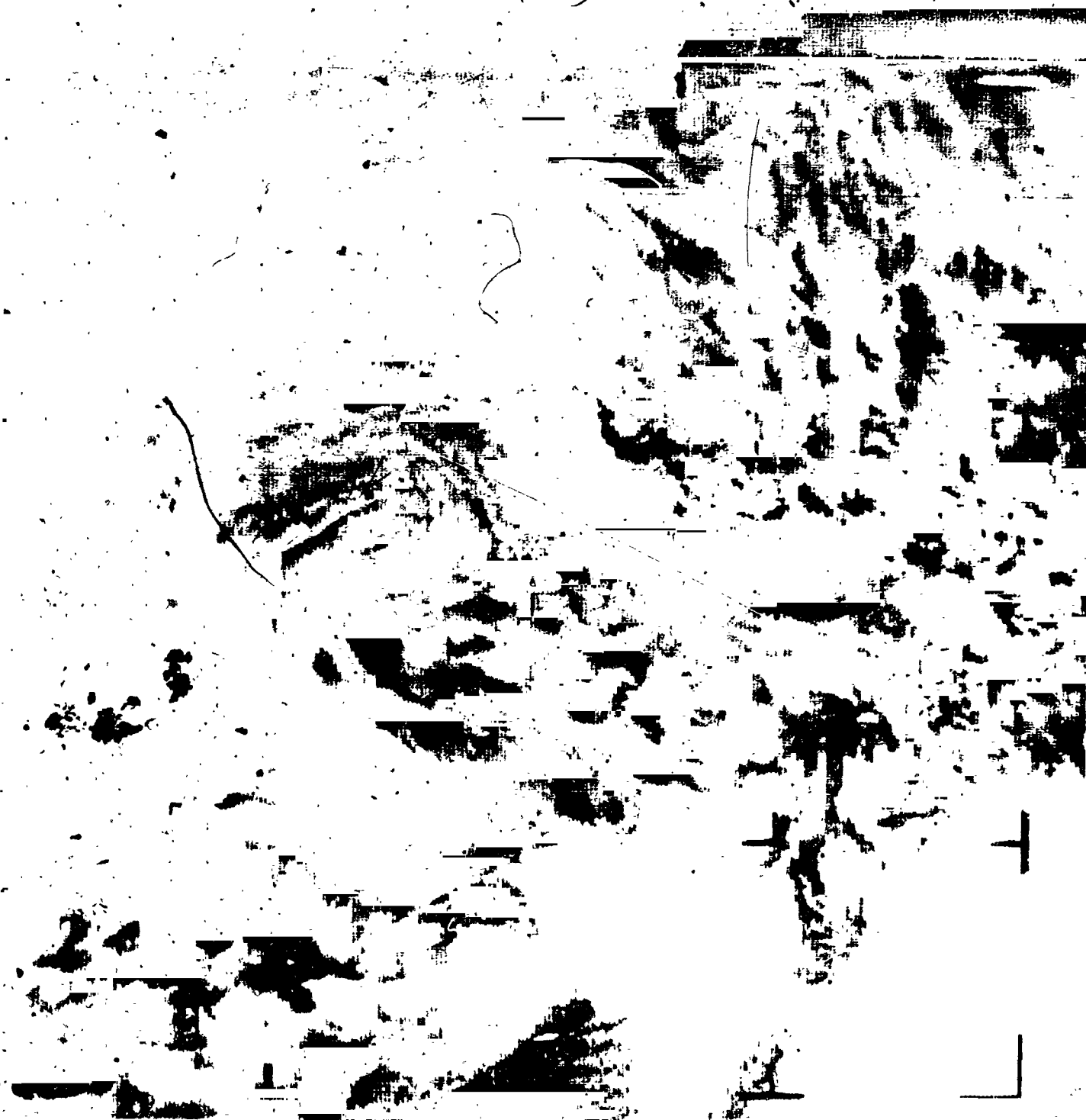


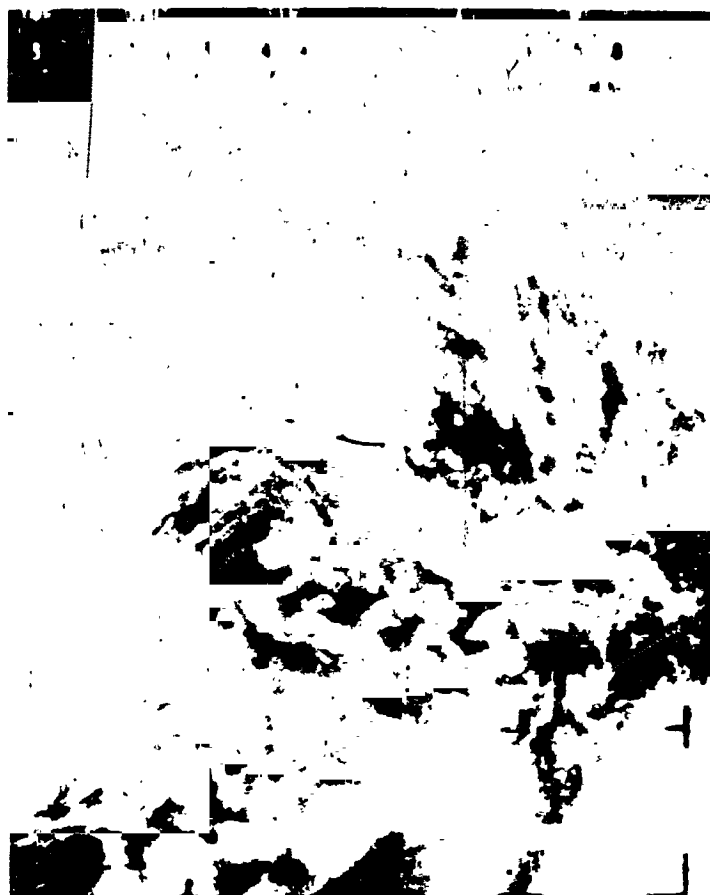
FIG. 1

(b) Bandwidth reduced 9:1 with peripheral cancellation





3  
BLACK AND WHITE  
ENHANCEMENT  
METHOD

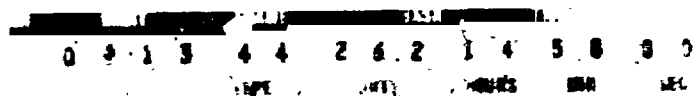


5  
LINE ENHANCEMENT  
METHOD

(d) Bandwidth reduced 9:1 with other experimental processing techniques

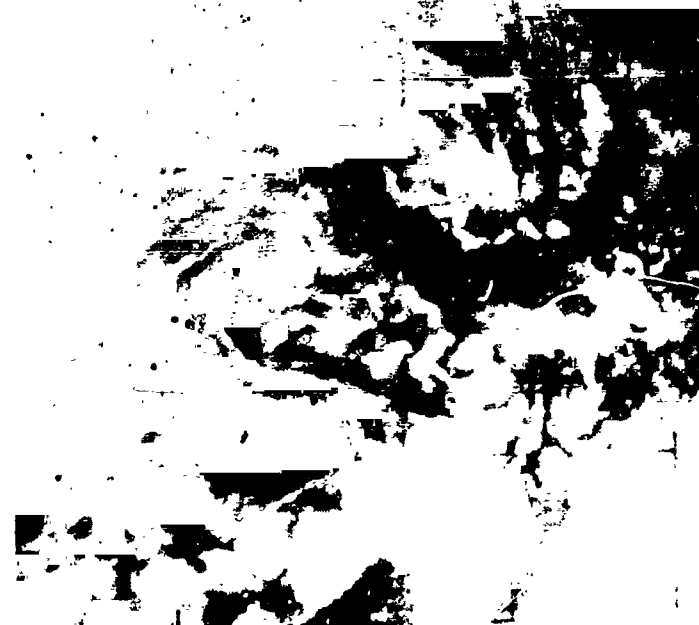
4

BLACK ENHANCEMENT  
METHOD



6

WHITE ENHANCEMENT  
METHOD



## FIG. 5 CLOUD CELLS AND LINES

LOCATION - Off the west coast of Chile, South America, along the Tropic of Capricorn.

PRINCIPAL PATTERN FEATURES - Electronic interference, cellular structure, and cloud lines.

The frame shows an off-shore cloud cover. The long curving rows of small scale cloud elements (cumulus) apparent in Area I are a typical cloud pattern in air that has begun a transit from land to water. Area II has a heavy, bright cloud cover, cellular as well as clustered, indicating a nucleus of strato-cumulus and cumulus - possible shower activity. Area III has cumulus clouds in a definitely cellular, but well separated, pattern. Area IV has an ill-defined dark grey appearance, due to electronic interference, which is superimposed on sheet-like clouds on the left and cellular clouds on the right.

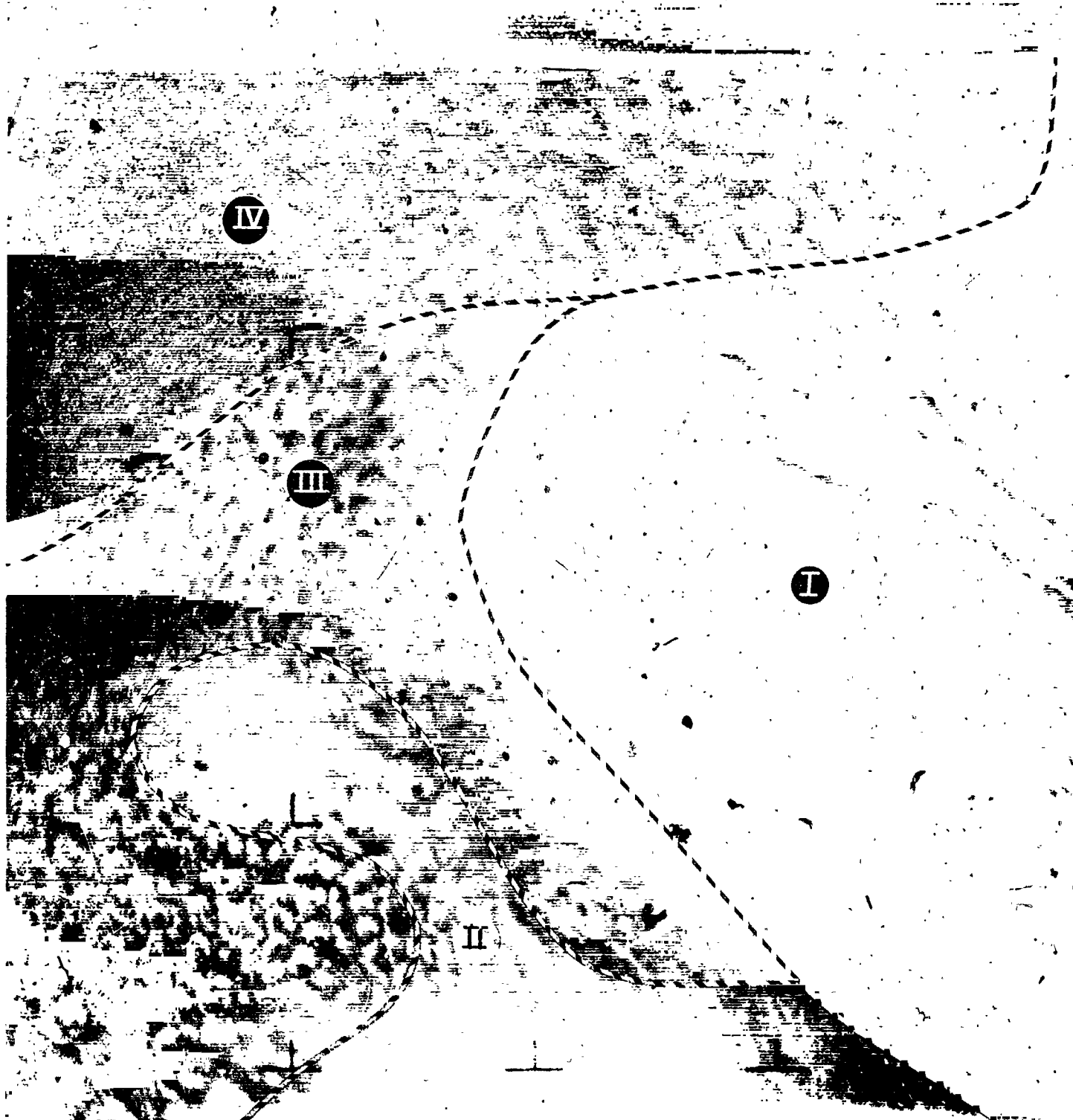
SUMMARY - The pattern in Area I is retained to a degree sufficient for interpretation only by Processes 3 and 6. Even here, there is serious loss of texture and detail so that an identification of these clouds as cumulus is difficult. In the other processes, the entire pattern in this area is obliterated or obscured.

The large-scale cumulus clusters in Area II are retained by all processes. There is loss of detail and pattern alteration in Processes 4 and 5 which seems to impose a cellular structure. In Processes 3 and 4, the cluster tends to blend into a smooth sheet.

The cellular structure of Area III is altered by Processes 4 and 5. They underestimate the cell size and present them as small-scale cumulus rather than cumulus of substantial vertical development. Processes 3 and 6 picture the clouds as individual blobs, similar to cumulonimbus, rather than cells. Process 2 preserves the pattern, but the brightness value is low and the cloud edge is soft and diffuse, more characteristic of strato-cumulus than cumulus.

The electronic interference in Area IV is greatly subdued by Process 2, allowing for a better interpretation of the cloud system than in the original. Processes 3 and 6 subdue the interference but also distort the individual cloud shapes. The overall pattern of a cloud sheet and cloud cells are recognizable, though indistinct. Processes 4 and 5 mitigate against any meaningful interpretation.

CAMR	ORBIT	FRAME	TAPE	DAYS	HOURS	MIN.
1	0313	07	262	16	45	34



(a) Unprocessed Nimbus original: Orbit 0313, Frame 7, Camera 1



FIG. 5

(b) Bandwidth reduced 9:1 with peripheral cancellation

5 3 1 3 0 2 6 2 1 6 4 5 3

TAPE

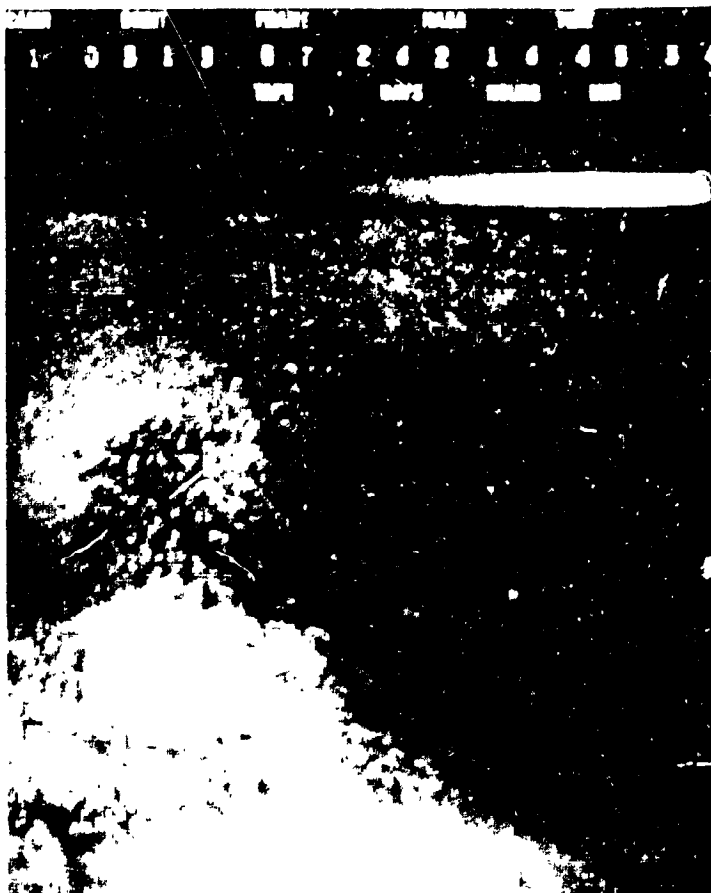
DAYS

HOURS

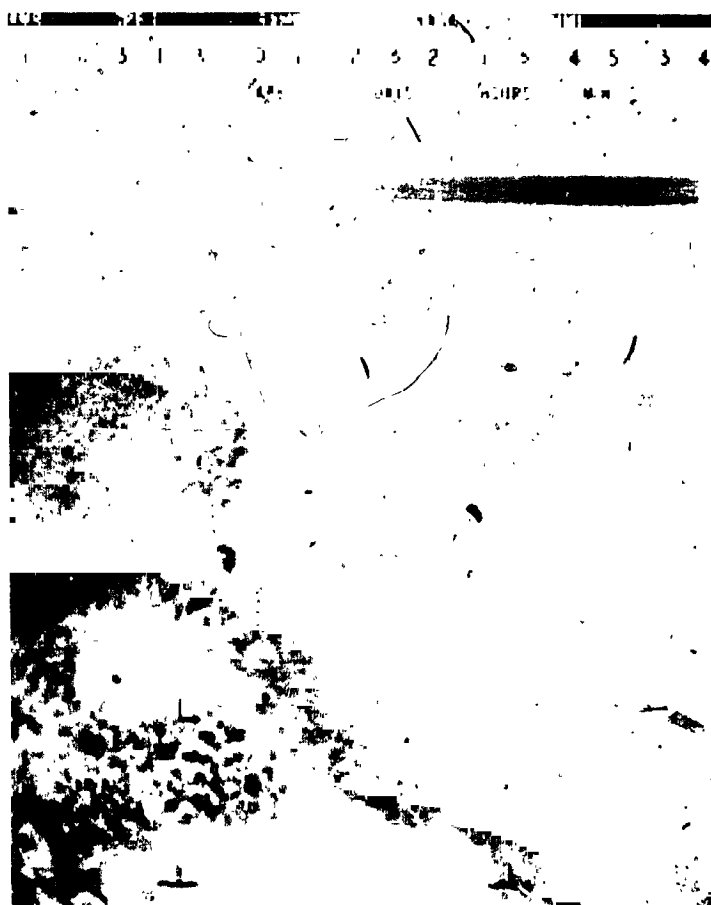
MIN

(c) Bandwidth reduced 9:1 with conventional averaging

3  
BLACK AND WHITE  
ENHANCEMENT  
METHOD

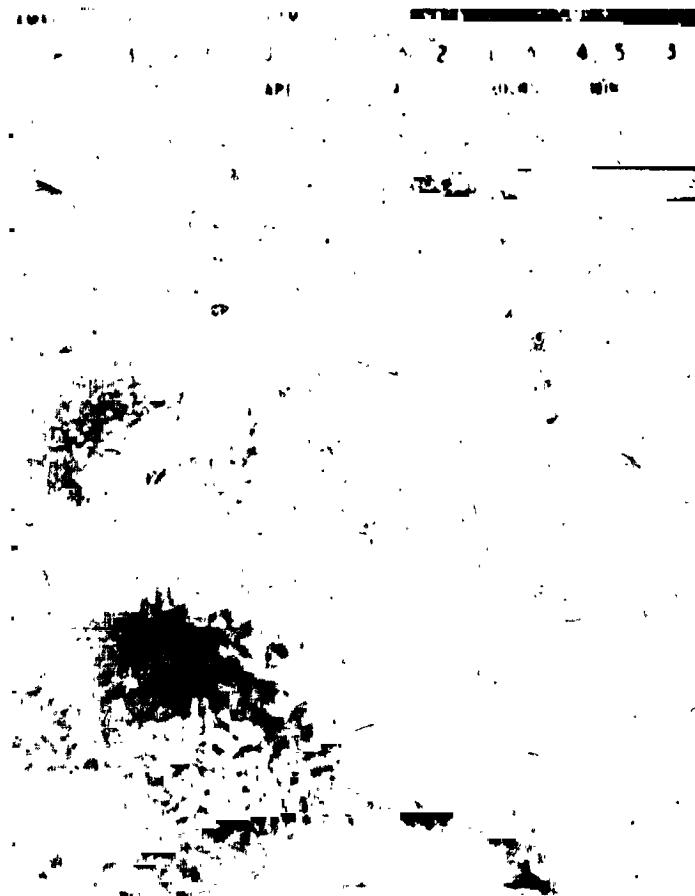


5  
LINE ENHANCEMENT  
METHOD



(d) Bandwidth reduced 9:1 with other experimental processing techniques

4  
BLACK ENHANCEMENT  
METHOD



6  
WHITE ENHANCEMENT  
METHOD





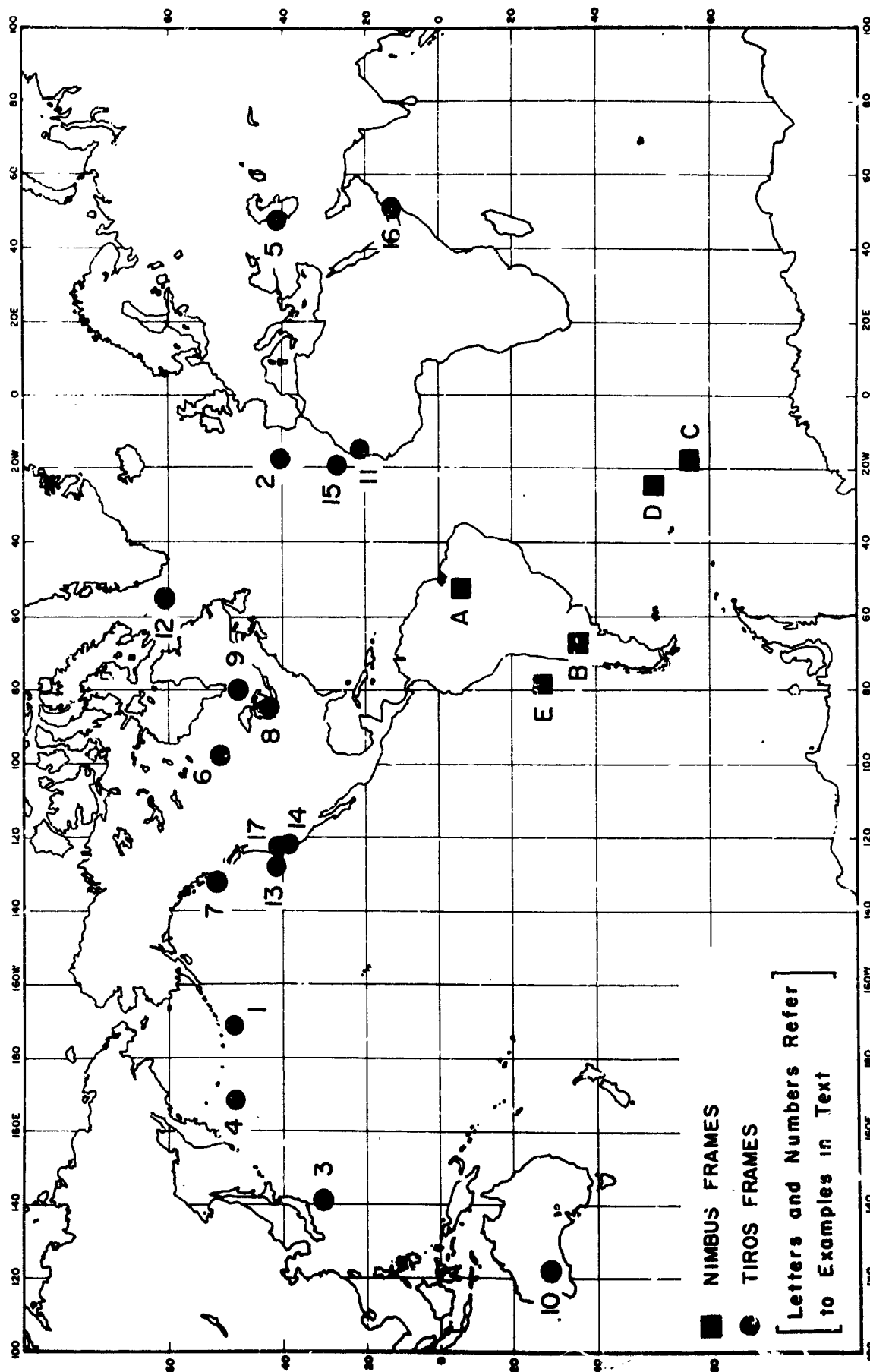


FIG. 6 DISTRIBUTION OF PHOTOGRAPHIC EXAMPLES

## V TIROS PHOTOGRAPHS

Satellite photographs provide a continuum of observations extending into areas that are devoid of conventional meteorological data. Further, they afford a refined evaluation of the extent of given cloud cover between stations in existing networks and provide corroboration of analysis or furnish the basis for adjustment of analysis and interpretations based on conventional observational data. They will, in time, provide greater insight into vertical and horizontal motions on all scales in the atmosphere. The meteorologist, in order to better utilize the satellite cloud photographs, must be acquainted with and be able to recognize the characteristic cloud features that have meteorological significance for analysis and interpretation.

This section presents 17 examples highlighting each significant meteorological feature commonly viewed in satellite photographs that should be preserved in any bandwidth reduction process. The examples were selected from the film catalogs of TIROS I, III, IV, V, VI and VII and portray features from which meteorological interpretations of varying complexity over both water and terrain can be drawn. They are believed to be representative of a wide range of patterns that will be encountered in processing any reasonably large sample of satellite photographs.

The 17 examples cover a gamut of meteorological situations ranging from broad-scale cloud systems associated with huge circulations to individual clouds. Of the former, the movement and intensity of cyclonic vortices (low-pressure systems) and their attendant frontal system, are of constant concern to the operational meteorologist. One of the most important situations (recognizable cloud arrays) is the cyclonic vortex, which has a distinct pattern consisting of cloud bands spiraling in toward the vortex center. Tropical storms also show a vortical appearance but are usually smaller in scale and their characteristic appearance is distinct from the former. Examples of both types of storms are included. Also, areal cloud coverage and type give some indication of the frontal

intensity and approximate stages of cyclone development. For example, during the decay stage of an occluded cyclone, the cloud pattern appears more fragmented (reduction of cloudiness) than it does in the earlier stages when a dense cloud shield extends in a broad continuous arc around the vortex center.

In addition to the large-scale circulations, cloud photographs reveal smaller circulations that often are not evident from an analysis of data from conventional networks of meteorological reporting stations. Often, these smaller systems develop into intense storms.

Atmospheric conditions, such as stability or instability, can also be deduced from the types and patterns of clouds that are observed. In general these deductions are based on texture (cellular, fibrous or smooth), pattern arrangements (random cells, bands, streets, striations, etc.), element spacing and size, and brightness (dark grey, grey, white or very white). Certain of the pattern arrangements such as random cells (solid, hollow, polygonal or fibrous), cumulus streets, striations, transverse waves and eddies, can be used to estimate wind conditions. Terrain features are another important consideration in cloud interpretations.

A tabulation of the significant features and the examples in which they occur is shown in Table II. It is apparent that any process of picture reproduction which eliminates or changes any one or more of these criteria will greatly influence the subsequent interpretation.

In each of the examples a brief descriptive summary is provided, which considers the significant meteorological features and the quality of reproduction by the peripheral cancellation method. No comments are made about the quality of the photograph obtained by the averaging process since it will be visually evident in every example that the peripheral cancellation process is superior to the averaging process in pattern retention capability. The overlay was designed to delineate the meteorological significance inherent in the cloud cover in the photographs in terms of such parameters as fronts, winds, etc.

The photographs selected portray wide angle, medium angle and narrow angle views. Initially, the photographic system of the TIROS series was

Table II  
DISTRIBUTION OF METEOROLOGICALLY SIGNIFICANT FEATURES IN PHOTOGRAPHIC EXAMPLES

Figure Number	1	2	3	4	5	6	7	8	9	10	11	12	13	14	15	16	17	18	19	20
	Cloud Vortex	Frontal Band	Cumulo-nimbus with Cirrus Streamers	Large Cumulus	Small Cumulus	Cumulus Streets	Strato Cumulus	Lee Waves (Strato-cumulus)	Induced Eddies	Stratus	Alto-stratus or Alto-cumulus	Cirrus	Transverse Bands in Cirrus	Striations in Cirrus	Snow Over Mountains	Snow	Ice	Coast-line	er-rain	Shadow
7	x	x			x	x					x			x						
8	x	x		x	x	x					x									
9	x			x	x	x					x	x								
10	x	x		x	x	x			x		x									
11	x	x		x	x	x					x	x								
12		x					x				x	x								
13		x					x				x	x								
14		x									x									
15	x	x									x									
16		x																		
17																				
18																				
19																				
20																				
21																				
22																				
23																				

comprised of a wide-angle camera and a narrow-angle camera (TIROS I). In later TIROS satellites only the wide- and medium-angle cameras were used. With the optical axis normal to the earth, the wide-angle camera viewed an area measuring some 700 miles on a side, the medium-angle camera viewed an area of about 475 miles on a side and the narrow-angle camera viewed roughly 80 miles on side. Most of the time these areas would be larger since only occasionally is the camera looking straight down. The resolution capabilities of the three cameras is about 1.4 miles per scan line for the wide-angle camera, 0.95 miles per scan line for the medium-angle camera, and 0.16 miles per scan line for the narrow-angle camera.

References in the summaries will be found at the end of the report.

**BLANK PAGE**

## FIG. 7 EXTRATROPICAL CYCLONE A

This photograph [Fig. 7 (a)] views a mature extratropical cyclone vortex, approximately 200 miles south of Adak in the Aleutian Chain. Such systems, with their attendant frontal bands, are among the most important synoptic weather-producing entities in temperate regions.

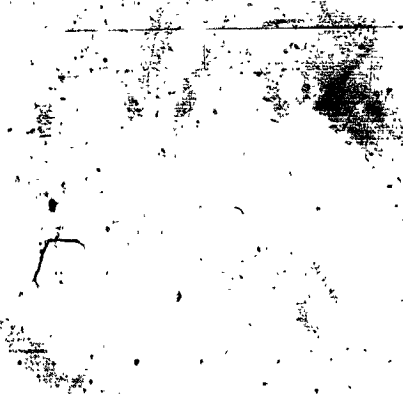
The size of this system is such that part of it extends beyond the frame of view. A small spiral vortex configuration of low cumuliform clouds is readily visible within, but separated from, the large spiral frontal band [Fig. 7 (b)]. The frontal band extending partially around the vortex is composed of middle and upper clouds, which tend to obscure the lower cloud forms. A thin cirrus shield extends beyond the edge of the frontal band. Striations within this cirrus shield are aligned with the upper winds. The relatively cloud-free area (lower left) is in the post-frontal cooler air. Cumulus clouds have formed within this unstable air mass and are aligned in "streets" parallel to the low-level wind flow. Experience in photo interpretation indicates that the cloud configuration of this extratropical cyclone places it in the mature stage in which the low aloft is situated over the surface low. This is reflected in the fact that the low-level cloud "streets" are nearly aligned with striations in the upper clouds.

Most major features and patterns are retained by the peripheral cancellation process [upper photo, Fig. 7 (c)] with rather good fidelity. The texture and detail of the frontal band is close to the original, though the high contrast in the processed frame tends to "thin cut" the cirrus cloud coverage. Some degradation of detail is apparent in cumulus clouds (left half of frame) by virtue of shrinking the element size and decreasing the contrast. As a result the extent of cumulus coverage is underestimated, the size of the individual cells is understated, and the lack of brilliance could possibly lead to an interpretation of limited cumulus development rather than the substantial cumulus buildups that the original photograph suggests.

PERIPHERAL  
CANCELLATION  
METHOD



CONVENTIONAL  
AVERAGING  
METHOD



(c) Bandwidth reduced 9:1



TIROS VII ORBIT 3312/3306T, FRAME 28 0136GMT 29 JANUARY 1964

WIDE ANGLE LENS

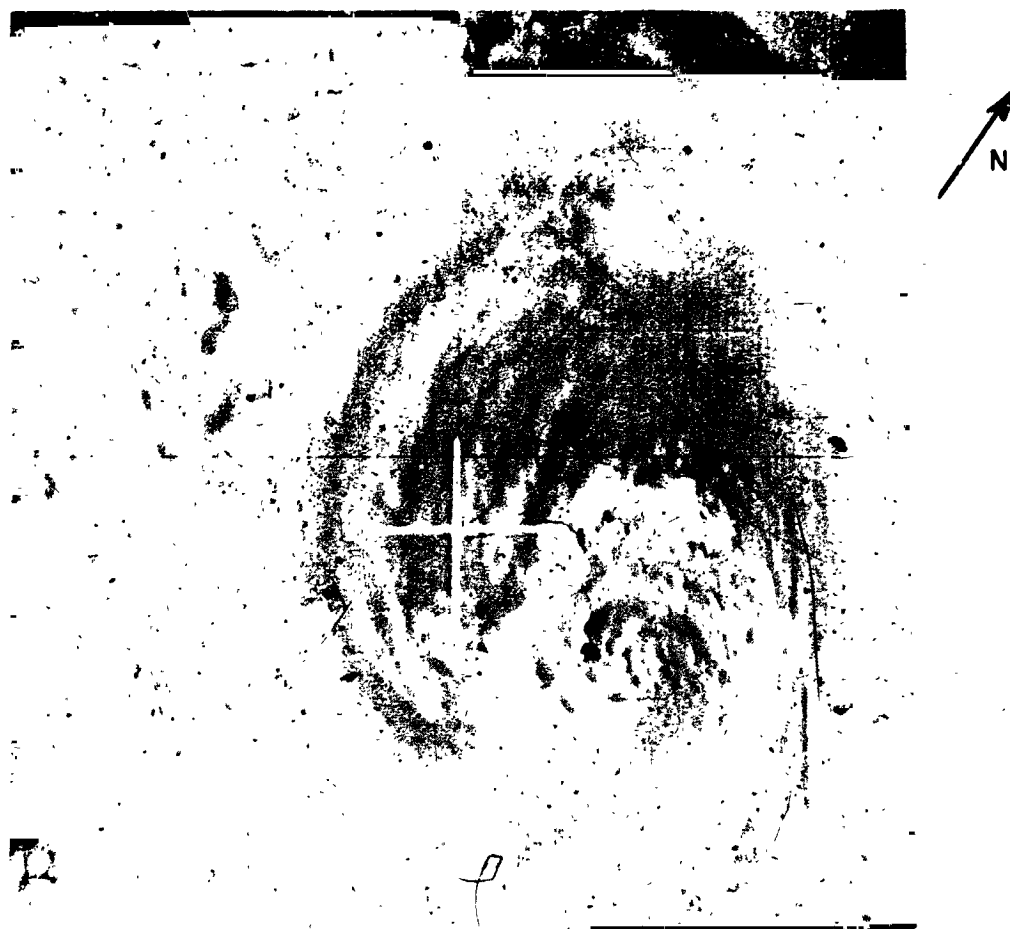


FIG. 7

SCALE: 1 in.  $\approx$  190 nm near mid-frame

(a) Unprocessed TIROS original

**BLANK PAGE**

WIDE ANGLE LENS

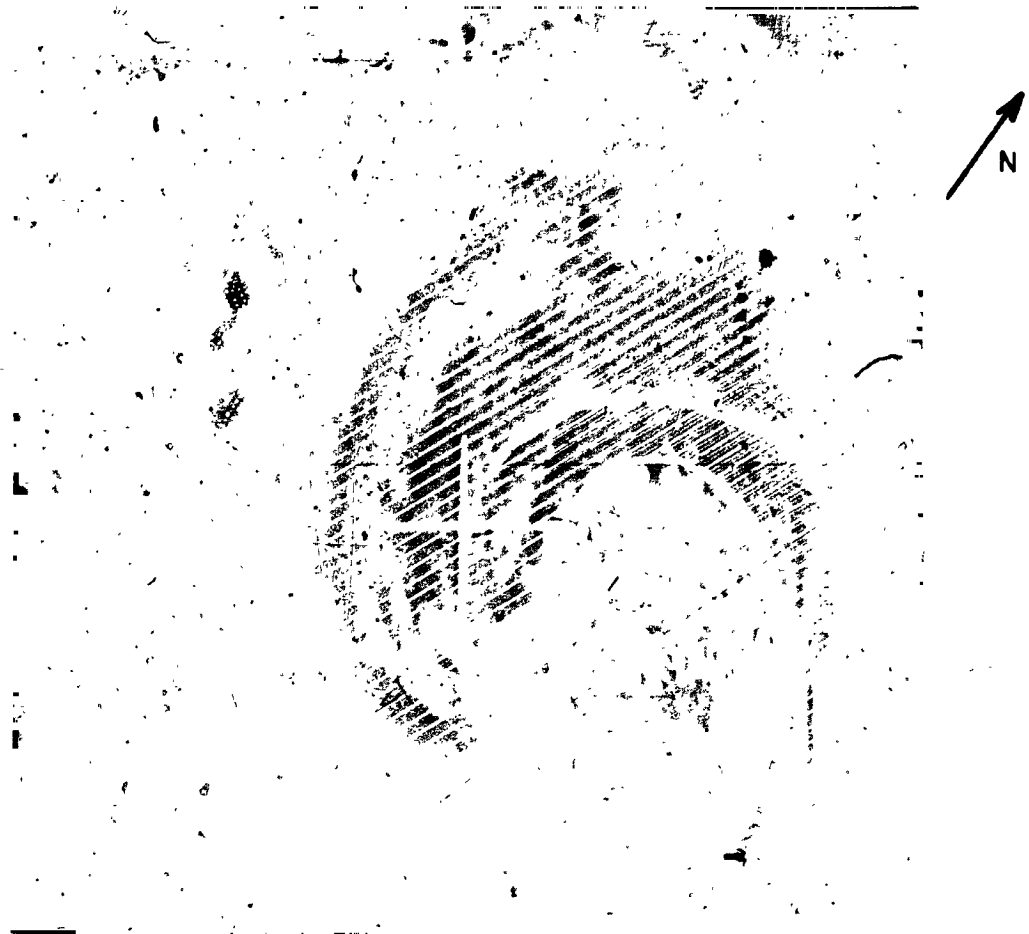




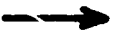



FIG. 7

SCALE: 1 in.  $\approx$  190 nm near mid-frame

- VORTEX CENTER
-  FRONTAL BAND (Middle and High Clouds)
-  CUMULIFORM CLOUDS (Cells) IN COLD AIR MASS
-  CIRRUS SHIELD
-  UPPER LEVEL WIND FLOW
-  LOW LEVEL WIND FLOW
-  OCCLUDED FRONT

(a) Unprocessed TIROS original

(b) Significant meteorological features of Fig. 7(a)

**BLANK PAGE**

## FIG. 8 EXTRATROPICAL CYCLONE B

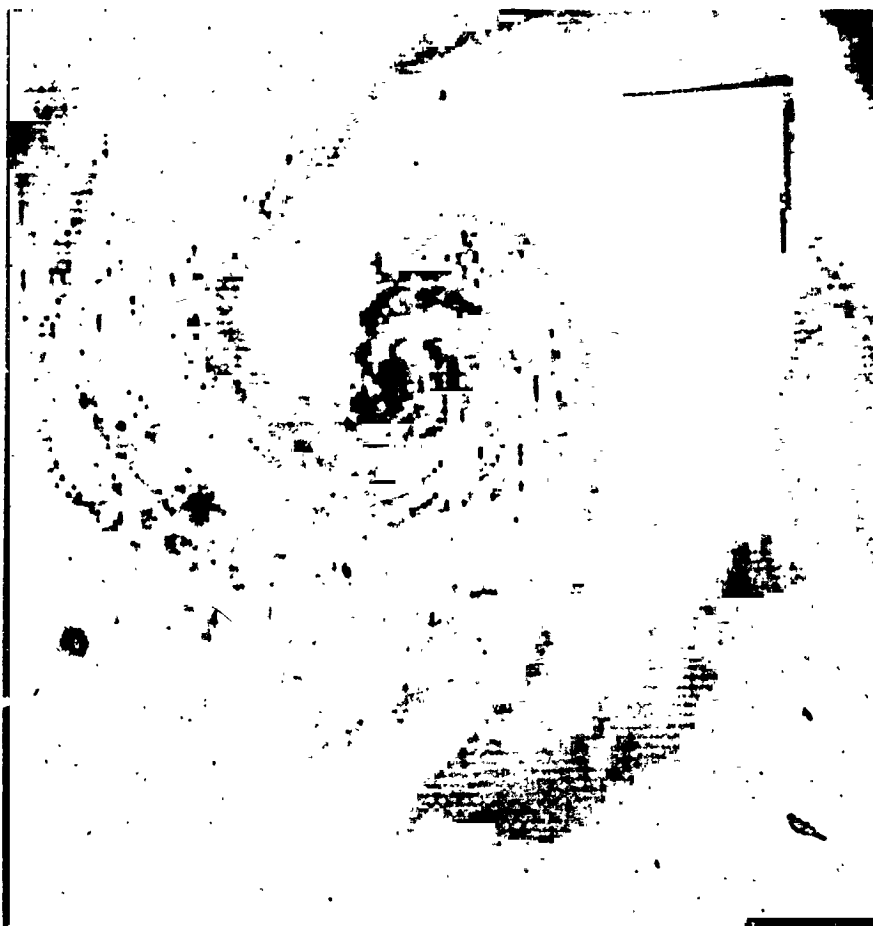
This view [Fig. 8 (a)] shows an extratropical vortex pattern associated with a fairly mature occluded cyclone system some 500 miles west of Portugal. The white appearing spiral band extending from the center is cloudiness along an occluded front. The cloud texture is bright and smooth indicating clouds of considerable thickness. Meteorological observations from ships in the area report a mixture of low, middle, and high clouds.

Cold air intrusion is taking place to the rear of the frontal band [Fig. 8 (b)] and is reflected by the relative cloud free area. The fact that it is spiraling into the very center itself indicates that occlusion has occurred. Some cumuliform cloudiness (individual white blobs) is developing in the post frontal area suggesting instability within the cold air mass. Cloud cell size immediately rearward of the frontal band is rather small, indicating that vertical development to greater heights is being prevented by a stable layer level aloft probably in combination with considerable wind speed shear in the vertical. Some of the cells farther back in the cold air are considerably larger, suggesting these cells are developing to greater heights, in a field where the vertical wind shear is not very large.

The location of the cloud vortex center on the photograph coincides with the location of the low-pressure center obtained from conventional data (not shown) closest to orbit time. Since the storm appearance indicates maturity, the center of the vortex cloud pattern also gives a close positioning of 500 mb (18,000 ft) low center since surface and 500 mb centers are nearly coincident in a mature and filling extratropical systems.

The major pattern is retained in all respects by the peripheral cancellation method [upper photo Fig. 8 (c)] with the exception that the black-and-white contrast is too strong, resulting in an overbright, hard-appearing frontal band. Clouds that were dark grey (as in the lower left of frame) tend to be totally obscured. Another noticeable result of the processing is the pronounced rectilinear effect along the cloud band edges and, particularly, in the cumuliform clouds. The effect renders the recognition of cellular patterns more difficult. By and large, cloud alignment is not affected. Interpretation of large-scale patterns is not affected; interpretation of the small-scale patterns has been affected to some degree but not to the point where it obscures the meteorological significance of the small-scale elements.

PERIPHERAL  
CANCELLATION  
METHOD



CONVENTIONAL  
AVERAGING  
METHOD



(c) Bandwidth reduced 9:1

TIROS IV ORBIT 1162/1161T, FRAME 21 1000GMT 30 APRIL 1962

WIDE ANGLE LENS



FIG. 8

SCALE: 1 in.  $\approx$  150 nm near mid-frame

(a) Unprocessed TIROS original

**BLANK PAGE**



WIDE ANGLE LENS

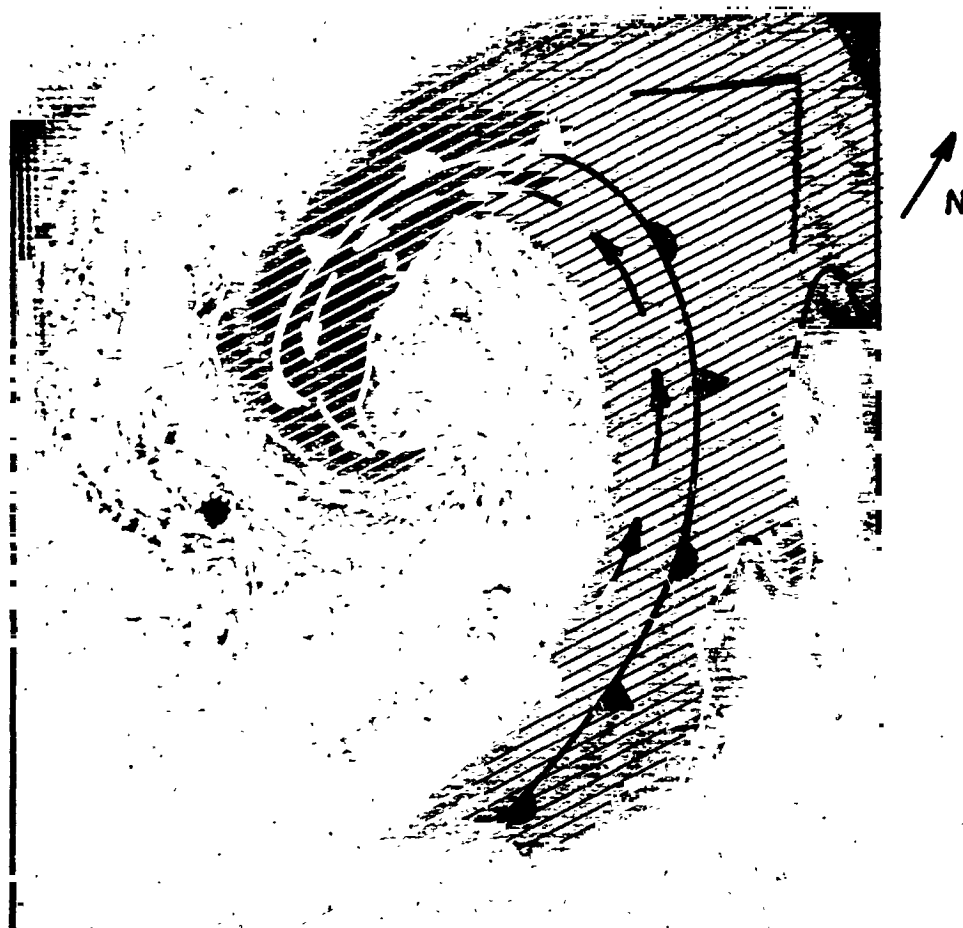


FIG. 8

SCALE: 1 in. = 150 nm near mid-frame

- VORTEX CENTER
- ▨ FRONTAL BAND (Upper and Middle Clouds)
- ☐ CUMULIFORM CLOUDS (Cells) IN COLD AIR-MASS
- LOW LEVEL WIND FLOW
- - - - - UPPER LEVEL WIND FLOW
- ☐ OCCLUDED FRONT

- (a) Unprocessed TIROS original
- (b) Significant meteorological features of Fig. 8(a)

## FIG. 9 TROPICAL CYCLONE

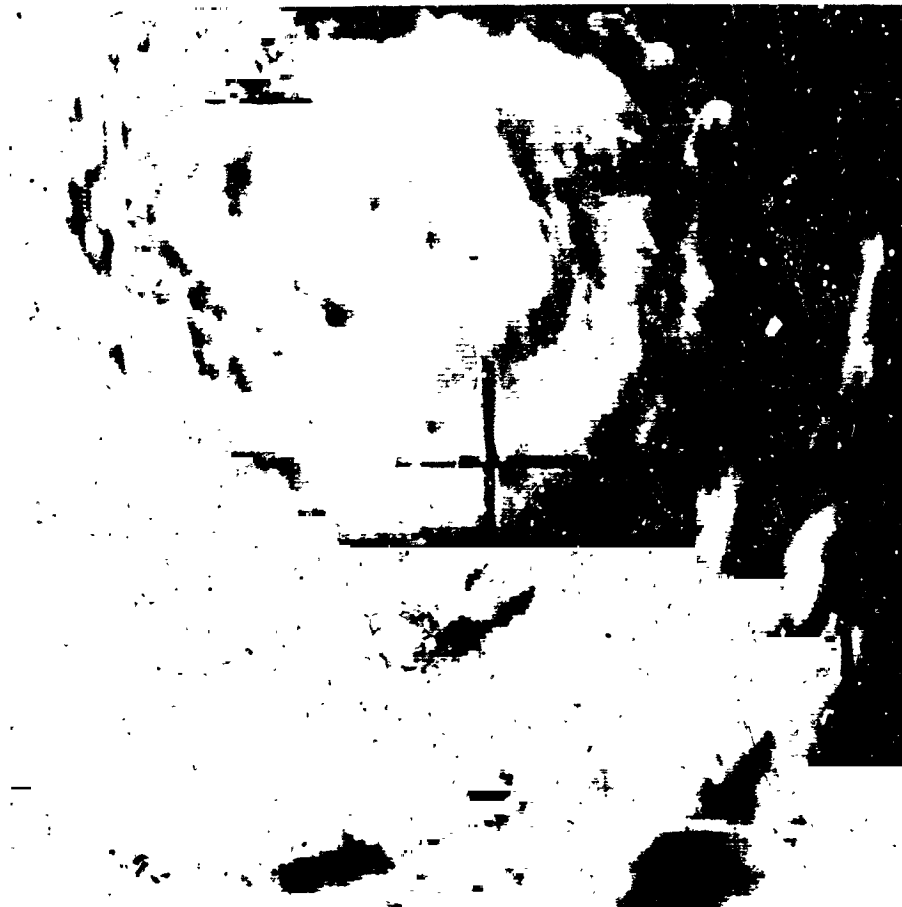
This photograph [Fig. 9 (a)] shows a well developed tropical cyclone (Typhoon Ruth) approximately 250 miles south-southwest of Japan. The "eye" of the typhoon is discernible as the small dark spot within the center of the vortical cloud mass. Wind speeds measured by aircrafts reach 95 knots near the center. In such storms, the maximum winds are usually confined to the small doughnut shaped "wall cloud" directly surrounding the eye [Fig. 9 (b)]. Although violent cumuliform cells are present (bright white elements), cirrus clouds from the tops of the large cumulonimbus cells partially obscure the spiral bands within the vortex itself. Outside of the main vortical cloud mass the area contains less cloudiness, although, cumulonimbus cloud bands are present on the lower right hand part of the frame. The area on the lower left hand part of the frame is relatively cloud-free, although there are some small individual cumulus.

Visual evidence of bands, both under and outside the cirrus canopy, gives clues to the structure of the upper air. The spiral cloud bands reflect general ascending motion in relatively moist air; at lower levels there is inflow relative to the band, while at upper levels there is outflow, (Tang, et al., 1963).

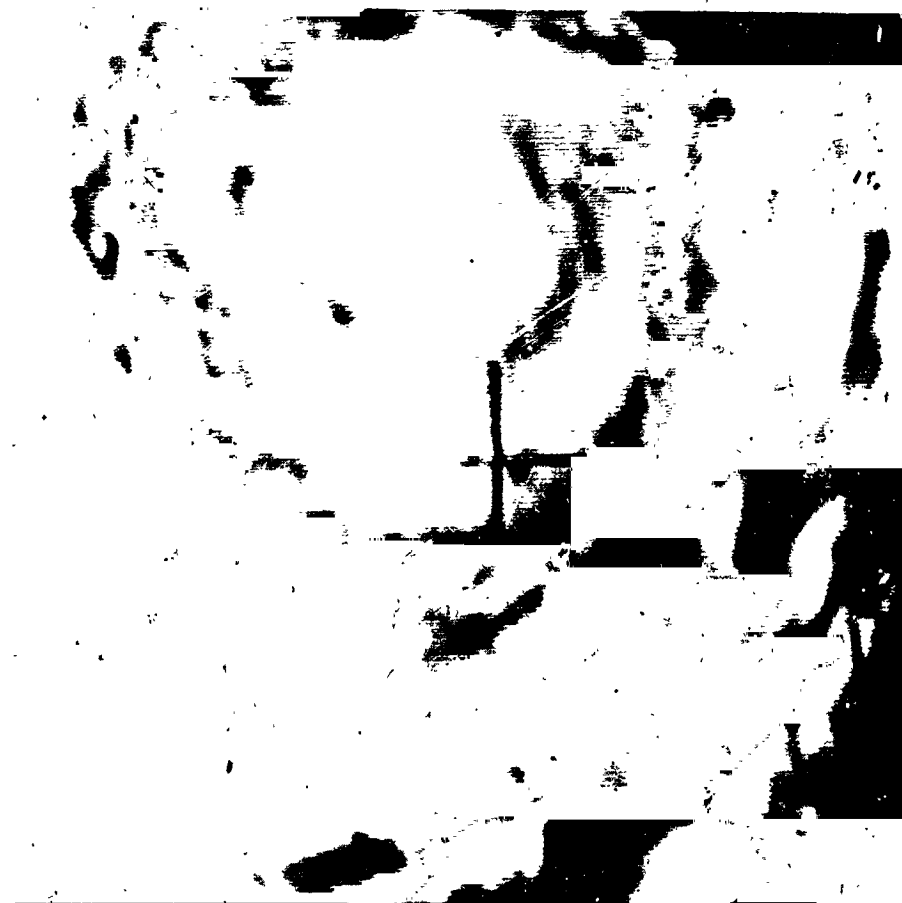
According to Widger, et al., (1964), the cirroform canopy thins or may even dissipate in some quadrants during the process of decay. In this photograph the cirrus shield appears quite thin, suggesting no further development of this storm. Some idea of storm movement can be gleaned from the fact that generally, the spiral bands are more clearly defined in the rear quadrants of the storm, while front quadrants usually show more convection with a thickening cirrus shield.

All features essential to the recognition of the tropical cyclone per se are well-retained by the peripheral cancellation process [upper photo Fig. 9 (c)]. There is, however, a pronounced diminution of element sizes. Due to the strong black-and-white contrast, the thin dark grey clouds have been obliterated (see clouds on upper right of frame), leaving only the brighter elements. Also the contrast makes the faint striations near the center of the cyclone less recognizable. The "eye" and wall cloud remain clearly evident, as are the bands of towering cumulus.

PERIPHERAL  
CANCELLATION  
METHOD



CONVENTIONAL  
AVERAGING  
METHOD



(c) Bandwidth reduced 9:1

TIROS V ORBIT 855/855T, FRAME 13 0351GMT 18 AUGUST 1962

WIDE ANGLE LENS

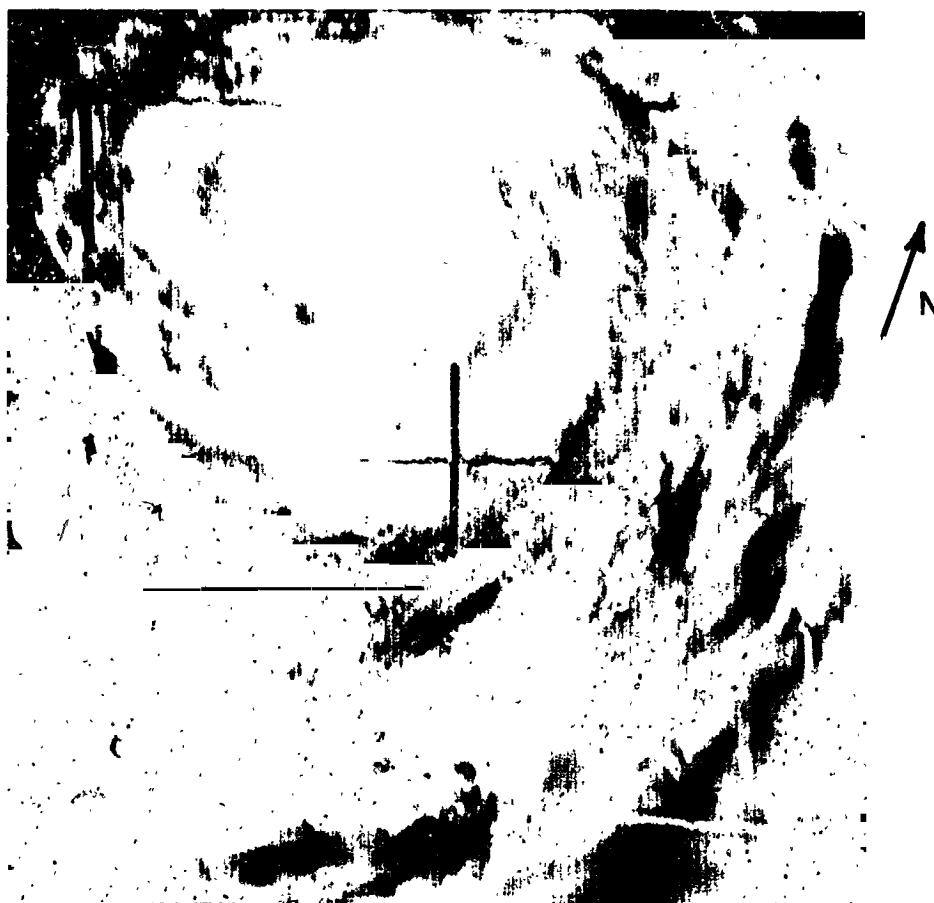


FIG. 9

SCALE: 1 in.  $\approx$  160 nm near mid-frame

(a) Unprocessed TIROS original

TIROS V ORBIT 855/855T, FRAME 13 0351GMT 18 AUGUST 1962

WIDE ANGLE LENS

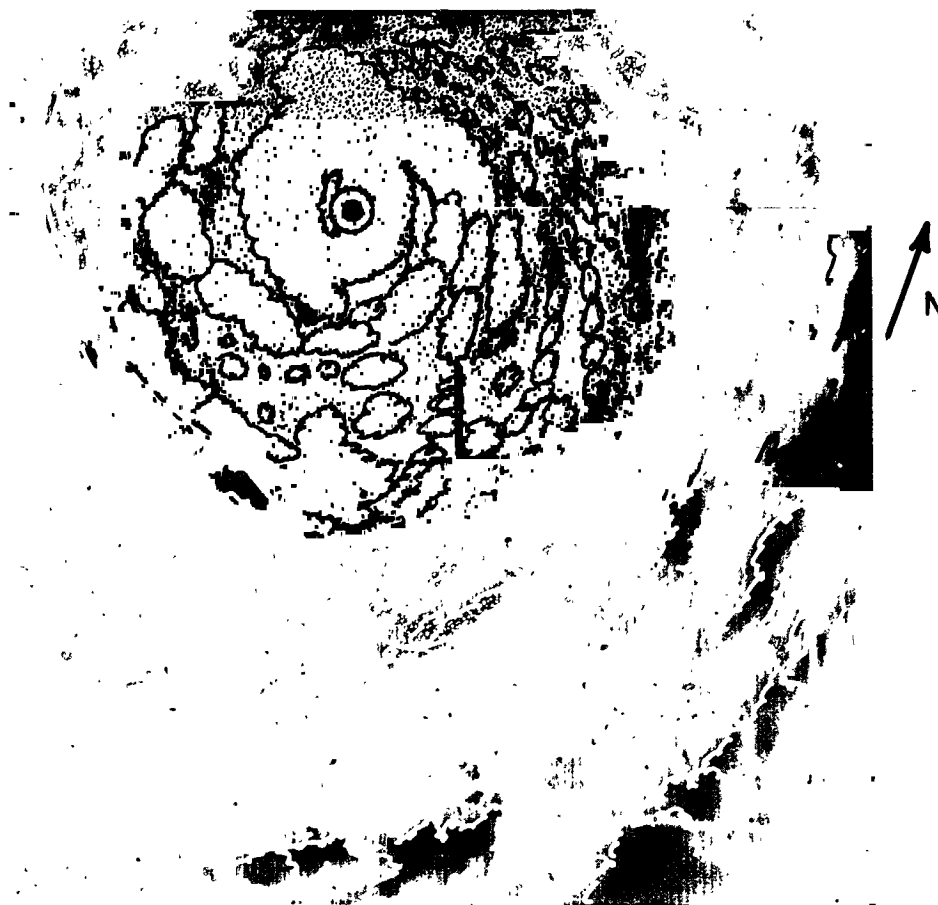





FIG. 9

SCALE: 1 in.  $\approx$  160 nm near mid-frame

- TYPHOON CENTER -- "eye"
- WALL CLOUD SURROUNDING EYE
-  CIRRUS SHIELD PARTIALLY OBSCURING UNDERLYING ORGANIZED BANDS OF TOWERING CUMULUS AND CUMULONIMBUS
-  BANDS OR ARMS OF TOWERING CUMULUS
-  AREA OF SMALL INDIVIDUAL CUMULUS (Cell Size 5-20nm)

(a) Unprocessed TIROS original

(b) Significant meteorological features of Fig. 9(a)

## FIG. 10 SECONDARY CYCLONIC CIRCULATIONS

This photograph [Fig. 10 (a)] shows two well-defined secondary cloud vortex patterns along the western periphery of a major cyclonic circulation. Frontal and vortex clouds from the major low [Fig. 10 (b)] are seen as the fairly solid cloud sheet near the horizon. Although these secondary vortex patterns or "eddies" bear some resemblance to larger circulations, they are, in actuality fairly small and are embedded in the flow of cool air from the northwest behind the principle cloud vortex associated with the major low.

The main significance of such secondary systems is that frequently, they develop into full-fledged storms with little advance warning from the analysis bases on the synoptic network reports. This is especially true in the area of the photograph, some 400 miles southeast of the Kamchatka Peninsula, an edge of which is visible on the northern tip of the frame. Surface temperatures as low as  $-26^{\circ}\text{F}$  are reported over this land mass, consequently there is a plentiful supply of cold air to be pushed seaward by the northerly surface winds. Cloudiness of a cumuliform and cellular appearance extends over most of the post frontal area suggesting that the cool air is becoming unstable due to its being heated by the warmer ocean surface. A small clear area just offshore can be seen along the coast. Here, the cold continental air has not yet picked up enough moisture in the lower levels for cumulus to form. Within the cumuliform clouds in the post frontal area, small cells are located along the northern or cold side of the jet stream. Apparently enough downward motion is taking place to suppress the vertical development of the cumuliform cells. Several areas in the photograph appear nearly cloudfree; here, both subsidence and low-level divergence act to prevent cloud development.

All cloud features and patterns are retained with good fidelity by the peripheral cancellation process [upper photo Fig. 10 (c)]. There is some loss of cloud amount due to the heightened black-and-white contrast absorbing the dark grey cloud. This is particularly roticeable in the upper right of the frame. Another apparent effect is the near elimination of some link spaces between clouds at the extreme lower left of the frame. These resulting effects, however, do not interfere greatly in the recognition and determination of features having meteorological significance. There is no pronounced rectilinear appearance to the individual cloud elements, as seen in some previous cases. The changing texture and grey scale throughout the original frame has been especially well preserved.

PERIPHERAL  
CANCELLATION  
METHOD



CONVENTIONAL  
AVERAGING  
METHOD



(c) Bandwidth reduced 9:1

TIROS VIII ORBIT 1088/1083T, FRAME 19 0304GMT 5 MARCH 1964

WIDE ANGLE LENS



FIG. 10

SCALE: 1 in.  $\approx$  160 nm near mid-frame

(a) Unprocessed TIROS original



TIROS VIII ORBIT 1088/1083T, FRAME 19 0304GMT 5 MARCH 1964

WIDE ANGLE LENS



FIG. 10

SCALE: 1 in.  $\approx$  160 nm near mid-frame

- VORTEX CENTER
- ▨ FRONTAL BAND (Upper and Middle Clouds)
- ☼ CUMULUS CLOUDS IN COLD AIR
- EDGE OF KAMCHATKA PENINSULA
- +— JET STREAM
- LOW LEVEL WIND FLOW
- ☾ OCCLUDED FRONT
- HORIZON

(a) Unprocessed TIROS original

(b) Significant meteorological features of Fig. 10(a)

## FIG. 11 SMALL-SCALE CYCLONE

This frame [Fig. 11(a)] shows a small-scale cyclonic vortex centered over the middle of the Caspian Sea. The vortex is entirely contained within the water area (about 150 miles wide) and its existence is not obvious from conventional land station reports despite the rather dense network around the sea area. Cloudiness in the vortex appears rather dense. However, there are striations that suggest cyclonic inflow around the center. In general, the appearance is similar to that of the vortex associated with tropical storms, except that the eye and wall cloud are missing.

An arm of cumuliform clouds extends to the northward from the vortex and a detached band of less dense clouds encircles the eastern edge of the vortex. Some detached cumulus cells are also present over the water surface. Cloudiness in the upper part of the frame reflects the remains of a weak cold front in that area.

The Caucasus Mountains [Fig. 11(b)], located on the west side of the frame, are snow-covered. Snow on mountains can be distinguished from cloud by the characteristic dendritic or lace-like appearance. Terrain throughout the area of the frame appears lighter than the water surface.

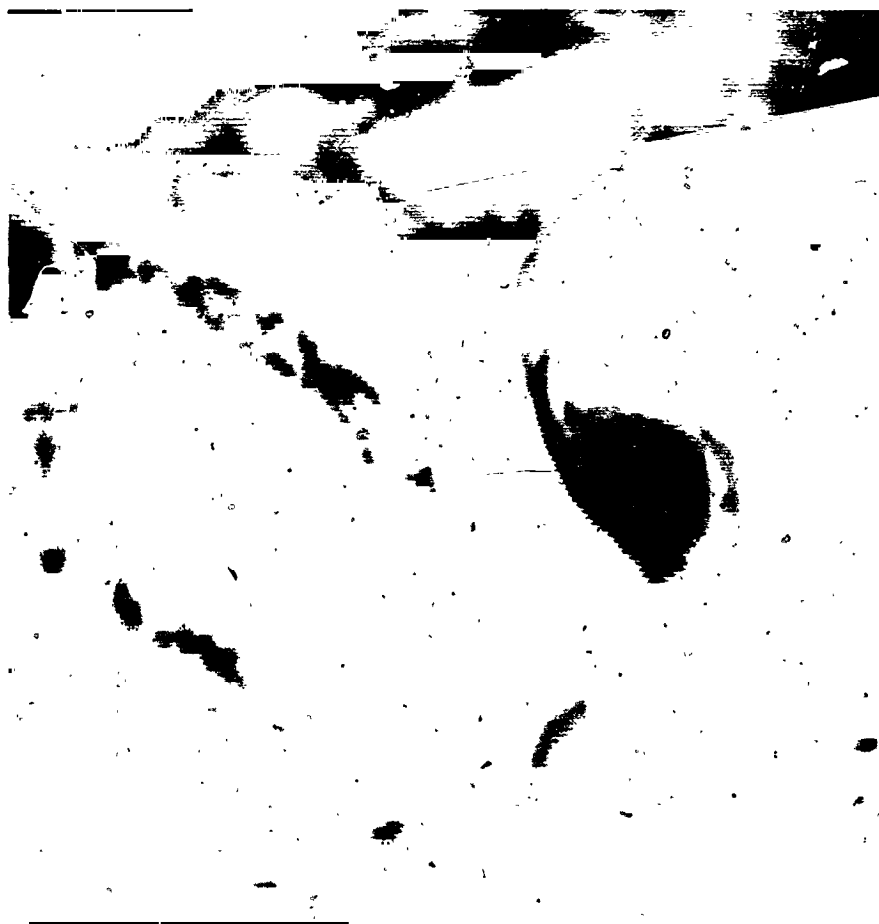
The importance of recognizing such secondary vortex systems is that, although they are fairly small in size, they can produce considerable weather, sometimes of a very violent nature and, because of their small size, frequently escape detection through barometric analysis based on conventional data.

All major features are retained by the peripheral cancellation process [upper photo Fig. 11(c)]. The depiction of terrain as well as contrast between water and land are especially well preserved. The cloud forms, in toto, are retained but the excessive black-and-white contrast or brightness obliterates the thin striations within the small cyclone that suggests the inherent rotational movement. Lack of these lines could lead to an interpretation of stratus cloud cover except that it is organized in a well defined circular shape rather than a spreading ill-defined amorphous type of boundary attendant upon stratus coverage or fog. The clouds in the upper portion of the frame are overbright and lack the wispy texture seen on the original. Snow cover on the Caucasus is preserved, although a rectilinear effect is present. The latter, however, is not so pronounced that it would lead to a misinterpretation for meteorological purposes.

PERIPHERAL  
CANCELLATION  
METHOD



CONVENTIONAL  
AVERAGING  
METHOD



(c) Bandwidth reduced 9:1

2

TIROS VII ORBIT 2278/2276T, FRAME 27 0924 GMT 20 NOVEMBER 1963

WIDE ANGLE LENS

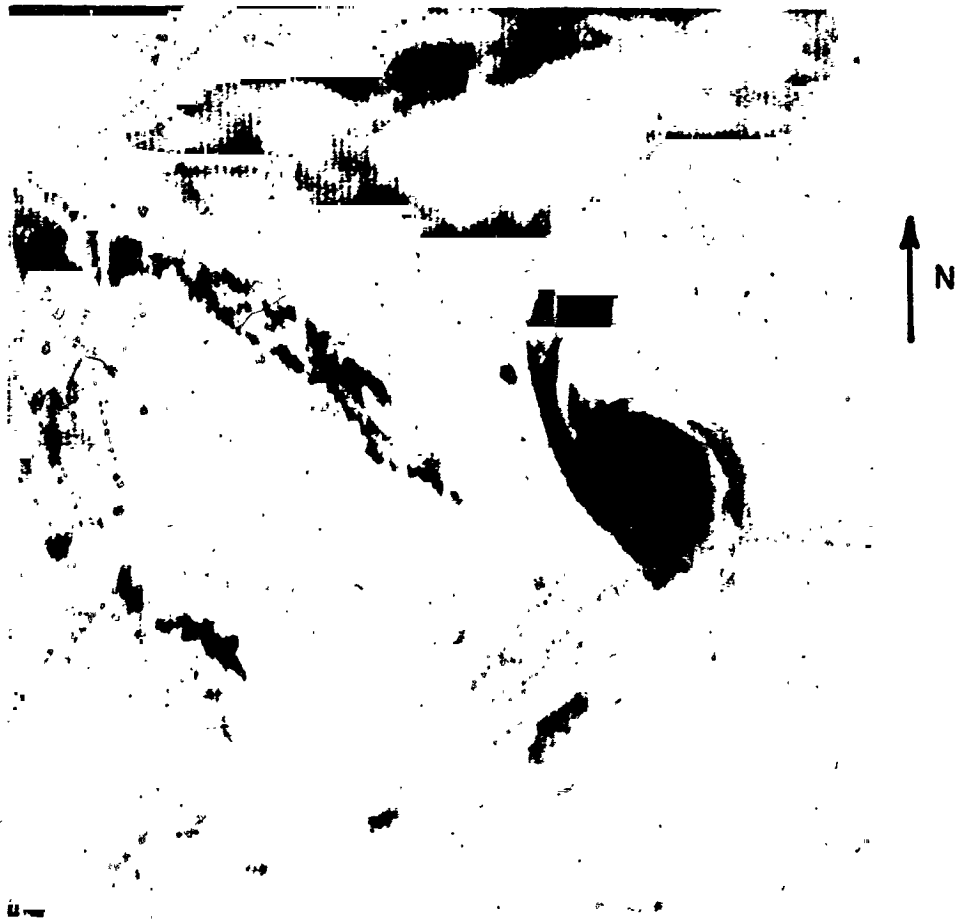


FIG. 11

SCALE: 1 in.  $\approx$  100 nm near mid-frame

(a) Unprocessed TIROS original

WIDE ANGLE LENS



FIG. 11

SCALE: 1 in.  $\approx$  100 nm near mid-frame

VORTEX CENTER



CLOUD VORTEX



SNOW COVER



CUMULUS CLOUD



COASTLINE OF CASPIAN SEA



FRONTAL BAND (Upper and Middle Clouds)

(a) Unprocessed TIROS original

(b) Significant meteorological features of Fig. 11(a)

## FIG. 12 CLOUDS COMPARED WITH ICE

This frame [Fig. 12(a)] views cloud cover over central Canada. Lake Winnipeg, most of Lake Winnipegosis, and Lake Manitoba [Fig. 12(b)] are visible, appearing as smooth, light-grey entities. This is due to the fact that in April the water surfaces in this area are frozen and, therefore, highly reflective. Each small island and bay is discernible. Two pronounced bands of cirrus streaks extend west to east across the upper part of the frame. Their appearance is somewhat greyer than the lake but whiter than the underlying terrain. Upper-level winds are aligned with the bands and striations.

Most of the clouds in the extreme upper left portion of the frame are associated with a cold front in this area and are reported as altocumulus with some high cirrus. The clouds in the lower part of the frame are part of a cloud system associated with a well-developed low to the south of the area encompassed by this frame. Cloudiness in the lower right sector appears uniform and fairly dense and consists of low clouds of bad weather (cumulus fractus), higher altocumulus and altostratus clouds along with rain and snow. In the lower left of the frame, the cloudiness appears broken and has a more lumpy appearance. Here, the cloudiness consists of broken stratocumulus with some overlying cirrus being present.

Some of the grey tone in and immediately adjacent to the center of the frame results from cloud cover composed of a thin sheet of altocumulus. However, the ice-covered lakes are still visible as white blobs through it, especially in the area east of Lake Winnipeg. Sufficient divergence is present in lower levels to keep the area relatively free of lower cloud forms.

Most of the patterns are retained by the peripheral cancellation process [upper photo Fig. 12(c)], though there is definite loss of detail or texture in small-scale or fibrous elements. In general, the black-and-white contrast has been heightened over that of the original.

The major ice-covered lake (upper right of center) is reproduced satisfactorily. The shoreline and cirrus cloud in the upper portion of the lake is retained especially well. The shoreline on the lower portion has a pronounced rectilinear edging. The smaller lakes (lower left of center) are not as well reproduced because of their small size.

The cirrus bands in the upper half of the frame retain their filmy texture, though the small lakes visible through the cirrus (upper right) are obscured in the processed frame. Stratocumulus elements (lower left) are retained, though the excessive brightness might lead to an interpretation of cumulus. The frontal clouds (lower right) are much too bright. They appear dense and without texture as compared to the original. Small cumulus (center far right) are obscured and not recognizable.

PERIPHERAL  
CANCELLATION  
METHOD



CONVENTIONAL  
AVERAGING  
METHOD



(c) Bandwidth reduced 9:1

TIROS VII ORBIT 4307/4306T<sub>2</sub> FRAME 16 1640GMT 5 APRIL 1964

WIDE ANGLE LENS



FIG. 12

SCALE: 1 in.  $\approx$  130 nm near mid-frame

(a) Unprocessed TIROS original



TIROS VII ORBIT 4307/4306T<sub>2</sub> FRAME 16 1640GMT 5 APRIL 1964

WIDE ANGLE LENS

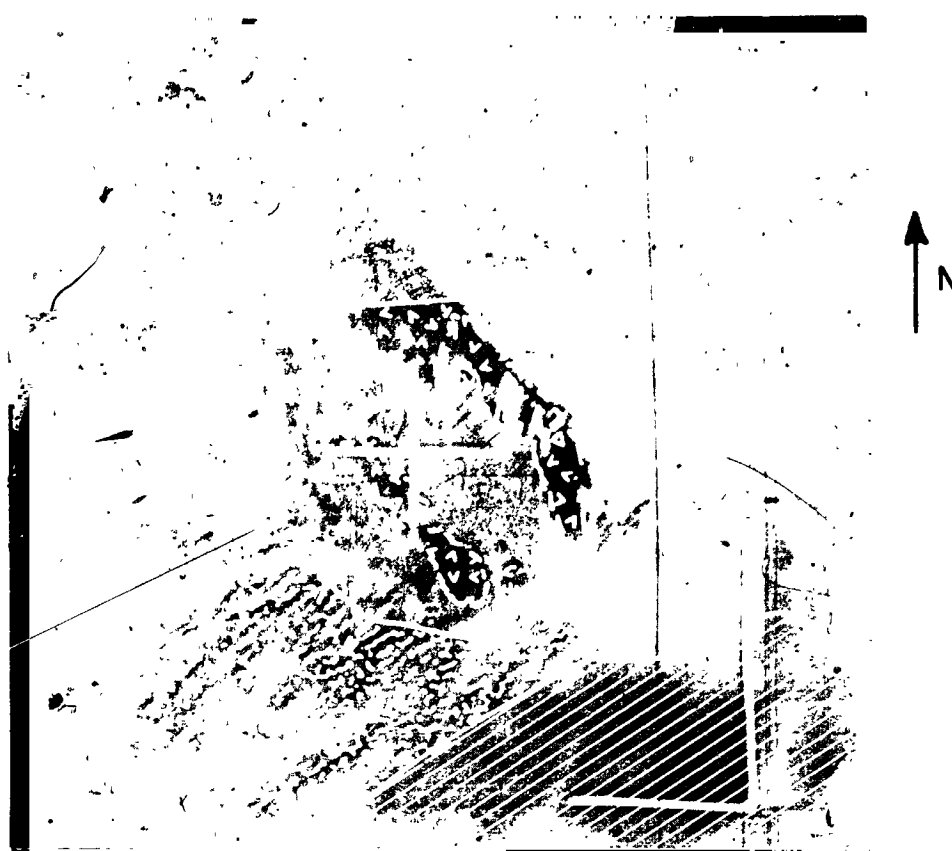









FIG. 12

SCALE: 1 in.  $\approx$  130 nm near mid-frame

-  **FRONTAL BAND (Upper and Middle Clouds)**
-  **CIRRUS BAND**
-  **ICE COVERED LAKES**
-  **STRATOCUMULUS**
-  **UPPER LEVEL WIND FLOW**
-  **COLD FRONT**
-  **LOW LEVEL WIND FLOW**

(a) Unprocessed TIROS original

(b) Significant meteorological features of Fig. 12(a)

### FIG. 13 FRONTAL BAND - SNOW-COVERED MOUNTAINS

This frame [Fig. 13(a)] views an area of British Columbia and the Pacific Ocean immediately adjacent. Parts of Queen Charlotte Islands are visible as small light grey areas near the center of the photo, see Fig. 13(b). The northern tip of Vancouver Island is barely discernible near the southern part of the frame, just off shore from the mountainous area. The marked dendritic appearance of the pattern on the right of the frame indicates snow cover on the Coastal Mountains. Water inlets, rivers, and valleys appear as fairly dark areas against the white background. The mountains and ocean area for some distance offshore are almost entirely cloud-free, indicating the extent to which the offshore winds have circulated the dry continental air to the seaward.

Most of the cloudiness appearing on the left side of the frame is associated with an occluded front. The texture of the cloudiness on each side of the frontal band appears thin, fibrous, and striated. These are altostratus and altocumulus clouds accompanied by higher cirrus clouds. Striations in such clouds are usually aligned with the winds at cloud level, which in this case are from the south.

In the far upper left of the frame, the cloudiness appears more cumuliform and cellular, typical of low stratocumulus or small cumulus in the immediate post-frontal area.

Retention of major features and patterns is good by the peripheral cancellation process [upper photo Fig. 13(c)]. Black-and-white contrast is stronger than in the original but does not interfere with the recognition and interpretation of significant elements.

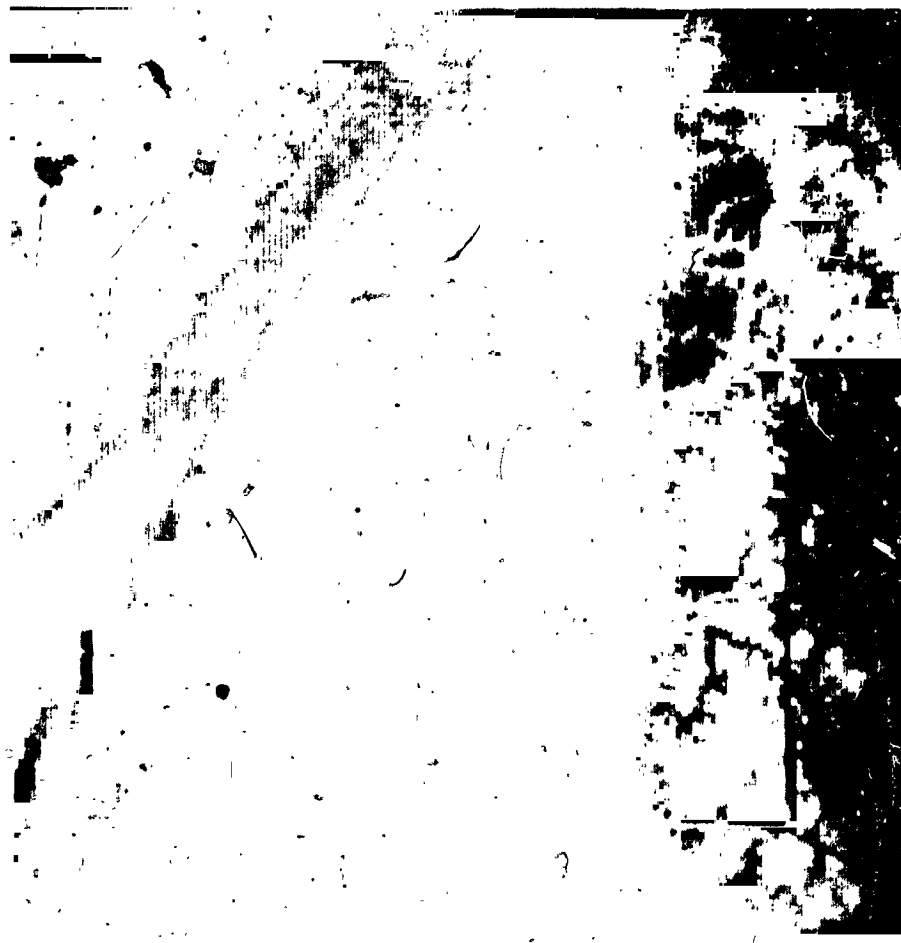
The snow pattern (far right) is well reproduced but a rectilinear effect becomes a bit too prominent in the far upper right. As a result of the heightened black-and-white contrast, the dark grey appearing islands in the center of the frame have been obscured, or, in the case of Vancouver Island, obliterated.

The frontal and high clouds on the left of the frame are retained. There is loss of texture at the lower left due to excessive contrast and small clouds in the far upper left have been obscured.

The pattern alterations are such that more likely it might lead to under-interpretation of the cloud patterns rather than misinterpretation.

/

PERIPHERAL  
CANCELLATION  
METHOD



CONVENTIONAL  
AVERAGING  
METHOD



(c) Bandwidth reduced 9:1

TIROS VII ORBIT 4323/4322T<sub>2</sub> FRAME 9 1835GMT 6 APRIL 1964

WIDE ANGLE LENS



FIG. 13

SCALE: 1 in.  $\approx$  150 nm near mid-frame

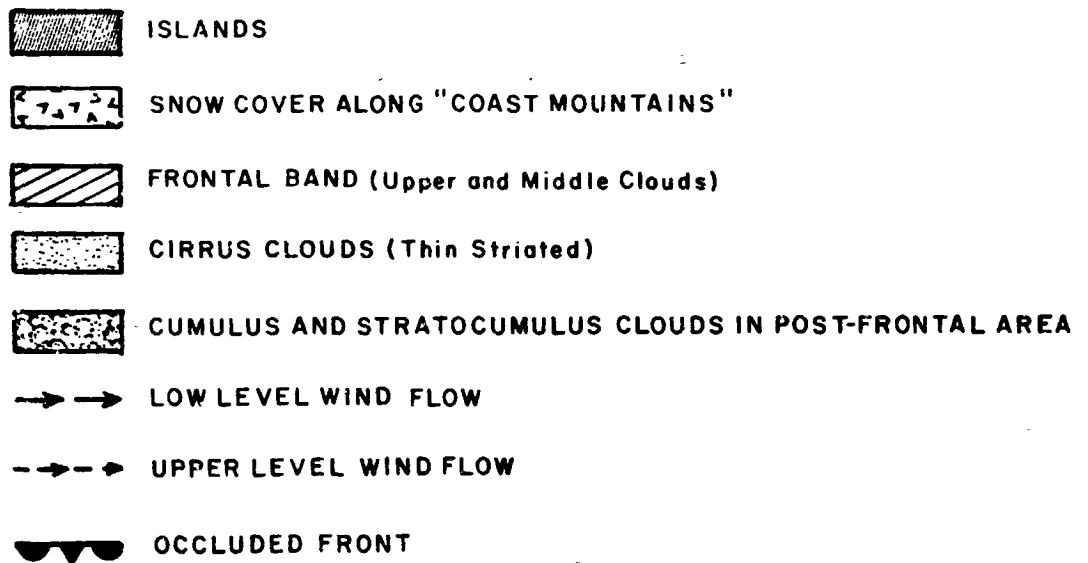
(a) Unprocessed TIROS original

WIDE ANGLE LENS



FIG. 13

SCALE: 1 in.  $\approx$  150 nm near mid-frame



(a) Unprocessed TIROS original

(b) Significant meteorological features of Fig. 13(a)

#### FIG. 14 FRONTAL SYSTEM A

This photograph [Fig. 14(a)] shows a broad curving frontal cloud mass associated with a well-developed cold front. The frame of view extends over the Great Lakes, New York and southeast Ontario. Lake Michigan is outlined on the overlay [Fig. 14(b)] but only sections of the shoreline are visible.

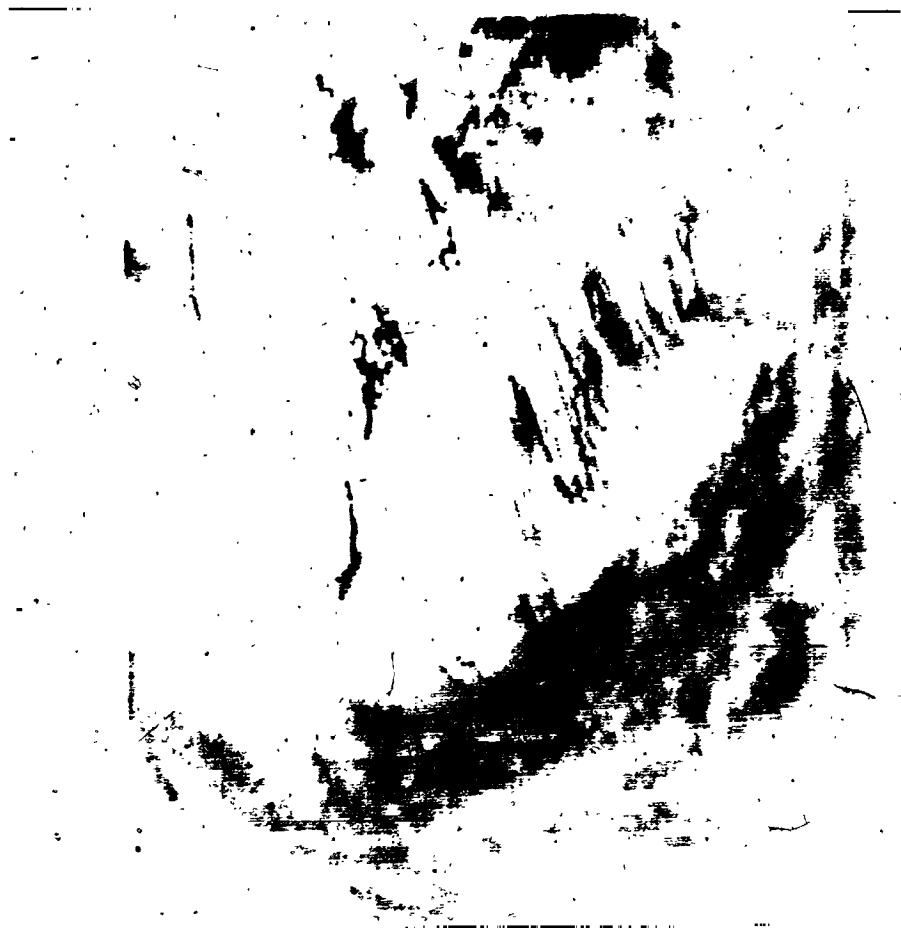
The low-pressure system from which the frontal arm originates is off the northeast corner of the frame and therefore not visible. Cloudiness along the frontal band is reported as stratocumulus, cumulus fractus of bad weather, and altocumulus typical of active frontal systems. The extensive area of the frontal clouds, along with the solid appearance of the cloud forms, are indications of strong frontal intensity.

The clearing north of the front results from the intrusion of colder air, associated with a well-developed high cell moving over the post-frontal region. Surface temperatures of ( $40^{\circ}\text{F}$ ) are reported in the cold air as compared to temperatures of ( $60^{\circ}\text{F}$ ) along the front itself. Most of the cloudiness over the postfrontal region is reported as stratocumulus clouds. The cloudiness over Lake Michigan is confined mostly to the eastern side of the lake indicating that the low cumuliform clouds that have developed over the lake due to heating are being drifted by a westerly kind. Over the Great Lakes farther east, the clouds indicate a wind from the northwest. Note that cell size is smallest to the north where the cumulus first develop and grow in size toward as they pick up moisture and increase in vertical development. A few altocumulus appear as the faint streaks aligned parallel to the upper wind. Some 20 miles behind the trailing edge of the frontal shield the cloudiness diminishes suggesting subsidence in the lower levels.

Most of the cloudiness to the south of the frontal band appears less dense. Cumulus clouds are visible, however. Some upper clouds are also present which tend to obscure the lower cloud forms.

The reproduction of this frame is exceedingly good by the peripheral cancellation method [upper photo Fig. 14(c)]. This may be due to the fact that, to begin with, the majority of cloud elements are on the bright end of the grey scale. The frontal band of upper and middle clouds retains its texture and detail despite a slight increase in the black-and-white contrast. Effects of the heightened contrast are apparent in the postfrontal area (upper right of center) where the very small scale, dark-grey cumulus elements have been obscured. This, however, is minor and would not interfere with the proper interpretation of the pattern. There is no major alteration of cloud character, texture or pattern.

PERIPHERAL  
CANCELLATION  
METHOD



CONVENTIONAL  
AVERAGING  
METHOD



(c) Bandwidth reduced 9:1

TIROSV ORBIT III9D, FRAME 6 1400GMT 5 SEPTEMBER 1962

WIDE ANGLE LENS



FIG. 14

SCALE: 1 in.  $\approx$  180 nm near mid-frame

(a) Unprocessed TIROS original



TIROSV ORBIT 1119D, FRAME 6 1400GMT 5 SEPTEMBER 1962

WIDE ANGLE LENS



FIG. 14

SCALE: 1 in. = 180 nm near mid-frame

H HIGH CELL



FRONTAL BAND (Upper and Middle Clouds)



CUMULIFORM CLOUDS



ALTOCUMULUS BANDS



LOW LEVEL WIND FLOW



UPPER LEVEL WIND FLOW



COLD FRONT



SHORELINE OF LAKE MICHIGAN

(a) Unprocessed TIROS original

(b) Significant meteorological features of Fig. 14(a)

## FIG. 15 FRONTAL SYSTEM B

This photograph [Fig. 15(a)] is a frame adjacent to the one shown in Fig. 14(a). It extends the view toward the northeast showing more of the cold frontal system and the cloud arm around the surface low located just north of Moosonee. Most of the low-level cumulus cloud streets in the post-frontal region are still visible although some have been lost due to the higher angle of view. The upper winds as shown on the overlay [Fig. 15(b)] cross these streets at a considerable angle as do the thin bands of altocumulus clouds, indicating that the upper wind flow is quite different from that at lower levels. The black streak through the center of the frame is interpreted as a cloud shadow cast on the lower cloudform by upper cirrus clouds. However, this is not conclusive, since it quite closely parallels the coastline on the eastern shore of James Bay. In any event, similar appearing rifts identified as shadows from bands of cirrus clouds in association with jet streams have been observed on other satellite photographs. They are of meteorological importance since they give evidence as to the location and orientation of strong jet stream winds.

Temperature soundings and wind aloft data are given as supplementary information and shows the large temperature differences at low levels between the warm air in the frontal zone and the cold air in the post frontal area. In addition, they show dramatically the difference in wind directions and speeds with altitude which match the attendant changes in cloud alignment, especially in the post frontal cold air. Flint, Moosonee, and Sault St. Marie all show northwest winds in the lower levels with strong westerly to southerly winds aloft. In general, the soundings within the frontal band show that cloudiness extends to high altitudes, whereas, within the cold post frontal air, cloud forms are present in only the very lowest levels.

The pattern retention by the peripheral cancellation process [upper photo Fig. 15(c)] is good but there is definite loss of texture, which could interfere to an extent with interpretation. The predominant loss of detail and texture occurs in the frontal band. Excessive black-and-white contrast results in a hard, dense and opaque appearance to the band, particularly in the lower portion, which could interfere with the proper interpretation of cloud type and atmospheric stability. Also, there is an induced "rectilinear effect" prominent in the clouds on the far right of the frame.

PERIPHERAL  
CANCELLATION  
METHOD



CONVENTIONAL  
AVERAGING  
METHOD



(c) Bandwidth reduced 9:1

TIROS V ORBIT III9D, FRAME 9 1400GMT 5 SEPTEMBER 1962  
WIDE ANGLE LENS

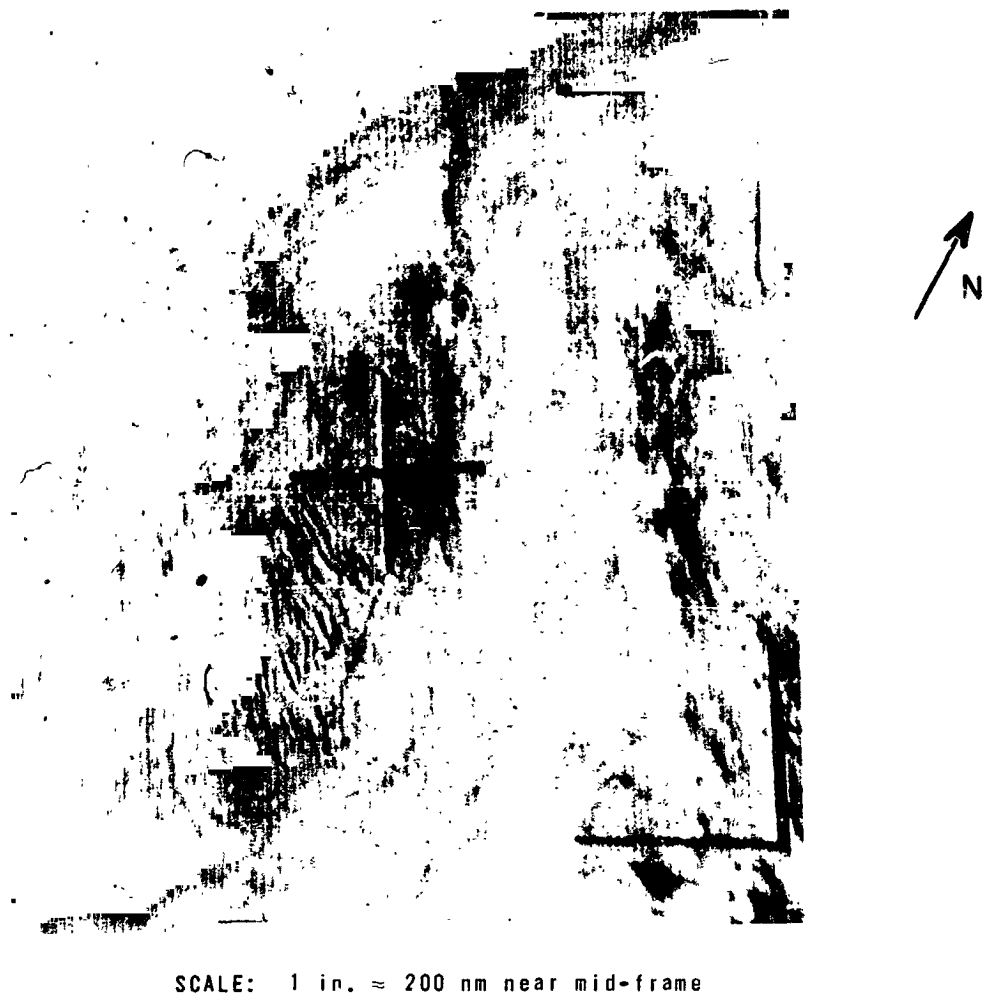


FIG. 15

(a) Unprocessed TIROS original

TIROS V ORBIT III9D, FRAME 9 1400GMT 5 SEPTEMBER 1962

WIDE ANGLE LENS

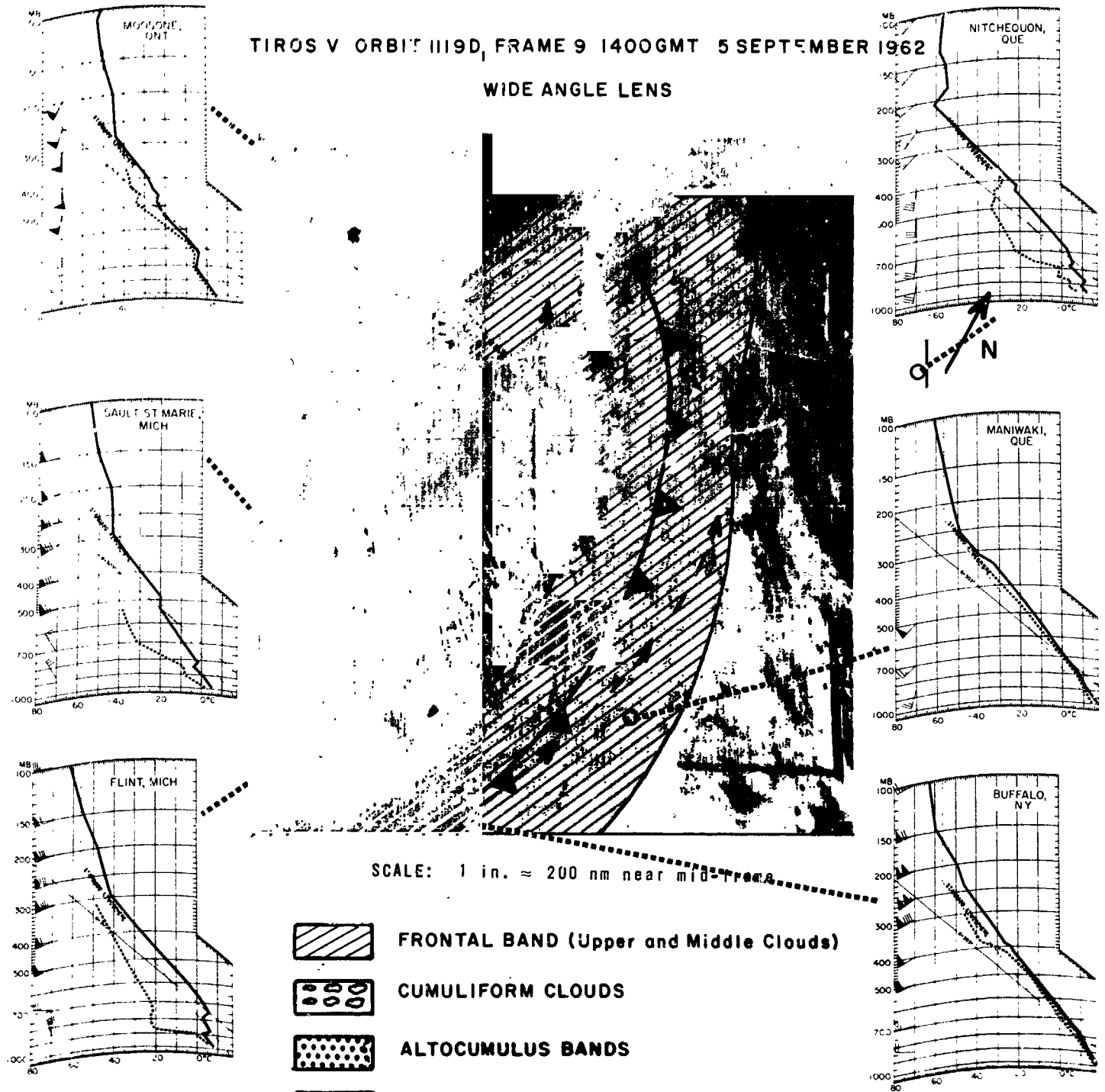


FIG. 15

RADIOSONDE  
LEGEND

(a) Unprocessed TIROS original

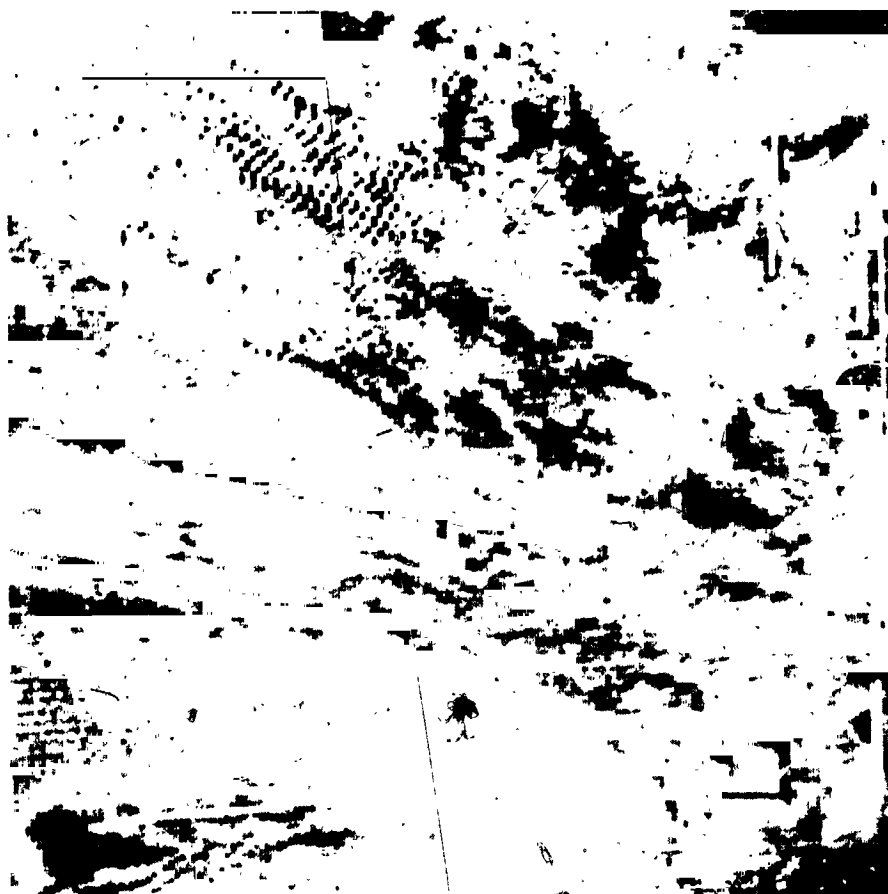
(b) Significant meteorological features of Fig. 15(a)

FIG. 16 LEE WAVE CLOUDS

This frame [Fig. 16(a)] presents a view of the cloud cover over southwest Australia. Visible in the upper left of the photograph is a system of lee wave clouds located downwind from the Kimberly Range (off the extreme upper left corner of the frame). Cloudform is identified as stratocumulus over the northern half of the frame. Lee waves are forming within this cloudform and appear as the parallel banded rows outlined on the overlay. The direction of the wind flow [Fig. 16(b)] is perpendicular to these transverse waves and observations show that the wind speed increases rapidly above the cloud level. A small portion of the southwest coast of Australia is visible in the lower portion of the frame. The band of cloudiness extending across the frame and crossing the coastline is believed to be associated with a weak cold front that appears to be curving southward off the lower right hand portion of the frame.

The overall pattern retention by the peripheral cancellation process [upper photo Fig. 16(c)] is considered good. The principal degradation in quality occurs as a result of heightened black-and-white contrast and induced scanning effects. The heightened contrast results in some loss of dark grey elements on the originals--note loss of coastline at bottom center of frame and small cumulus clouds scattered throughout the frame. The heightened contrast also results in some textural loss to clouds, particularly noticeable in the merging of cloud elements within the major cloud band just below the center of the frame. Processing induces rectilinear patterns that are noticeable in the upper portion of the frame. The principal result is the merging of small cloud and diffusion of the edges. It does not interfere greatly with the proper interpretation, especially, of the lee wave cloud.

PERIPHERAL  
CANCELLATION  
METHOD



CONVENTIONAL  
AVERAGING  
METHOD



(c) Bandwidth reduced 9:1

TIROS IV ORBIT 570/569T<sub>2</sub> FRAME 16 0515GMT 20 MARCH 1962

MEDIUM ANGLE LENS



FIG. 16

SCALE: 1 in.  $\approx$  120 nm near mid-frame

(a) Unprocessed TIROS original



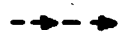




TIROS IV ORBIT 570/569T<sub>2</sub> FRAME 16 0515GMT 20 MARCH 1962  
MEDIUM ANGLE LENS



FIG. 15

SCALE: 1 in.  $\approx$  120 nm near mid-frame

-  LEE WAVE CLOUDS (Stratocumulus)
-  FRONTAL BAND (Altostratus and Altopumulus)
-  UPPER LEVEL WIND FLOW
-  LOW LEVEL WIND FLOW
-  VISIBLE COASTLINE

- (a) Unprocessed TIROS original
- (b) Significant meteorological features of Fig. 16(a)

## FIG. 17 CIRRUS CLOUDS

This frame [Fig. 17(a)] views a cirrus band over the northwest coast of Africa. Cape Blanc, as well as other coastal irregularities are readily distinguishable, see Fig. 17(b). The cirrus cloudiness appears partially as striations, but mostly as transverse waves, i.e., perpendicular to the flow. At best, cirrus clouds are somewhat hard to see on satellite photographs because of their thin filmy appearance and this is especially true when the underlying surface is highly reflective, such as lower clouds, snow or light colored terrain. In this photograph the light colored sand and soils are highly reflective and, although the cirrus is clearly visible over water, it is not seen in such fine detail over land. However, shadows cast upon the lighter soils from the more dense parts of the cirrus bands and striations indicate that the cirrus extends inland to considerable distances.

The wave-like patterns that frequently occur in cirrus clouds can be used to delineate jet streams and wind directions. Bundgaard has shown that transverse waves in cirrus are associated with small wind shears in the vertical; elongated waves or striations are parallel to the general wind flow with large shear values. In the case illustrated both types of cloud form are evident highlighting the rapid change of shear over a limited distance. Upper winds at cirrus level were of jet-stream speeds.

Although oscillations can be present without sufficient moisture to form characteristic high-level clouds, such cloudiness (waves and striations) when photographed is proof that oscillations are present, as well as the conditions necessary for their occurrence. Aircraft traverses have shown that such areas of transverse waves have been known to contain considerable turbulence.

The pattern retention by the peripheral cancellation process [upper photo Fig. 17(c)] is considered fair. In general, the texture and pattern detail of the cirrus cloud is preserved. Because of the heightened black-and-white contrast, the dark grey cirrus over the ocean (left of frame) is virtually obliterated. Over the land, there is darkening in the upper and lower right of the frame. Over the water, the loss of dark grey elements would result in an underestimation of cloud distribution. Over land the darkening could imply a change in terrain cover or presence of lakes, etc., which could lead to a misinterpretation of the facts. The cirrus band is reproduced to a degree that misinterpretation is not likely.

PERIPHERAL  
CANCELLATION  
METHOD



CONVENTIONAL  
AVERAGING  
METHOD



(c) Bandwidth reduced 9:1

TIROS VII ORBIT 3462/3461T, FRAME 12 1315GMT 8 FEBRUARY 1964

WIDE ANGLE LENS



FIG. 17

SCALE: 1 in. = 100 nm near mid-frame

(a) Unprocessed TIROS original

WIDE ANGLE LENS



FIG. 17

SCALE: 1 in.  $\approx$  100 nm near mid-frame



TRANSVERSE WAVES IN CIRRUS CLOUDS



LONGITUDINAL WAVES (Striations) IN CIRRUS CLOUDS



UPPER LEVEL WIND FLOW

A

CAP BLANC



COASTLINE

(a) Unprocessed TIROS original

(b) Significant meteorological features of Fig. 17(a)

## FIG. 18 CELLULAR PATTERNS — ICE AND SNOW

This photograph [Fig. 18(a)] shows the patterning of cumuliform clouds in Davis Strait and Labrador Sea between Newfoundland and Greenland. The interior of Greenland, being snow covered, appears as a featureless white sheet. Its rough coastline with numerous bays and inlets shows up clearly, see Fig. 18(b). Davis Strait is ice covered.

Cold continental air ( $-5^{\circ}\text{F}$  at the surface) is flowing from the arctic interior, across Davis Strait, to the southeast over warm water. Immediately offshore the sky is generally cloudfree. Soon, however, cumuliform clouds develop and become organized into cloud streets aligned with the low-level winds.

Farther offshore, the cells get progressively larger as the air is warmed to greater depths. From the appearance of the cellular structure near the southern edge of the frame, it would be judged that clouds have reached the stage where upper clouds from the cell tops are spreading out to partially obscure the cellular forms.

An anti-cyclonic circulation is present just to the left of frame center. The cloud patterning in this area tends to conform to the anticyclonic circulation shown by the low-level winds. Although high cells are often totally free of clouds due to subsidence, here the contrast in air and water temperature is so great that the subsidence present is not sufficient to overcome the instability produced.

The pattern and textural characteristics within the frame are fairly well-reproduced by the peripheral cancellation process [upper photo Fig. 18(c)]. The coastline of Greenland (upper right) is distinct as are the rows of cumulus just offshore. The pack ice in the far upper left remains as in the original, although much brighter. This heightened black-and-white contrast is also apparent in the clouds at the extreme lower right, in which the contrast tends to merge some of the cloud elements. A noticeable pattern change is apparent in the scattered clouds in the lower left of center where processing has introduced a rectilinear patterning to the cloud, which could possibly interfere with the proper identification of cloud type and cloud alignment.

PERIPHERAL  
CANCELLATION  
METHOD



CONVENTIONAL  
AVERAGING  
METHOD



(c) Bandwidth reduced 9:1

WIDE ANGLE LENS



FIG. 18

SCALE: 1 in.  $\approx$  150 nm near mid-frame

(a) Unprocessed TIROS original



WIDE ANGLE LENS

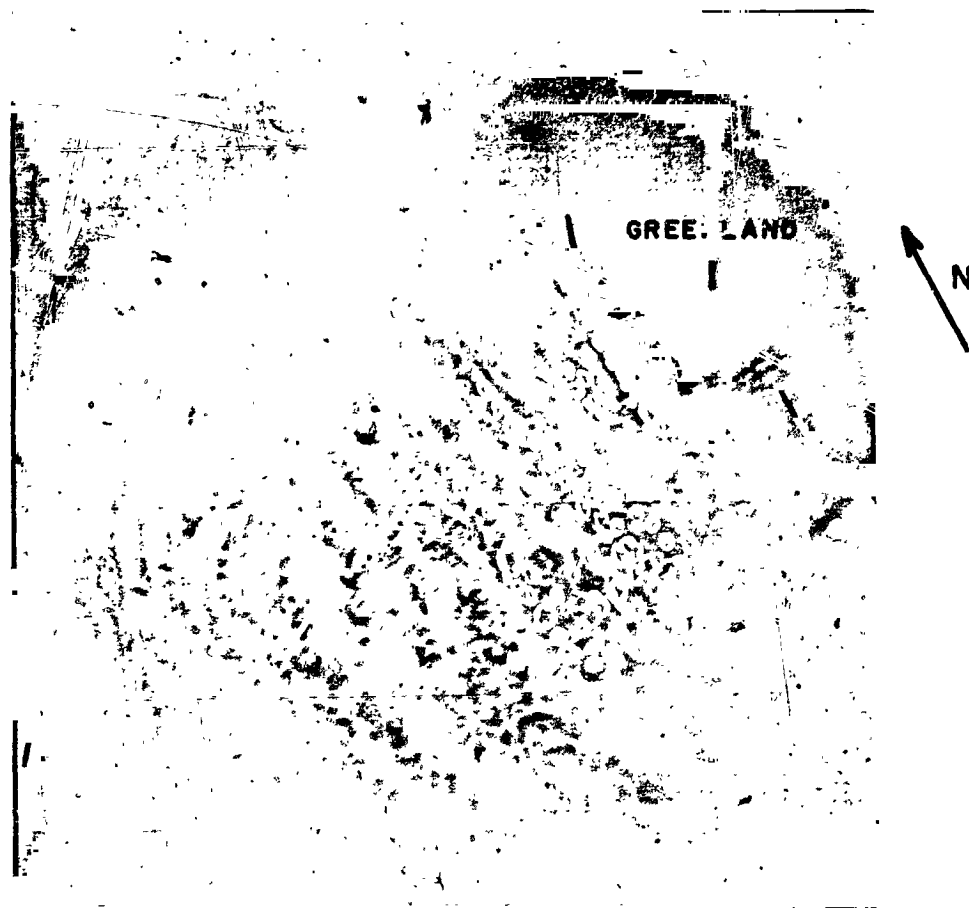







FIG. 18

SCALE: 1 in.  $\approx$  150 nm near mid-frame

-  CLOUD-FREE AREA ALONG COASTLINE OR ICELINE
-  CUMULUS CLOUDS
-  CIRRUS CLOUDS
-  LOW LEVEL WIND FLOW
-  COASTLINE OR ICELINE
- H** HIGH CELL

(a) Unprocessed TIROS original

(b) Significant meteorological features of Fig. 18(a)

FIG. 19 COASTAL STRATUS

This frame [Fig. 19(a)] views an area along the Northern California Coast. The terrain shows up fairly black with practically no variation in the grey scale. Scattered cumulus and stratocumulus over the land area are visible as the white blobs or patches (upper right of frame), see Fig. 19(b). Considerable cloudiness seen as the mottled and striated whiteness at lower left of frame, extends over the ocean area. The edge of the cloudiness extends several miles inland of the coastline, covering identifying coastal features. Out to sea the cloud cover transforms from a smooth, featureless appearance (identified as stratus along the coast), to a lumpy, cellular appearance (identified as stratocumulus). The area of more uniform cloudiness seen at the bottom of the frame is identified as altostratus clouds on the northward edge of a small vortex centered further to the southward.

Satellite photographs, in some areas such as this, can give indirect clues as to wind conditions. For example, when north-northwest winds prevail off the coast of California, they give rise to upwelling water from depths up to 200 meters which results in a fairly low surface water temperature. This maintains a fairly dense stratus cover along the immediate coast. Farther offshore, where no upwelling is occurring, sea surface temperatures are somewhat warmer. This is immediately reflected in the type of low cloud cover (stratocumulus).

The uniform cloud cover at the bottom of the frame is somewhat striated or banded. These striations or bands are aligned with the easterly circulation that would be present on the northern periphery of the cyclonic circulation.

The pattern retention for this example is considered good. Some loss of cloud amount is noted due to increased black-and-white contrast absorbing some of the dark grey elements into black. This is apparent in the cumulus coverage over land (upper right of frame), particularly along the edges, but not exclusively so. Due to processing procedures, there is a definite rectilinear pattern impressed on the clouds. Neither of these effects just discussed would interfere seriously with the proper interpretation of cloud types, but there might be some underestimation of cloud coverage.

Over the ocean (lower left of frame) the cellular structure is preserved by the peripheral cancellation process [Fig. 19(c)] as is the sheet-like character of the clouds along the coast and at the bottom of the frame. Excessive contrast, however, has made the clouds too white and dense in several places (lower part of coast and at the very bottom of the frame). Grey-scale graduations, however, are preserved rather well.

PERIPHERAL  
CANCELLATION  
METHOD



CONVENTIONAL  
AVERAGING  
METHOD



(c) Bandwidth reduced 9:1

TIROS IV ORBIT 738/738T<sub>2</sub> FRAME 16 2235GMT 31MARCH 1962  
MEDIUM ANGLE LENS



FIG. 19

SCALE: 1 in.  $\approx$  125 nm near mid-frame

(a) Unprocessed TIROS original

MEDIUM ANGLE LENS

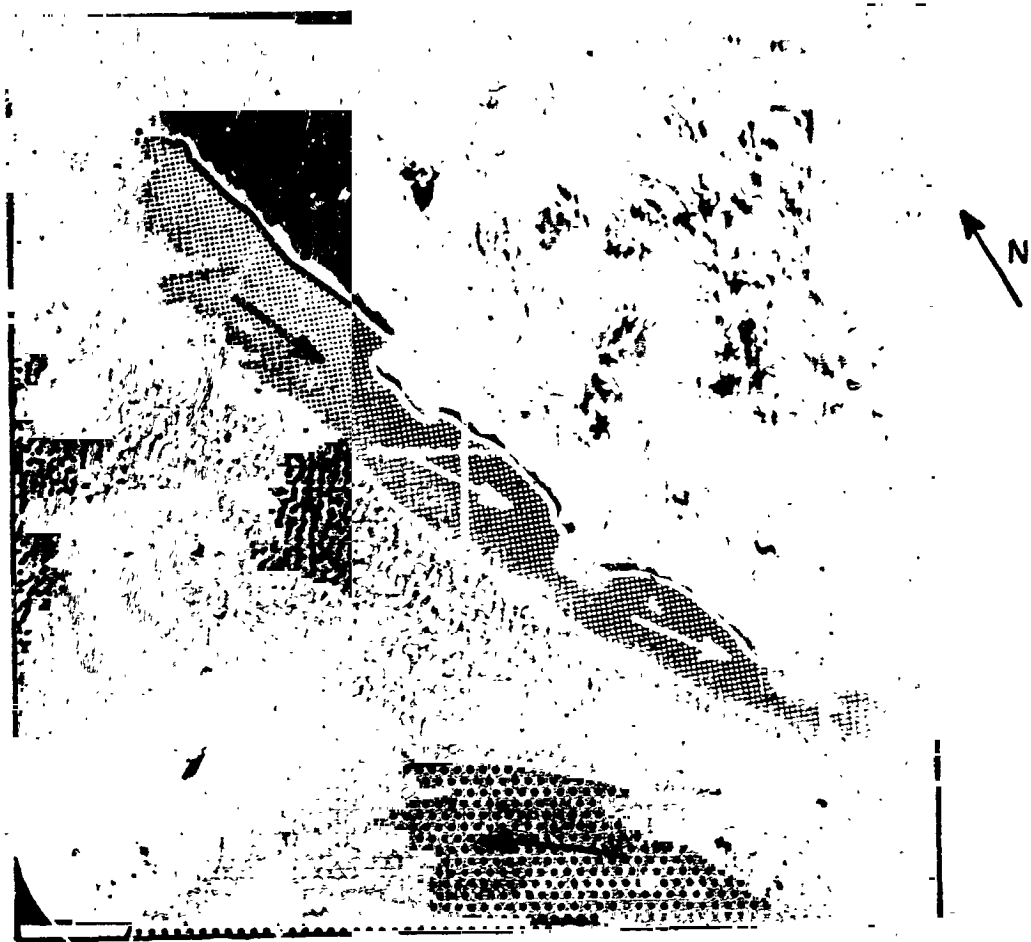


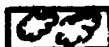

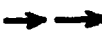


FIG. 10

SCALE: 1 in.  $\approx$  125 nm near mid-frame

-  COASTAL STRATUS
-  STRATOCUMULUS
-  TOWERING CUMULUS OVER LAND
-  ALTOSTRATUS (Edge of Small Vortex)
-  LOW LEVEL WIND FLOW

(a) Unprocessed TIROS original

(b) Significant meteorological features of Fig. 19(a)

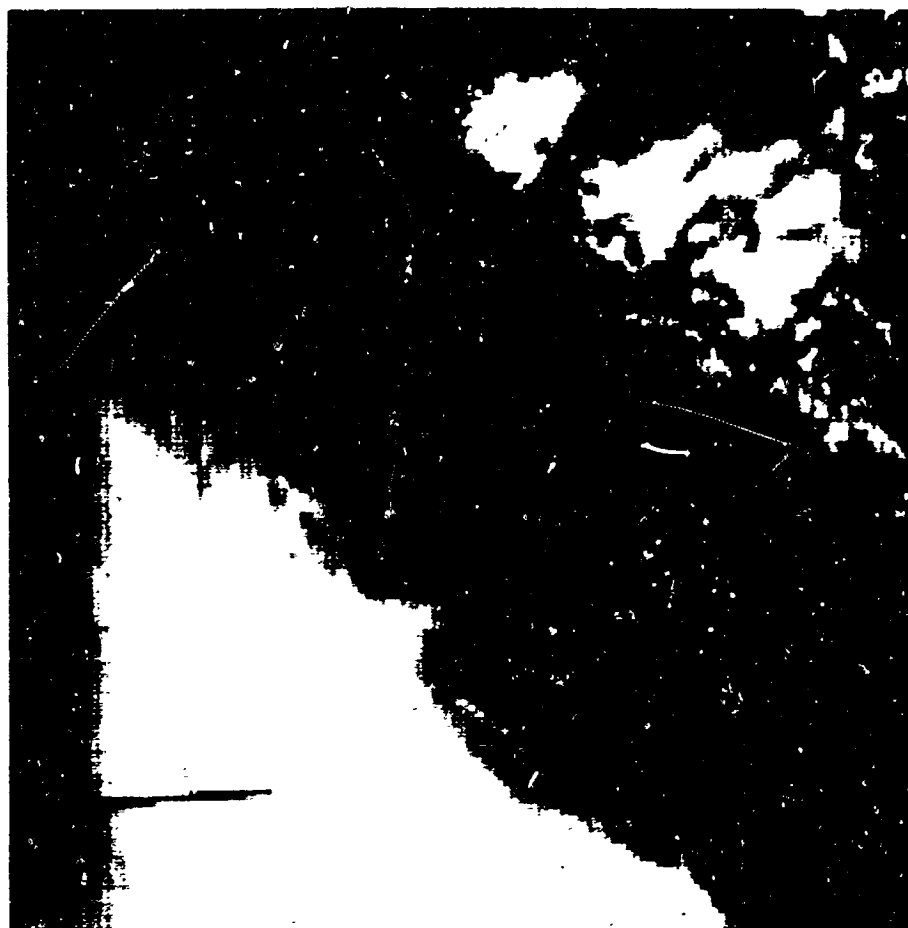
FIG. 20 CUMULONIMBUS WITH CIRRUS PLUMES

This photograph [Fig. 20(a)] presents a view of the Western United States and the Pacific Ocean off California. The broad white cloud mass in the lower left is ocean stratus lying along the California Coast, see Fig. 20(b). Although the stratus covers some of the coastal area, other sections are visible. Dry continental air covers the area inland from the coast and is characterized by the extensive cloud free area. The snow cover along the Sierra Nevada has the characteristic dendritic appearance, which generally makes it distinguishable from cloud cover.

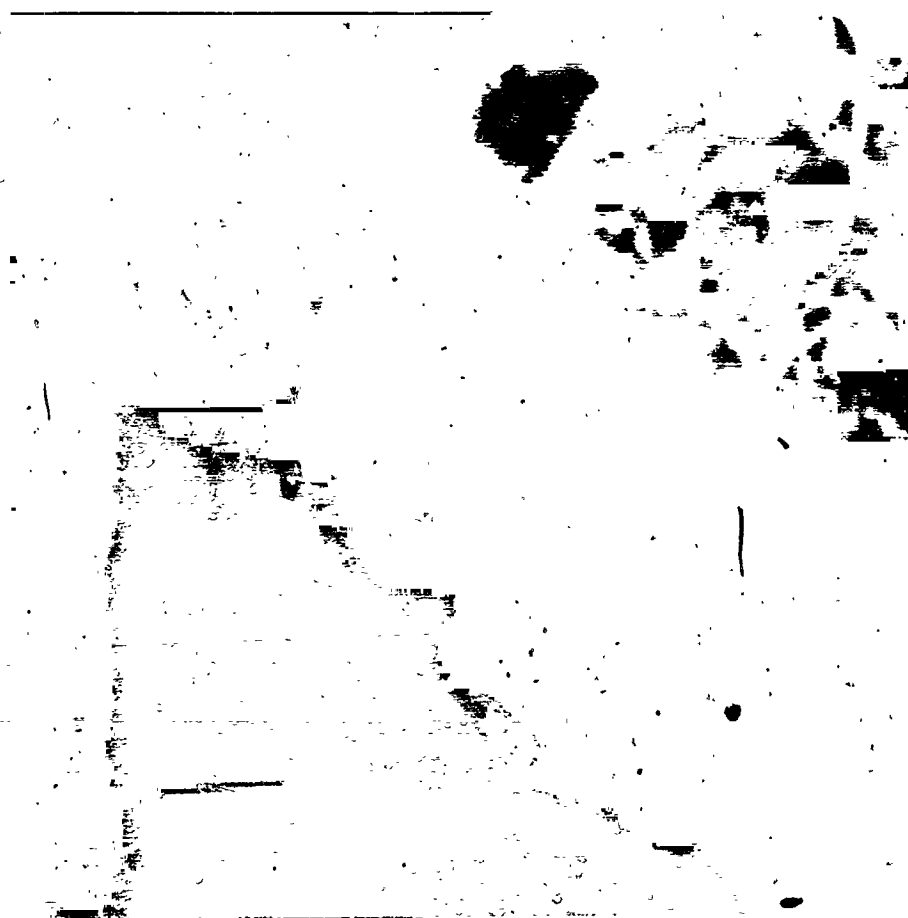
The scattered small-scale clouds in the upper left of the frame are isolated cumulus cells that have developed over the terrain during the day, but have limited vertical development. On the other hand, the moderate-size bright white clouds in the upper right are those that have reached the stage where the anvil tops of cirrus have developed and are being blown downstream by fairly strong upper-level winds. These cumulonimbus cells are forming at the crest of the Sierra Nevada. Their windward or southwest side is hard edged, as compared to the lee or northeast edge, which is being hidden by the higher cirrus plumes. The presence of coastal stratus immediately offshore implies that upwelling of cold water is occurring. Northwestern low-level wind flow is reported by conventional meteorological observations.

The overall pattern retention by the peripheral cancellation method [upper photo Fig. 20(c)] is good but excessive black-and-white contrast has deleted a considerable amount of texture and small detail. In addition, there is a pronounced rectilinear pattern induced on the cumulus cloud edges at the upper right of the frame. A considerable amount of the contrast between hard and soft edges of the cumulonimbus cells has been lost. The lack of filmy texture does not allow an evaluation of the upper level winds. Snow cover on the mountains is made less easily recognizable due to the rectilinear pattern. The dark terrain is made even darker making an interpretation of terrain more difficult. The cumulus clouds (upper left) are depleted in size by absorption of the dark grey areas. Excessive contrast also renders the coastal stratus too bright, thereby taking on an appearance of possibly dense, middle clouds. The subtle striations apparent in the original, are not retained.

PERIPHERAL  
CANCELLATION  
METHOD



CONVENTIONAL  
AVERAGING  
METHOD



(c) Bandwidth reduced 9:1

TIROS V ORBIT 049D, FRAME 20 2252GMT 22 JUNE 1962  
MEDIUM ANGLE LENS



FIG. 20

SCALE: 1 in.  $\approx$  75 nm near mid-frame

(a) Unprocessed TIROS original



TIROS V ORBIT 0490, FRAME 20 2252GMT 22 JUNE 1962  
MEDIUM ANGLE LENS

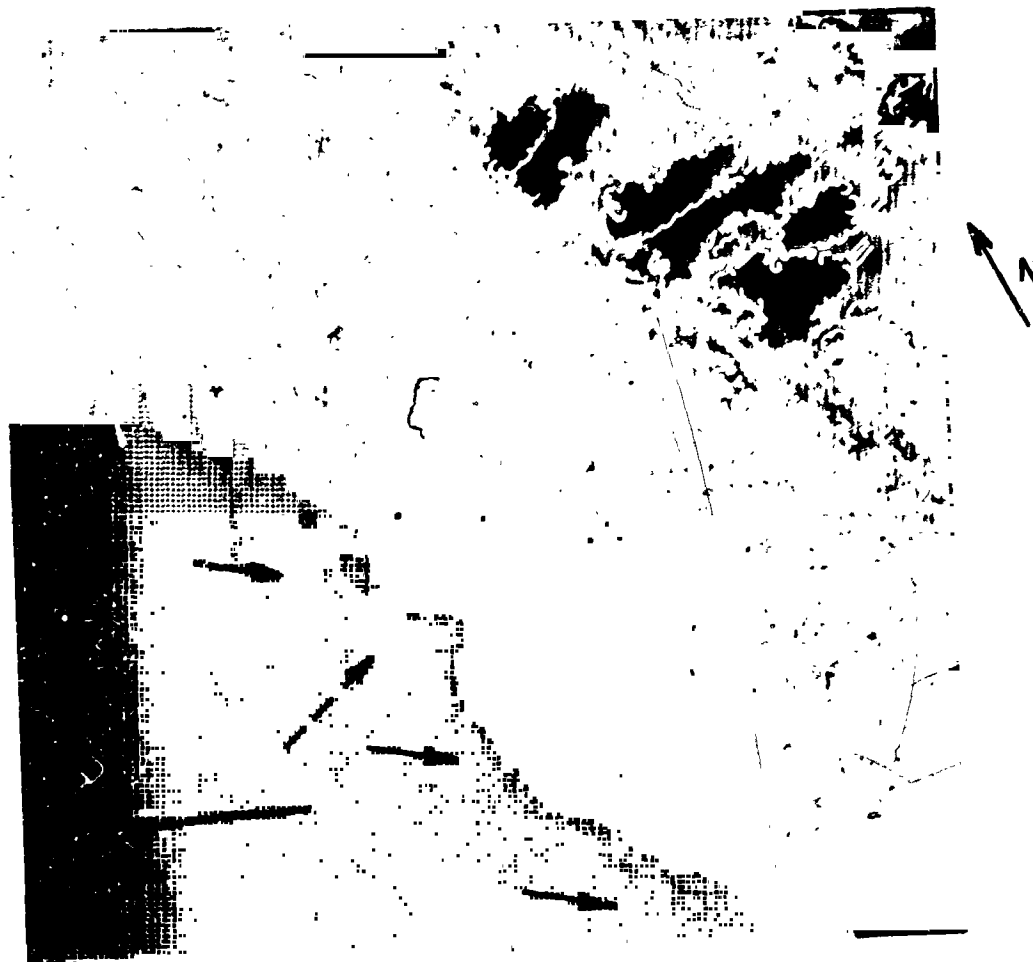

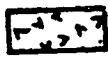


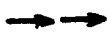



FIG. 20

SCALE: 1 in. = 75 nm near mid-frame

-  CUMULONIMBUS WITH CIRRUS STREAMERS
-  SNOW COVER ON SIERRA NEVADAS
-  COASTAL STRATUS
-  CUMULUS OVER TERRAIN
-  LOW LEVEL WIND FLOW
-  UPPER LEVEL WIND FLOW
- M** MONTEREY BAY

(a) Unprocessed TIROS original

(b) Significant meteorological features of Fig. 20(a)

## FIG. 21 EDDIES INDUCED BY ISLANDS

This frame [Fig. 21(a)] shows an area off the northwest coast of Africa just southeast of the Canary Islands. The islands are not visible in this photograph but are located just off the northeast corner of the frame. The eddies and swirls seen on the frame are being induced in a field of predominately stratocumulus cloud, see Fig. 21(b). Under favorable conditions occurrences of such swirls are common downwind from islands. An island terrain of 1000 feet or more induces eddies into the wind flow which can cause the cloud forms downwind from the obstruction to appear as swirls. This generally occurs with a pronounced low-level inversion and a wind speed of 10 to 20 knots. Consequently, when satellite photographs show such swirls and the position of the island or islands are known, wind directions and approximate speeds can be deduced.

To the south of the swirls, the cloud patterning becomes rowed, with the rows aligned with the surface winds. Clouds in these rows are also predominately stratocumulus. Cumuliform cloudiness seen on the left side of the frame, is associated with a zone of convergence around the periphery of a quasi-permanent oceanic high. The cumuliform structure of these clouds is barely apparent, especially near the horizon near the northwest edge of the photo due to the high nadir angles involved.

The general pattern retention by the peripheral cancellation method [upper photo Fig. 21(c)] is good; the eddy formations are clearly recognizable. There are some small, though undesirable, pattern changes apparent in the processed frame. For example, excessive contrast has brightened and merged some of the elements in the clouds on the lower right such that the rows, so clearly evident on the original, are not distinct. They appear more as a cloud sheet (interrupted by breaks), a pattern that would have a different meteorological significance from that of the original. This same excessive contrast also obscures the individual cumulus element in the cloud line (upper left) but this probably would not lead to a serious misinterpretation.

Also undesirable is the definite checkerboard effect to the clouds in the upper right, though it also probably would not interfere with the proper identification and interpretation of the clouds.

PERIPHERAL  
CANCELLATION  
METHOD



CONVENTIONAL  
AVERAGING  
METHOD



(c) Bandwidth reduced 9:1

TIROS V ORBIT 186/187T<sub>2</sub> FRAME 18 1400GMT 2 JULY 1962  
MEDIUM ANGLE LENS



FIG. 21

SCALE: 1 in.  $\approx$  120 nm near mid-frame

(a) Unprocessed TIROS original

TIROS V ORBIT 188/187T<sub>2</sub> FRAME 18 1400GMT 2 JULY 1962

MEDIUM ANGLE LENS



FIG. 21

SCALE: 1 in.  $\approx$  120 nm near mid-frame



EDDIES IN STRATOCUMULUS



STRATOCUMULUS IN ROWS



CUMULUS CLOUDS IN CONVERGENCE ZONE



LOW LEVEL WIND FLOW



HORIZON

H

HIGH CELL

(a) Unprocessed TIROS original

(b) Significant meteorological features of Fig. 21(a)

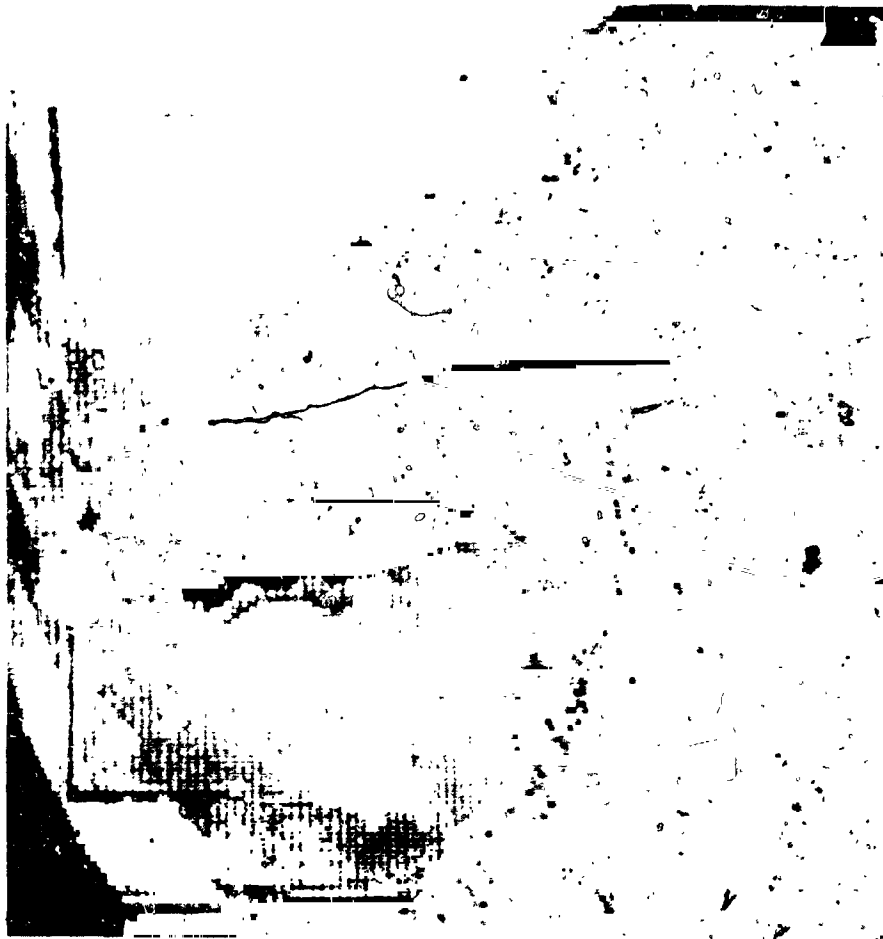
FIG. 22 CLOUD "STREETS"

This frame [Fig. 22(a)] views the entrance to the Gulf of Aden. The photograph is marked by strong contrast between the bright highly reflective land and the less reflective water. Clouds over the water are seen as thin "streets," grey to white in tone, curving into the Gulf of Aden, see Fig. 22(b). These are identified as lines of cumulus, separated by about 10 miles, with alignment parallel to the direction of the surface wind flow. The relative cloud-free zone offshore along the coasts suggests that a morning land breeze is circulating dry continental air outward over the water surface. The cloud streets demark the line along which the dry air flowing southward or westward from the land converges with the moist air flowing westward over the water.

Small cumuli, such as seen in this photograph, are of limited vertical development. Cloud growth is usually being prevented by marked wind shear or a temperature inversion near the cloud tops. According to Malkus, 1963, a marked shearing imposed aloft upon the convective layer brings in cross-wind modes, oriented with the upper shear. This then can be used as a tool in the interpretation of such photographs as this. Since no cross wind modes are present, it could be assumed that no directional wind shear is present to cloud tops and that cloud growth is resulting from an inversion rather than from a wind shear.

The pattern retention of the terrain by the peripheral cancellation process [upper photo Fig. 22(c)] is considered fair but the pattern retention of the small cumulus streets over the water is considered as poor. In the former case the coastline is sharp and distinct. Excessive black-and-white contrast, however, obscures or obliterates certain of the terrain features. This degradation is particularly prominent in the upper left of the frame, where grey-scale is entirely absent. Over the water the curvilinear rowing of the clouds, which is of major meteorological significance in terms of this frame, is not well reproduced. The excessive contrast has obscured the dark grey clouds, destroying the appearance of curving rows. Only scattered, bright, elements remain. In this example, the interpretation of the meteorological significance is greatly hampered.

PERIPHERAL  
CANCELLATION  
METHOD



CONVENTIONAL  
AVERAGING  
METHOD



(c) Bandwidth reduced 9:1

TIROS IV ORBIT 1238/1287T, FRAME 25 0449GMT 9 MAY 1962

WIDE ANGLE LENS



FIG 22

SCALE: 1 in.  $\approx$  130 nm near mid-frame

(a) Unprocessed TIROS original



WIDE ANGLE LENS

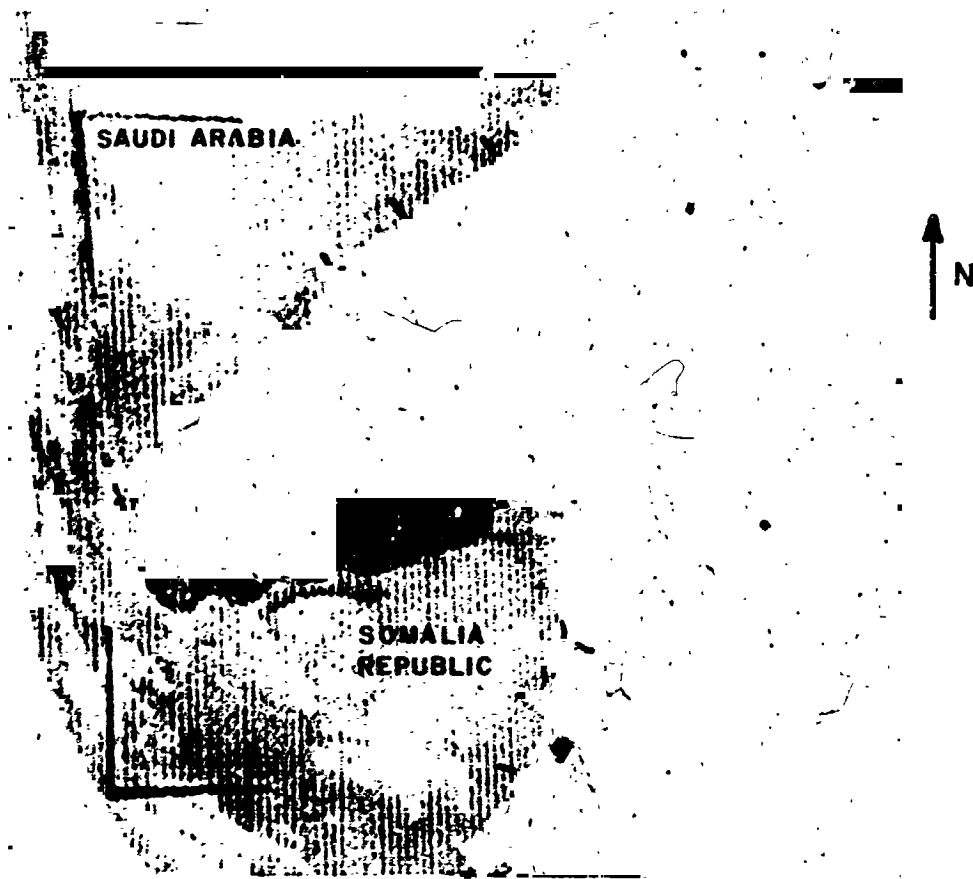


FIG. 22

SCALE: 1 in.  $\approx$  130 nm near mid-frame



CUMULUS CLOUD "STREETS"



COASTLINE



LOW LEVEL WIND FLOW

(a) Unprocessed TIROS original

(b) Significant meteorological features of Fig. 22(a)

### FIG. 23 AIR MASS CONVECTIVE CLOUDS

This frame [Fig. 23(a)] views the area along the California Coast from Ukiah northward. Coastline can be seen on the lower left hand side of the frame, the darker area on the extreme left being ocean, see Fig. 23(b).

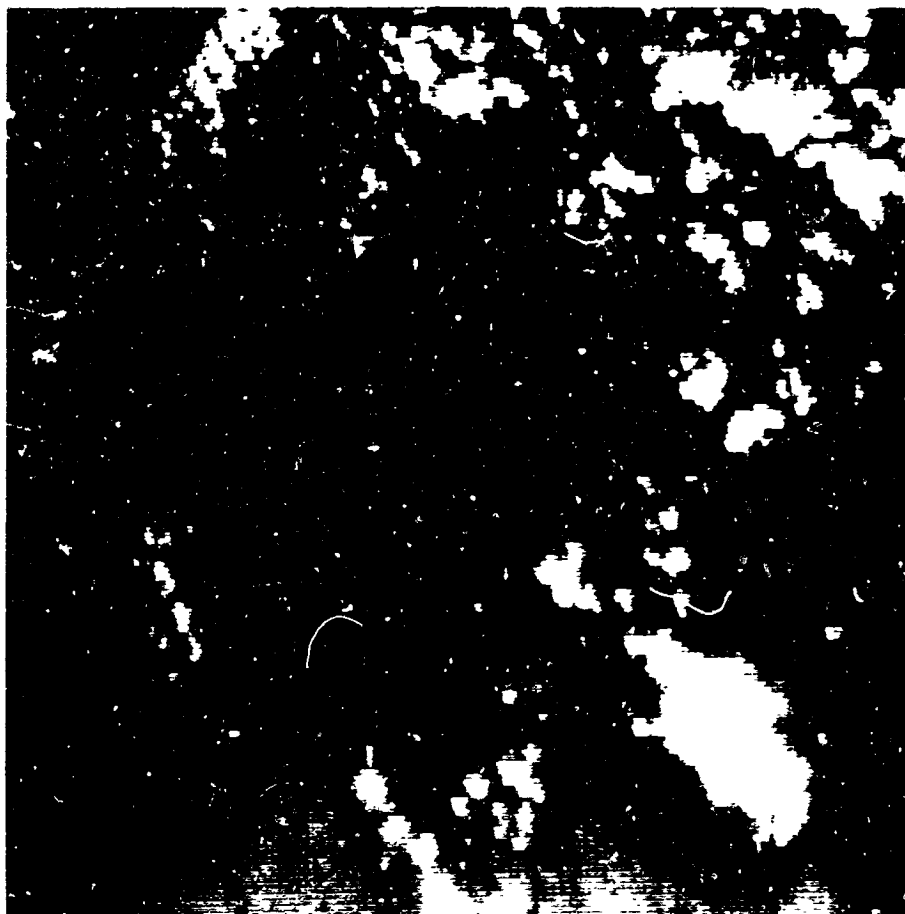
The large cells on the right side of the frame are cumulonimbus of 2-5 mill cell diameter. The appearance of the cells, hard edged on the windward side and soft edged on the leeward side, is the visual clue that the upper part of the cloud (cirrus) is being drifted downwind with the high-level winds. The smaller cells on the left side of the frame are smaller cumulus clouds (cell diameter 1/2 to 2 miles). They are forming over the mountainous terrain inland of the coastline and have not reached heights where cirrus is being drifted downstream. Individual cells are aligned in rows or "streets" with the northwesterly low-level wind flow. In certain instances, such as this, cloud patterns allow for the delineation of wind direction at both low and high levels.

The overall pattern retention by the peripheral cancellation process [upper photo Fig. 23(c)] is considered as good. A slight alteration in the pattern does occur as the result of heightened black-and-white contrast. For example, some of the cloud clusters, particularly in the right half of the frame, are merged into huge clusters because of the obscuration of the dark area delineating the boundaries between single cloud elements. This could lead to a misinterpretation of storm intensity. The distinction of texture between hard cloud edges on the windward side and soft edges on the lee side indicating cirrus is no longer evident due to excessive brightness.

On the left half of the frame, the contrast has absorbed some of the dark grey cumulus, leaving less cloud cover than on the original. The rowed pattern, however, has not been disturbed.

There is a slight though undesirable checkerboard effect to the small cumulus throughout the frame, but particularly noticeable in the right half of the frame.

PERIPHERAL  
CANCELLATION  
METHOD



CONVENTIONAL  
AVERAGING  
METHOD



(c) Bandwidth reduced 9:1

TIROS I ORBIT 603/603T, FRAME 14 0031GMT 13 MAY 1960  
NARROW ANGLE LENS



FIG. 23

SCALE: 1 in.  $\approx$  25 nm near mid-frame

(a) Unprocessed TIROS original

TIROS I ORBIT 603/603T, FRAME 14 0031GMT 13 MAY 1960  
NARROW ANGLE LENS

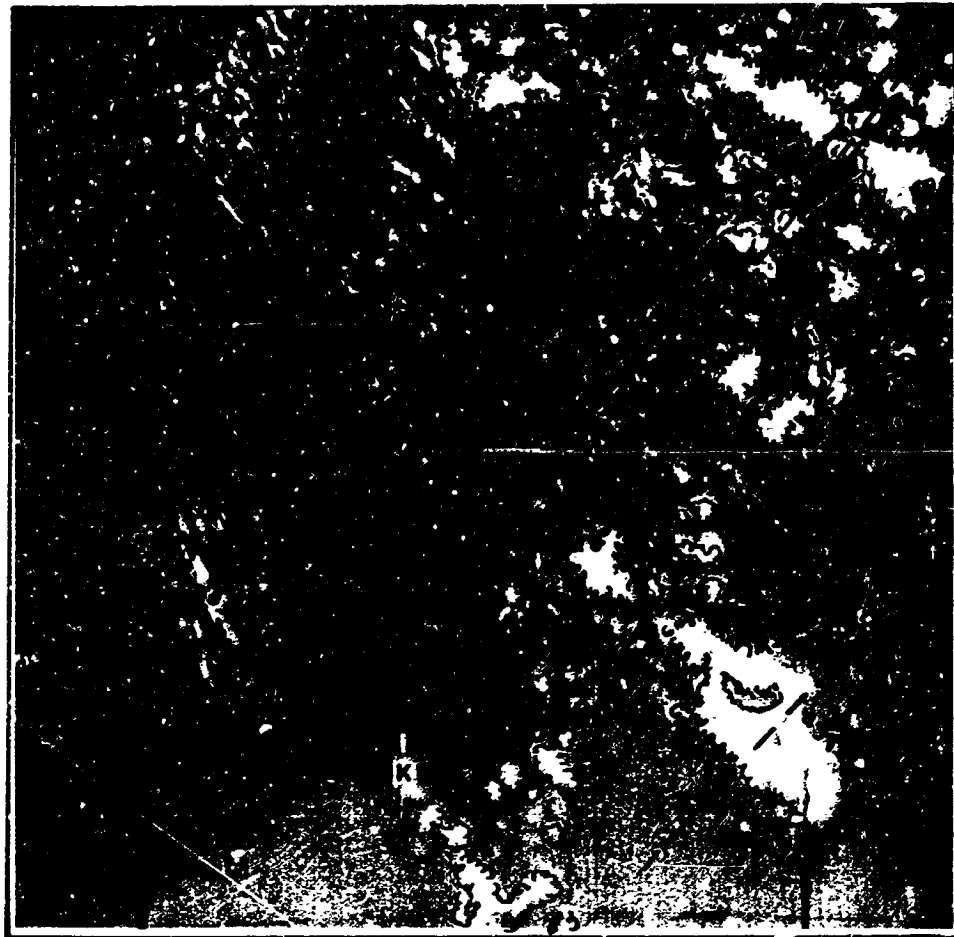


FIG. 23

SCALE: 1 in.  $\approx$  25 nm near mid-frame



LOW LEVEL CUMULUS



CUMULONIMBUS WITH CIRRUS STREAMERS



LOW LEVEL WIND FLOW



UPPER LEVEL WIND FLOW



COASTLINE

(a) Unprocessed TIROS original

(b) Significant meteorological features of Fig. 23(a)

## VI DETAILED TECHNICAL DESCRIPTION

### A. Scanner

The design of a drum scanner calls for a pair of connected rotating drums and a stable platform for the input and output optical systems. The platform must translate accurately relative to the rotating drum. It was decided that the most economical and rapid approach would be to avoid the design of this drum-platform system and employ a lathe bed as a basic mechanism. A small South Bend lathe bed was purchased and modified as follows:

A large traveling platform was rigidly attached to the sliding (transverse) carriage of the lathe. A double drum structure was supported between the headstock and tailstock of the lathe. Figure 24 shows the scanner with the leftmost drum enclosed in a light-tight box. This drum holds the input copy while the right drum serves to hold the film on which is printed the output picture. The input drum is provided with a bright light source for illuminating the input copy. This of course must be optically shielded from the output drum on which the film is placed. The light-tight box serves this function. Signals derived from the sensing head are delivered to a rack of electronic equipment where they are processed and fed to the modulated light source for exposing the output film.

The two drums are identical in size, each 12 inches in length and 12 inches in circumference. The feed rate on the transverse table is adjustable over a range that allows scanning densities from 4 lines to 500 lines per inch. Such a system is necessarily a one-to-one magnification system; that is, the size of the output film image is the same as the input picture.

Original Nimbus pictures were prepared by printing on 8 x 10-inch photographic paper. The picture area covered a 7 x 7-inch square; the identification data at the top of the picture extended the image area to a 7 x 9-inch rectangle. It was necessary to print the originals "backward,"

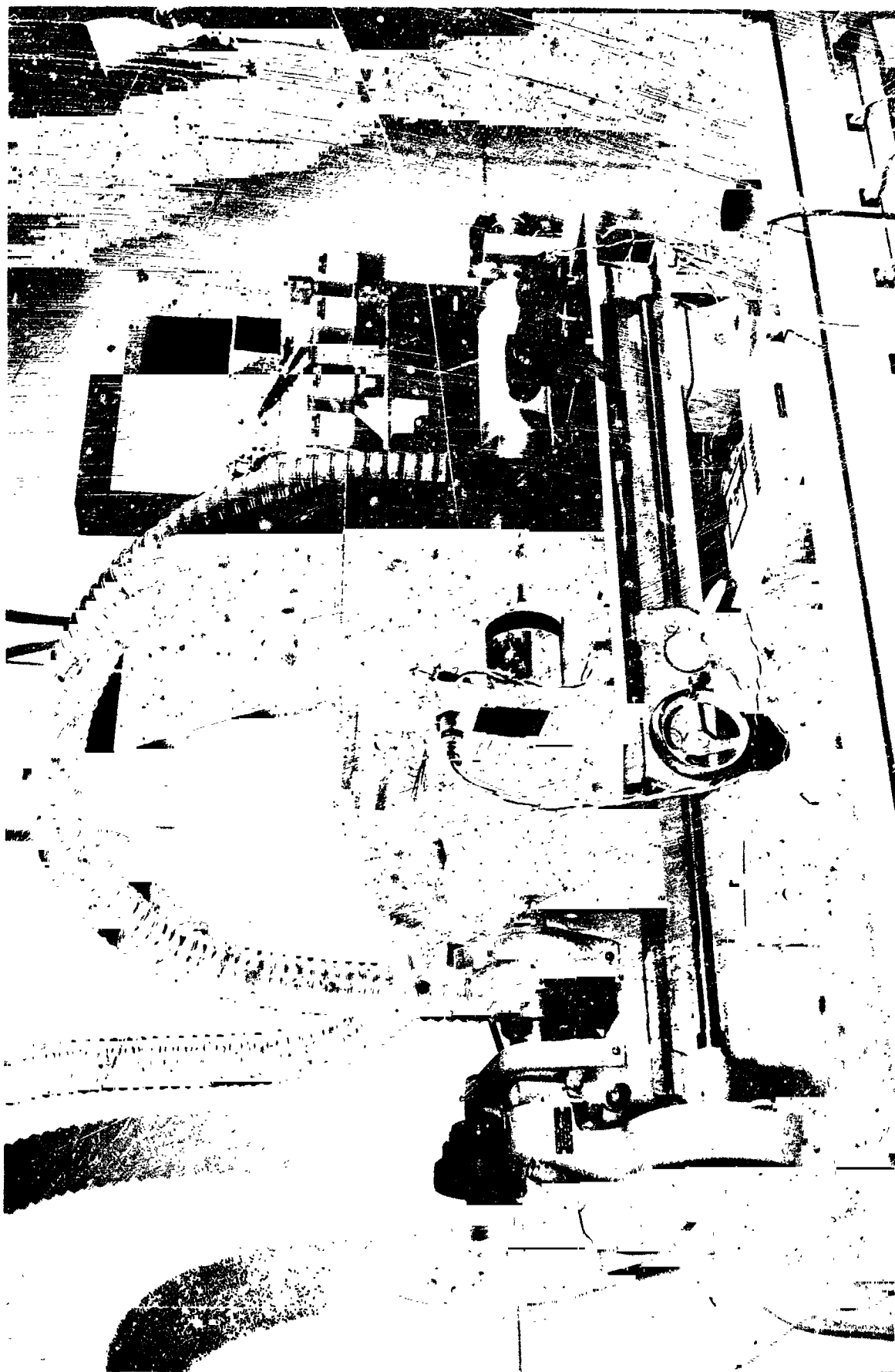


FIG. 24 NIMBUS SCANNER

that is, reading right to left. This was necessary since the output film picture is a negative and ordinary contact prints made from these negatives would be backward if this step were not taken.

The 800 scanning lines of the original picture covered 7 inches of drum surface. Figure 25 shows a simplified block diagram of the overall system.

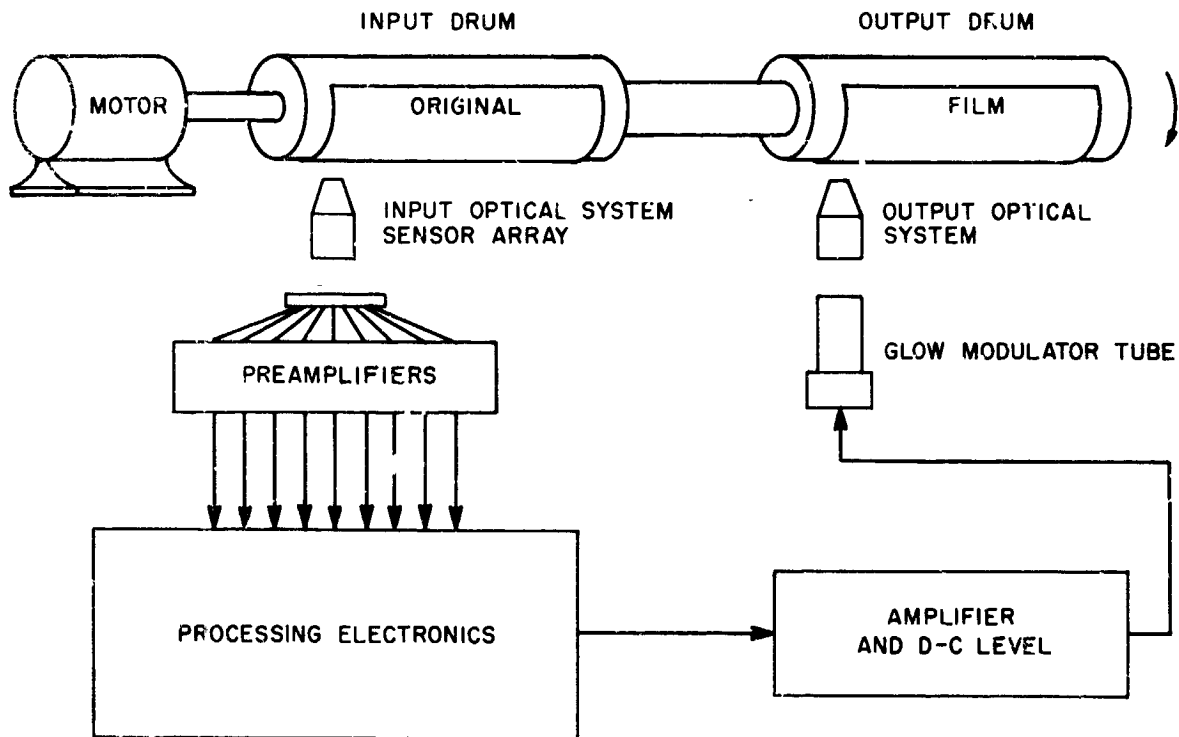


FIG. 25 SIMPLIFIED BLOCK DIAGRAM OF SYSTEM

#### B. The Input System

The input system comprises the input drum, a light source, the sensor head, the optical system, and the preamplifier. Several light sources were considered for illuminating the input copy. The best lamp tried was a General Electric DLS projection lamp with internal "cool" mirror. This lamp has a parabolic mirror within the vacuum envelope to focus the light from the filament to a small area in front of the bulb. The mirror coating is designed to reflect and focus only the visible light, allowing the infrared radiation to be transmitted through the



mirror. This allows slow scanning speeds without the possibility of overheating the copy being scanned. The filament receives power from a dc supply to ensure that no hum modulation of the video signal takes place.

A ten-power microscope objective images the illuminated area of the input copy on to the surface of the sensor head. The sensors are Texas Instrument Type LSX-600 photo transistors. They are very small NPN units with sufficient sensitivity to yield signals in the range of 0.25 to 0.5 ma as they were used in this scanner. Each phototransistor is a small cylinder 0.06 inch long and 0.06 inch in diameter. To obtain signals from a matrix of picture elements, two approaches are possible. The more straight-forward of them calls for a simple matrix of photo devices. Such a head was constructed with the sensors separated by 0.10 inch. Nine sensors were used in a  $3 \times 3$  array. Another approach uses delay lines in conjunction with a single line of photo sensors to generate the matrix of signals. Figure 26 shows such an arrangement.

Five delay lines of five taps each are used. The delay of each section is equal to the time of one picture element. At the points marked 1-25, the appropriate signals exist for processing with a  $5 \times 5$  matrix. The arrangement with delay lines is to be preferred, since equalization is somewhat easier. Delay lines, however, restrict the operation of the scanner to a fixed line scanning rate.

### C. The Output System

To expose the output film, a light source is required, capable of being modulated at rates up to a few kilocycles. Incandescent galvanometer-type modulatable sources were considered, as were fixed sources with variable-attenuation filters such as KDP or ADP. The simplest approach involved the use of Sylvania Glow-Modulator tube that can be directly modulated over a sufficient range. These devices are cold-cathode light sources with an essentially linear relationship between light output and cathode current. Spectrally, they emit strongly in the blue and ultra-violet portions of the spectrum and are therefore compatible with photographic film sensitivities. Experiments were conducted early in the

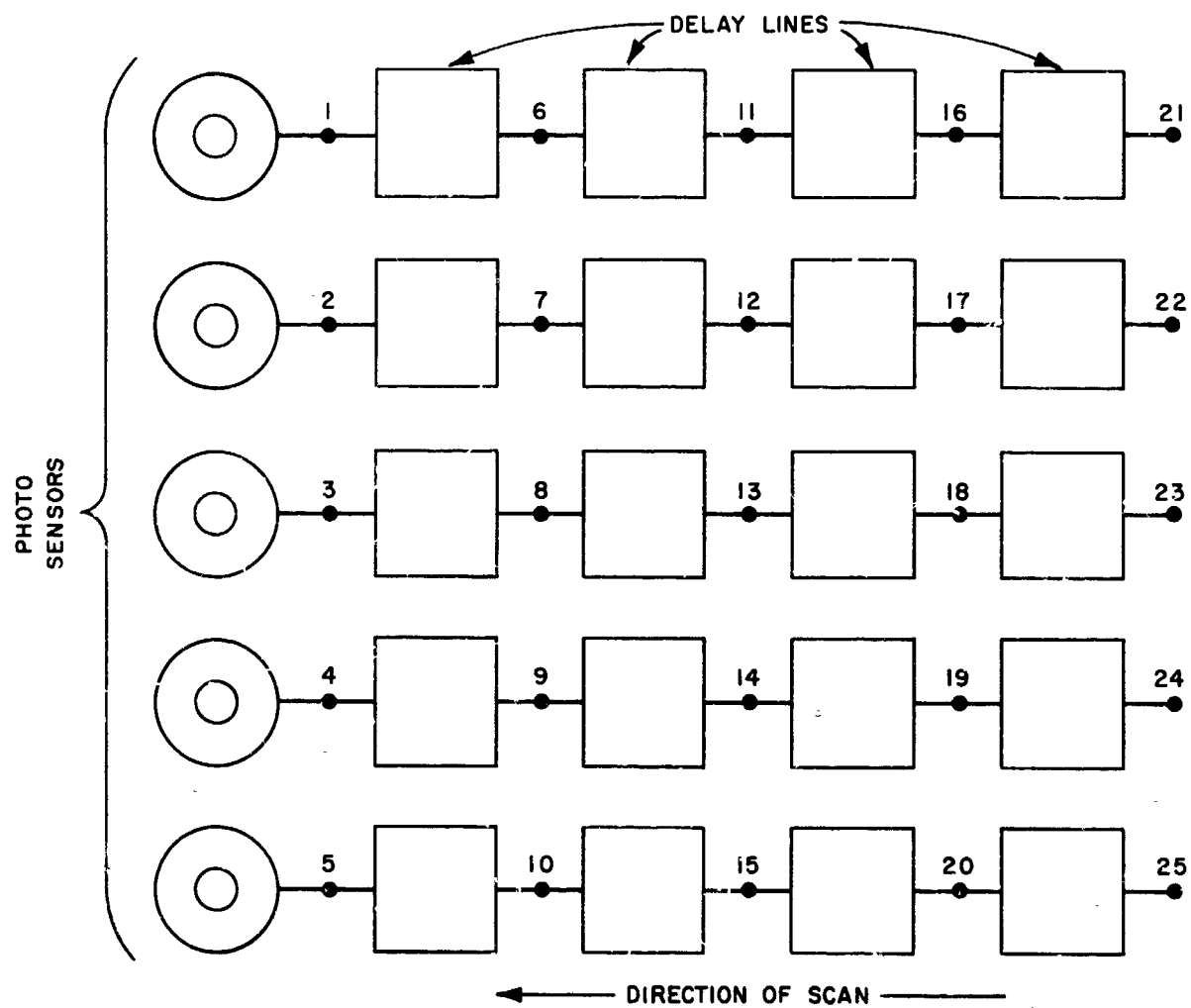


FIG. 26 DELAY-LINE SENSING ARRAY

project to determine the best operating range of these light sources. The available data indicated that the glow-modulator tubes would operate from essentially zero light out at zero current up to full output at 30-40 ma. However, some hysteresis was noted at the low light levels. This is consistent with the theory of operation of the tube, since a threshold condition exists at the low current level where the light-emitting crater is formed. Some work was done with simple gamma correction to attempt to compensate for this nonlinearity at low output level. Better results were obtained by restricting operation to the linear range of the glow tube. The resulting contrast range on the negative is reduced but with clean signals (very low noise levels) this reduced contrast on the negative can be restored in the printing process by using grades of photographic paper designed for higher contrast.

In selecting a film for printout, the factors considered included orthochromaticity (panchromatic film would present darkroom problems), long linear transfer characteristic, and availability. Film speed was not a particularly important factor since the scan rates could be adjusted to suit any situation. Kodak Gravure Copy film was selected as the output medium. It has an ASA speed rating of 12 and a long linear grey scale, suitable for holding highlight contrast present in most cloud pictures. It is readily available and can be used with an appropriate safelight, simplifying dark room procedure.

The output optical system employs a dual condenser lens and a microscope objective. The crater light source is imaged directly on to the film surface with no further aperturing. Flare is kept to a minimum by the use of black baffles within the barrel of the optical structure. The image size of the crater is made equal to the line spacing to produce a relatively "continuous" picture.

#### D. Bandwidth Compaction Algorithms

All of the picture processing in the early phase of the effort involved the use of the simple  $3 \times 3$  matrix sensor array. Many potential processing algorithms were conceived and most were implemental and tested

during the effort. To evaluate the specific algorithms it is necessary to compare processed pictures to the originals to see the extent of detail lost in the processing. It cannot be expected that reduction of bandwidth of 9:1 can be effected in a picture without influencing the meteorological information in the picture. The most realistic comparison is between processed pictures and pictures where 9:1 bandwidth reduction has been made by simple, conventional averaging. Described below are all of the bandwidth compaction algorithms together with an interpretation of their usefulness and application.

#### 1. Conventional Averaging

To provide a basis for comparison, pictures were processed by performing a simple averaging of the nine input video signals to produce a single print-out signal. The nine signals are summed by a simple resistive network. This type of averaging is equivalent to using a larger scanning aperture in the original picture. Detail contrast is drastically reduced.

#### 2. Selection of Blackest Element

With this process the blackest of the nine input elements is selected by a simple analog diode gate. For thin black detail in large white backgrounds, this technique enhances the detail structure. Figure 27(a) shows a typical small black detail in an original picture. Figure 27(b) shows the reduction in contrast caused by averaging over three of the original elements. Figure 27(c) shows that the detail contrast has been preserved by selecting the blackest element within the aperture. The feature has been enlarged in size and its contrast is equal to the original contrast.

Such a processing technique performs bandwidth reduction and yields much better results than simple averaging for this type of detail. For cloud streets, thin bands in large cloud sheets and some terrain features, this process yields very satisfactory results. Dendritic patterns can be accentuated, enhancing the meteorologist's ability to identify snow fields.

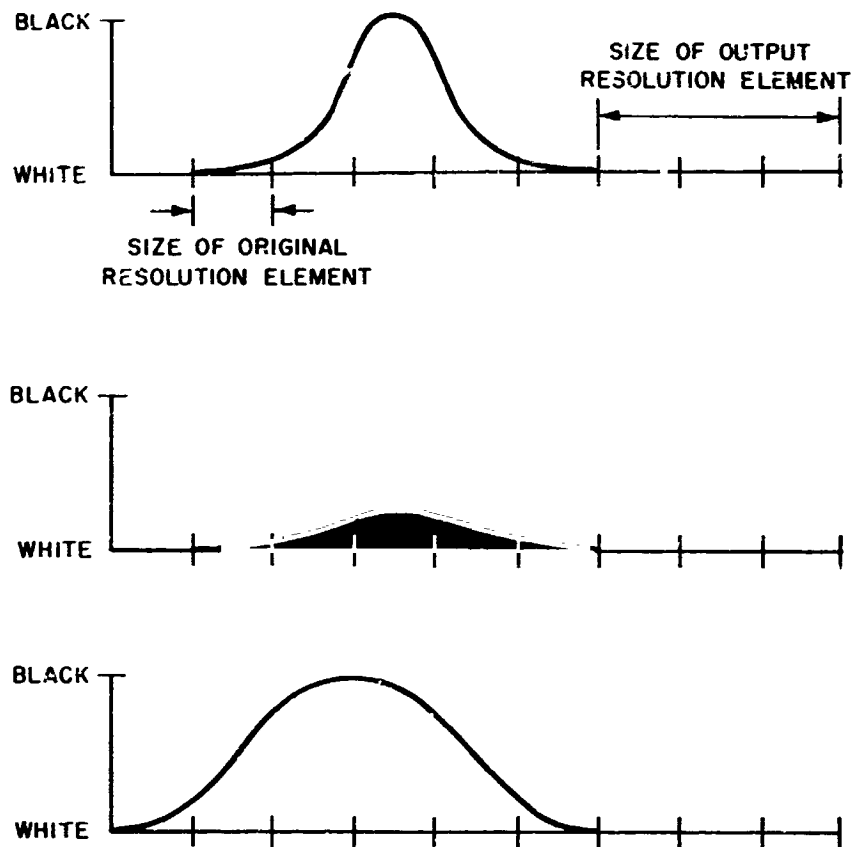


FIG. 27 SELECTION OF BLACKEST ELEMENT  
 (a) One-dimensional light distribution  
 (b) Reduction of contrast by averaging  
 (c) Preservation of contrast by selection of blackest element

Figure 28 shows a block diagram of the circuitry used to combine the derived black signal with the average signal. As can be seen from the figure, the signal corresponding to the blackest element together with the average signal is delivered to a difference amplifier whose gain is  $K$ . The output of this amplifier is summed together with the average signal to form the output  $O$ , where:

$$O = A + K(B - A)$$

It can be seen that the output is always equal to the average in broad areas with no detail (where  $B$  equals  $A$ ). For  $K = 1$  the output is identically equal to  $B$ . Setting  $K$  greater than 1 yields interesting results.

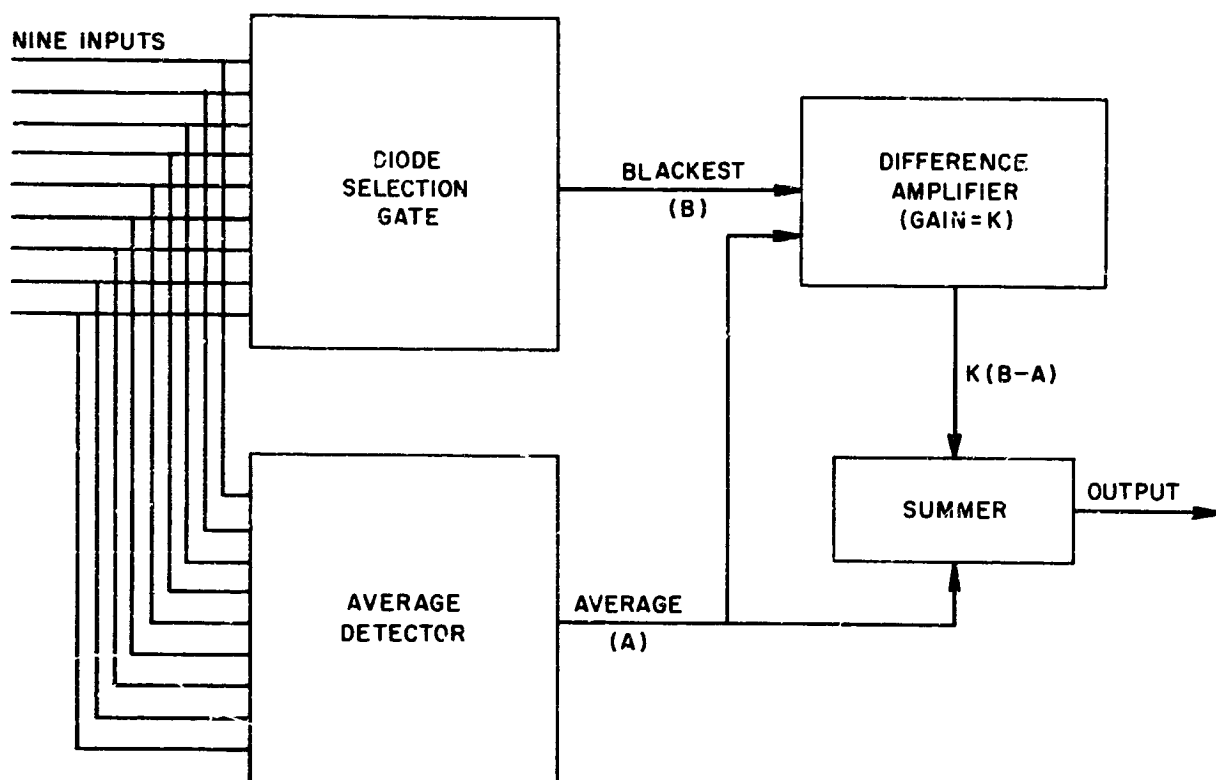


FIG. 28 BLOCK DIAGRAM OF COMBINING CIRCUIT

It allows not only preservation of detail contrast appearing in the original, but can actually increase this contrast. Such enhancement can be put to good use in view of the highly subjective nature of the useful information in the picture. It can also help compensate for some of the aperture losses in the camera, the communication link, and the display. If such enhancement helps the meteorologist to correctly interpret the data, then it is useful.

The disadvantage of this type of processing becomes obvious when one considers what happens to fine white detail when the processing algorithm calls for selection of the blackest element. In order for the output signal to correspond to white, it is necessary to have all of the nine inputs at a level corresponding to white. For if one of the nine is darker than the others, the output will equal this darkest element. In other words, all small white detail (whose size is less than the  $3 \times 3$  input array) will be lost.

### 3. Selection of Whitest Element

With a simple analog diode gate, the whitest of the nine input signals can be derived. The implementation is very similar to the previously described black-selection technique. The output signal  $O$  that results can be expressed as

$$O = A + K(W - A) ,$$

where  $A$  is the average,  $W$ , the whitest and  $K$ , the difference amplifier gain. This arrangement preserves contrast for small white detail in large black backgrounds. This can preserve the usefulness of a picture that has small cumulus cloud cells over dark terrain or water. The disadvantage here is obvious, since small black features will be lost. The situation is analogous to the previous one with the image polarities reversed.

### 4. Combination of Blackest and Whitest Enhancement

In an attempt to retain some of the advantages of both of the previously described processing methods, signals representative of the blackest and whitest were generated and combined as shown in Fig. 29.

The difference in amplifier gains ( $K$ 's) can be adjusted to favor the type of structure in a particular meteorological situation. It can be seen from the processed pictures that the results were far less than perfect. The pictures have a general defocused look and look similar to the pictures made by simple averaging.

The circuitry shown was very flexible and by simple adjustment of the  $K$ 's several outputs could be formed:

$$\begin{array}{ll} O = A & \text{both } K\text{'s} = 0 \\ O = B & K_1 = 1, K_2 = 0 \\ O = W & K_1 = 0, K_2 = 1 \\ O = \frac{B + W}{2} & K_1 = 1/2, K_2 = 1/2 \end{array}$$

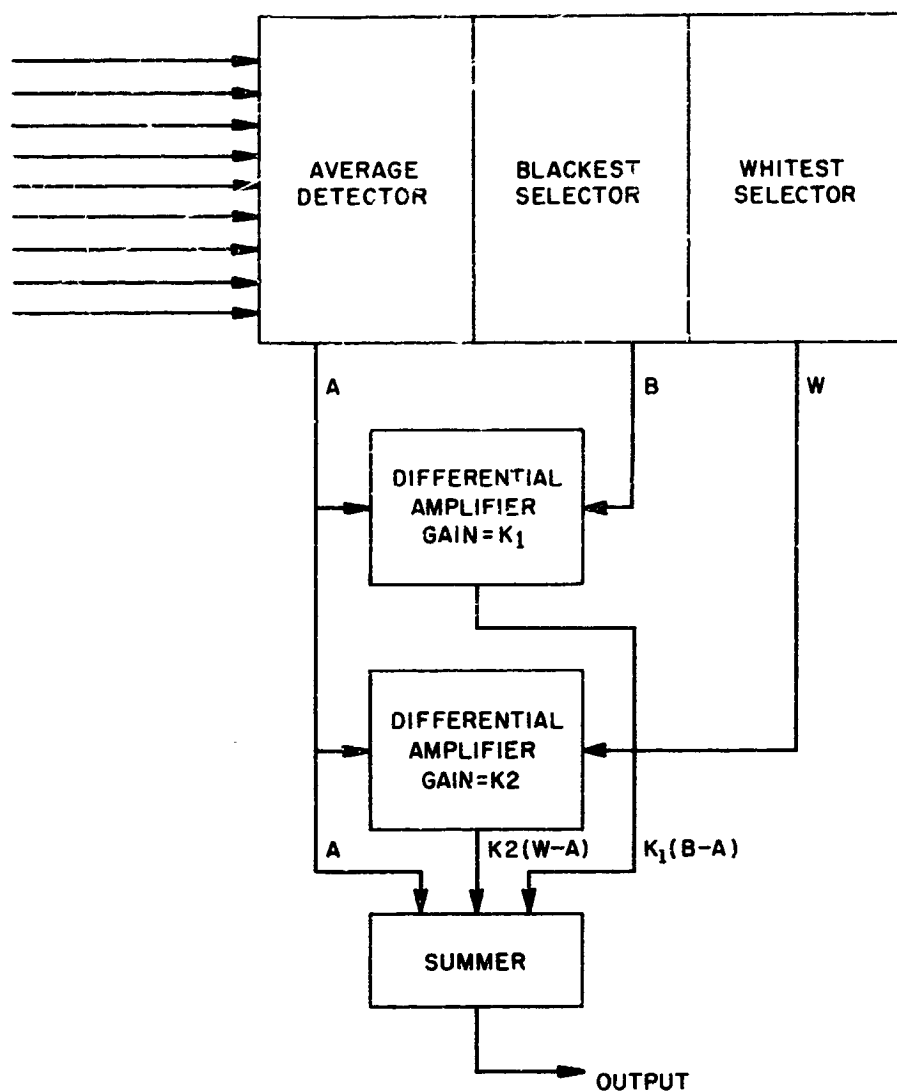


FIG. 29 BLOCK DIAGRAM OF BLACKEST-PLUS-WHITEST CIRCUIT

This circuit was used to produce all of the processed pictures where bandwidth compaction was accomplished by averaging, black selection, white selection, and combination black-white selection.

##### 5. Selection of Second Blackest or Whitest

In the processes previously described, small detail structure can determine the nature of the output signal. As would be expected this renders the system susceptible to noise. A small impulse-noise spike can be interpreted as signal detail and enhanced in the output. To reduce the likelihood of this and to decrease the system sensitivity to noise, it is possible to select the second blackest (or whitest).



This means that in order for noise to influence the output, noise spikes encompassing two or more elements must exist within the aperture simultaneously. In high-impulse-noise situations this condition occurs much less often than the appearance of single noise spikes within the aperture. Desired features, however, generally consist of more than one element within the aperture.

Selection of the second blackest of course can result in some loss of detail contrast. However, this can largely be compensated by "over-enhancing" the signal. As described previously, this involves increasing the gain of the differential amplifiers.

The noise problem in general is discussed more thoroughly in Appendix A.

To select the second blackest of nine input elements the following algorithm suffices: First, all possible groups of eight elements are gated to select the blackest of each group. (There are, of course, nine such groups.) The blackest original element will appear in all of the groups but one. The nine resultant signals are then gated, this time selecting the whitest of the nine. The derived signal will be the second blackest. A similar procedure leads to the second whitest signal.

#### 6. Line Structure Enhancement

The technique of diode analog gating can be applied to detecting the presence of line structure within the aperture. Circuitry was constructed to enhance lines in the twelve possible orientations within a  $3 \times 3$  array (three horizontal, three vertical, and two diagonal of three each in addition to four diagonal of two each in the corners). To enhance black lines, the algorithm given here is followed: First, each possible group of three elements in a row is diode gated to select the whitest. (There are eight of these groups.) Thus, the output of a single group will be black only if all three within the group are black. (In analog logic, gating the AND function for black is accomplished by OR gating for white. The two are equivalent.) The signals derived from the eight groups are gated to select the blackest. The output then

follows not the blackest element, but the blackest group of elements sampled three in a row.

A similar algorithm will generate an output signal that follows the whitest line within the matrix.

## 7. Peripheral Cancellation

During the course of the project, many pictures were processed by all of the previously described algorithms. The close inspection and evaluation of these processed pictures uncovered unexpected effects of the processing methods. For example, there was an undesirable loss of resolution of coarser lines which are comparable to the size of the large aperture of the processed picture. This was caused by the "tail" of a coarser line or point causing elements adjacent to it to experience density changes comparable to those at the center of the line or point. This is illustrated in Fig. 30, which shows a one-dimensional distribution

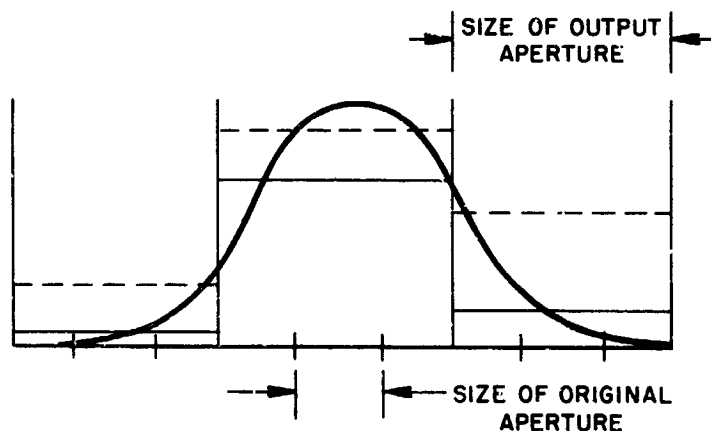


FIG. 30 ONE-DIMENSIONAL DISTRIBUTION OF LIGHT

of light values that encompasses three lower resolution elements. The solid line is the average of each coarse element, whereas the dashed line is the peak value of the matrix of cells within the larger aperture. The figure shows the apparent loss of contrast of the presentation representing peak values. This problem is aggravated when the detail contrast is exaggerated, namely, when an excessive amount of the  $(B - A)$  signal is added to the average signal. This results in the dashed

lines at the two side elements being further raised in intensity while that of the center element remains unchanged, significantly reducing the apparent resolution.

This phenomenon was observed in some of the processed pictures when comparing pictures representing conventional averaging to pictures which preserve or enhance detail contrast. The most obvious difference between the two is the apparent sharpness of the latter due to the contrast preservation of the original fine line information. However, in coarser line information, the effective broadening of lines is quite apparent. For example, the identification characters at the top of the Nimbus picture appeared less readable on the processed picture, which preserved the peak black level. White areas adjacent to and within the characters, such as the center of the letter O, were rendered a value of grey intermediate between the original white and the black value of the character lines themselves. Thus, the process that resulted in preservation of thin-line detail appeared to also cause a thickening of broad-line information. One solution involves an exploration of the area immediately surrounding the scanning aperture. A decision is then made as to the nature of the information within the aperture. For example, if an edge of the aperture contains a dark line or point, it is either due to fine detail that should be preserved, or due to a "tail" of a larger adjacent structure that should not be preserved. Thus, the information adjacent to the scanning aperture is used to determine how the information within the aperture is used. In one method of implementation, an array of photocells as shown in Fig. 31 is placed around the entire periphery of the original  $3 \times 3$  scanning aperture. The outputs of the peripheral photocells are linearly subtracted from the outputs of the adjacent photocell within the scanning aperture. Thus the outputs of A and G are subtracted from 1, B is subtracted from 2, C and D from 3, etc. The resultant outputs from the nine aperture photocells, following the subtraction of the peripheral neighbors, are then logically combined by the methods discussed previously, such as an OR circuit whose output is the blackest of the nine. This system will provide the desired all-black output for the case of an isolated thin line or dot anywhere within the

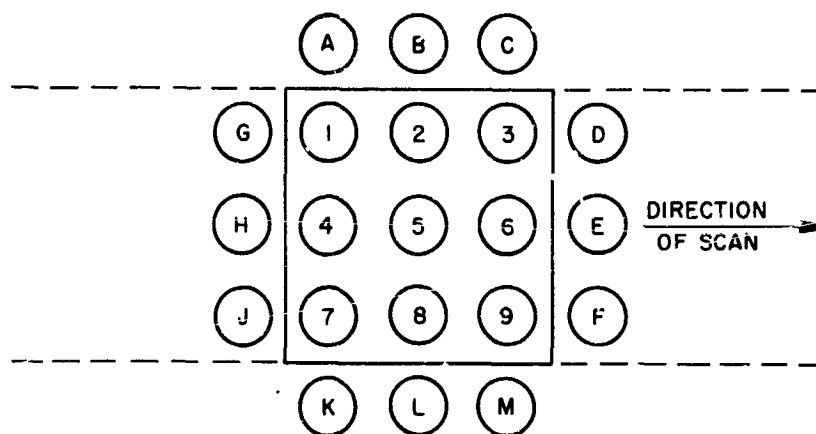


FIG. 31 MATRIX ARRAY OF PHOTOCELLS

scanning aperture. For the case of tails or adjacent broad dark lines, however, the subtraction of the associated peripheral photocell will cancel the output of the photocell within the aperture, preventing the element from becoming black. The broadening effect of dark lines will then be eliminated. One anticipated problem with the system described was the cancellation of information which occurs at the border of adjacent scanning lines. For example, assume the one-dimensional intensity distribution shown in Fig. 32 exists at the border of two scan lines and thus appears first on photocells K, L, and M and 7, 8, and 9; and then on the following scan line on photocells A, B, and C and 1, 2, and 3.

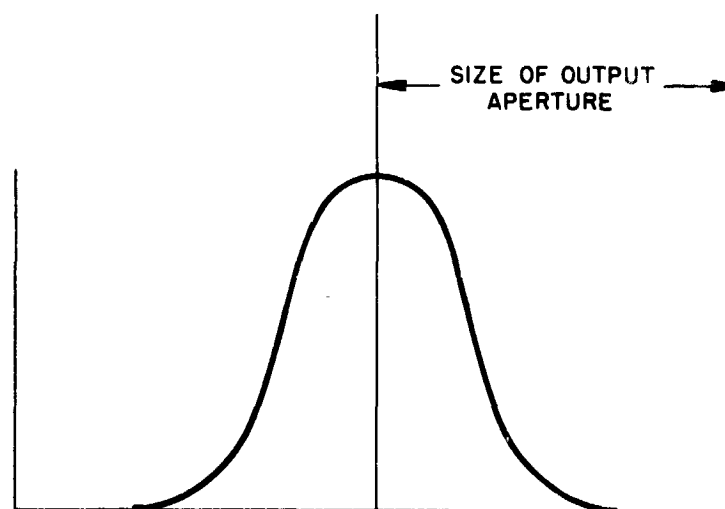


FIG. 32 INTENSITY DISTRIBUTION FOR A FEATURE THAT OCCURS BETWEEN SCANNING LINES

A linear subtraction process would completely eliminate this feature. This will not be the case if this same distribution exists in a vertical line normal to the direction of scan, since the feature will move through the aperture and occupy positions removed from the peripheral diodes, thus resulting in the desired output signal. To alleviate the problem, the lower peripheral photocells K, L, and M (or upper peripheral cells A, B, and C) could be removed. This essentially means that any feature such as shown in Fig. 32 that is cancelled during one scan line is reproduced in the subsequent scan line. The disadvantage, of course, is the susceptibility of the lower edge to tails of adjacent features. This can be attributed to the conventional quantization error of line scanned systems known as "Kell factor". A broad diagonal line crossing many scan lines will alternately appear as one and two elements as it would in any sampled system. This is not a problem normal to the scan direction, where elements are sampled continuously.

A better solution, and one which avoids the necessity of eliminating the three peripheral sensors K, L, and M involves the use of a nonlinear operation between a peripheral sensor and its associated interior sensor. In brief, a determination is made as to which of the two sensors (one interior and its associated peripheral neighbors) is blackest. If the exterior signal is blackest the corresponding interior element is removed from further determinations. This is done by causing the output from that element to be driven to a level outside the black-white logic levels with polarity selected such that its presence will be overlooked by subsequent circuitry.

Thus, any of the previously described processing techniques can be implemented after this peripheral cancellation is accomplished. The specific circuitry that was implemented and that represented by far the best results in terms of evaluation of the pictures produced is described here.

First, peripheral cancellation was done for black details; that is, each interior signal was removed if its exterior neighbor was blacker.

Then the blackest of the remaining interior elements is derived. Peripheral cancellation was then done for white detail; that is, each interior signal was removed if its exterior neighbor was whiter. The whitest of the remaining interior elements is derived. Two signals now exist: a peripherally-corrected blackest and a peripherally-corrected whitest. A third signal is now generated, which is the simple average of the nine interior signals. These three signals are now delivered to a unit that performs as follows: Let the signal representative of the blackest be called B, the whitest W, and the average A. Two signals, B-A and W-A, are generated. A determination is made of the larger of these. If B-A is larger, the output signal follows the B signal. If W-A is larger, the output follows the W signal. It can be seen that in large light areas of cloud pictures with fine black detail the B-A signal will, in general, be the larger. The B signal is used in such an area. Conversely in areas primarily dark with small white features the W-A signal predominates and the W signal is used. Here again a combination of the output correction signal with the average signal can be made and as in previous discussions an output O is generated:

$$O = A + K(C - A) ,$$

where C is the correction signal (either B or W depending on the area under the aperture) and K a controlled variable (amplifier gain). For practical reasons, the entire  $5 \times 5$  sensing matrix could not be implemented during the course of this study. Instead a  $4 \times 5$  matrix was constructed using four sensing phototransistors and a five-tap delay line as described in this section under Part B.

#### E. Test Charts

In addition to the many cloud pictures that were processed, two originals were made for test purposes. Test Chart No. 1, shown in Fig. 33, is an array of resolution wedges. The larger wedges vary from slightly less than 5 lines per inch up to 20 lines per inch. (The numbers at the edge of the wedge indicate the resolution in lines per inch.) The smaller wedges vary from about 8 lines per inch to 40 lines

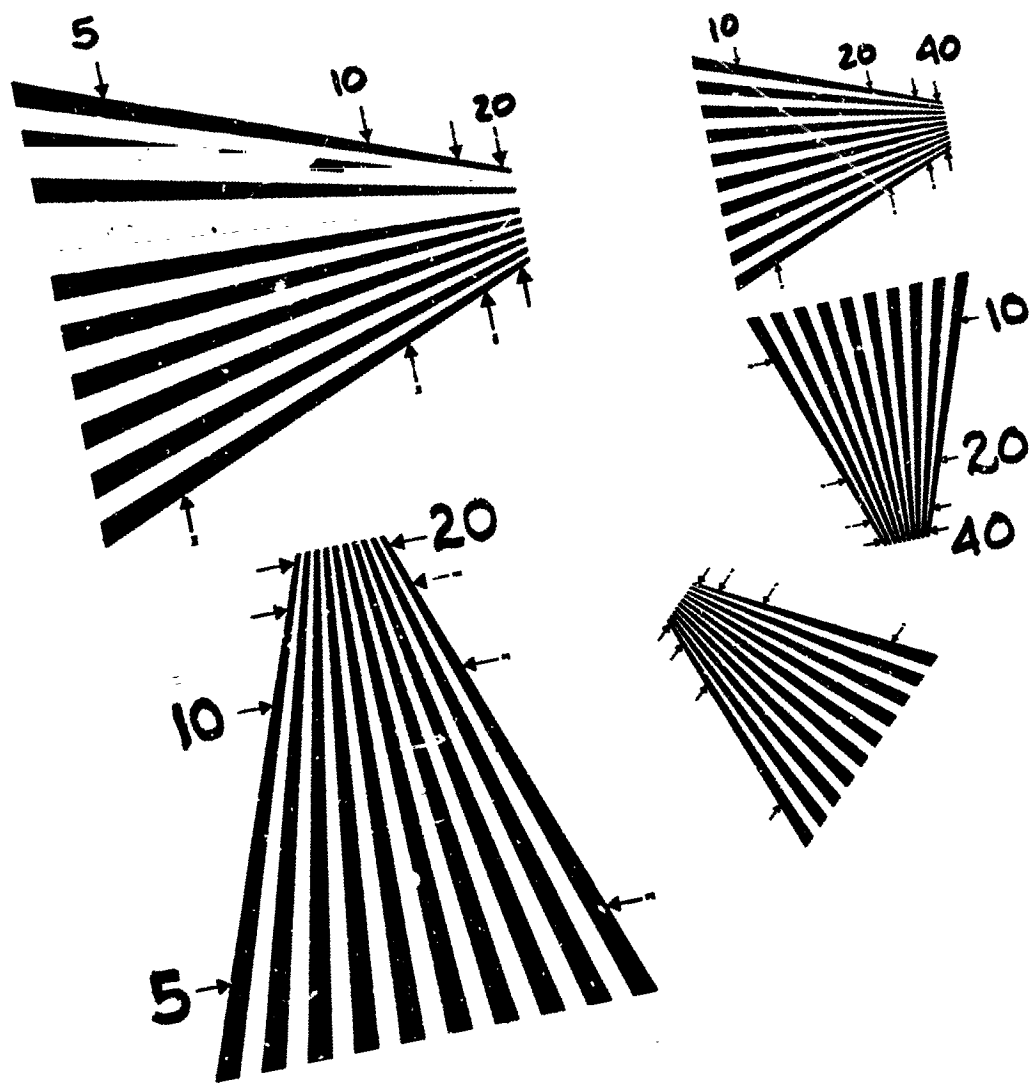


FIG. 33 ORIGINAL OF TEST CHART NO. 1.

per inch. This test chart was reduced in resolution by simple averaging (Fig. 34) and by the process which performs peripheral cancellation (Fig. 35). This chart serves to show how simple averaging reduces detail contrast while processing preserves it. The two uppermost wedges in Fig. 34 show loss of contrast starting at approximately 15 lines per inch. At 30 lines per inch the modulation has been reduced to zero. However, the processed picture Fig. 35 shows that the contrast has been preserved up to 30 lines per inch, where it goes to zero abruptly. Of course, no repetitive detail can exist beyond the system resolution limit of 30 lines per inch.

Test Chart No. 2, shown in Fig. 36, includes the picture of a girl and a grey scale test strip. Figure 37 shows this original reduced by simple averaging, while Fig. 38 was processed with peripheral cancellation. The grey scale demonstrates that the processing does not affect broad areas. The only detectable difference here is the sharpness of the transition between grey steps in the processed picture. In the photograph of the girl the processed version (Fig. 38) shows retention of contrast in areas of fine detail. The girl's hair, the highlight on the belt and the textured area below the belt are areas where the detail contrast is lost by averaging and preserved in the processed picture. This picture was processed with detail contrast exaggerated more than necessary for this type of picture since the scanner adjustments were set to yield the best results for cloud pictures.



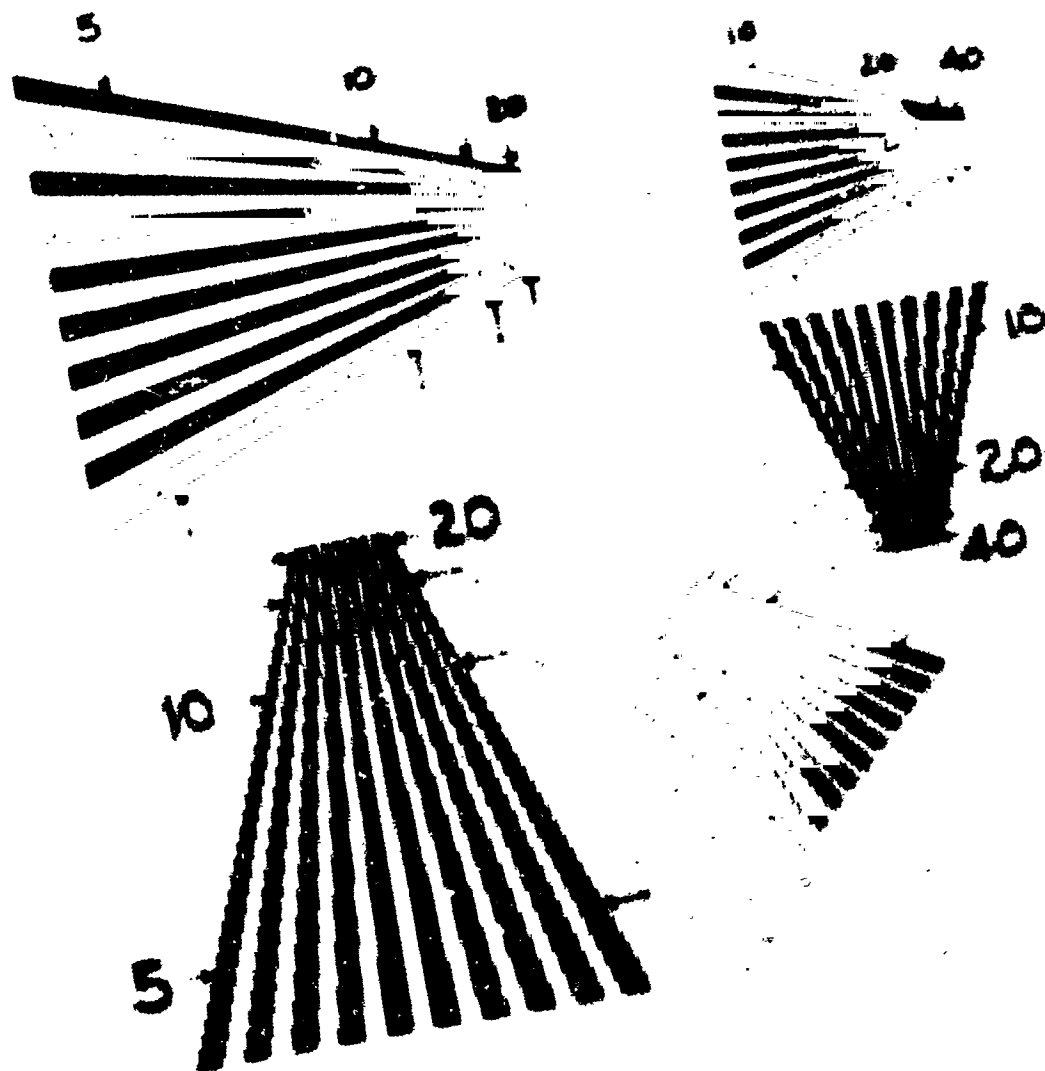


FIG. 34 TEST CHART NO. 1 REDUCED 9:1 BY SIMPLE AVERAGING

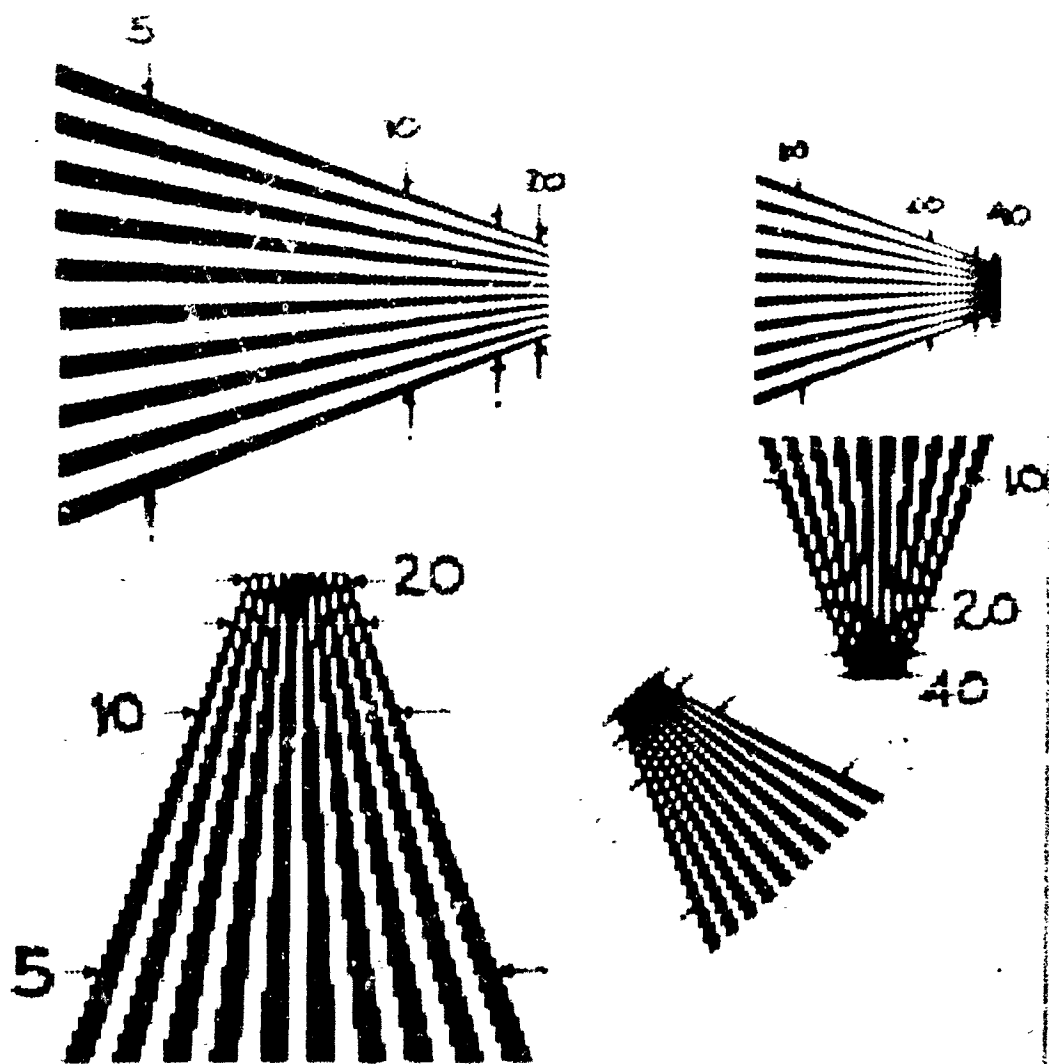


FIG. 35 TEST CHART NO. 2 REDUCED 9:1 BY PERIPHERAL CANCELLATION



FIG. 36 ORIGINAL OF TEST CHART NO. 2



FIG. 37 TEST CHART NO. 2 REDUCED 9:1 BY SIMPLE AVERAGING



FIG. 38 TEST CHART NO. 2 REDUCED 9:1 BY PERIPHERAL CANCELLATION

## VII CONCLUSIONS

### A. General

Bandwidth compression of pictorial information can be effected by simple low-pass spatial filtering. Such filtering (averaging) reduces contrast in areas of fine detail. Loss of this detail contrast reduces the picture's significance and usefulness to a meteorologist.

Many processing techniques were studied to determine if bandwidth compression could be done while retaining that detail contrast so important to correct picture interpretation. Several of these solved the problem for certain types while drastically degrading other types.

The final processing algorithm, detail-contrast enhancement with peripheral cancellation, appears to be decisively better than simple averaging for bandwidth compaction. The pictures obviously have more "sparkle" unlike the pictures that have been averaged, which look defocused. (Simple averaging is in many ways the equivalent of defocusing the image.)

More important, of course, is that the processed pictures are much to be preferred for their retention of meteorologically significant features.

Further, it appears that the best system would use a single processing algorithm for all pictures as opposed to maintaining a library of processing techniques and selection based on picture content. The latter system requires much more complicated equipment, a real-time visual monitor, and trained personnel to perform the selection.

### B. Errors

Performing data compression operations on satellite pictures rather than on tapes produces two types of errors: those that result in degradation of resolution and those that result in picture distortion. The degradations are primarily brought about by the various limiting apertures

that have been interposed between the rescanned picture and the original electrical signal stored on the tape. Any optical presentation or rescan of the picture essentially convolves the picture with the scanning aperture and results in a degraded picture. This is a particularly significant loss for the types of data-compaction systems that have been pursued in this study. If data compaction were to be accomplished by integration over a number of elements, the interposing of various scanning apertures prior to this integration process would not be serious, since the apertures do not seriously alter the integrated average of a group of elements. In this case, however, concentration is on the preservation of the detail contrast of small features, which would normally be lost in the integration process. A loss in small-area detail contrast, due to the many scanning apertures, is immediately felt as a loss in the ability to preserve the fine-line features in the original data.

In addition to the aperture losses, a quantization loss is experienced in the vertical direction because of the line structure. For example, any picture information of a size equal to the limiting resolution that happens to fall between two scan lines appears at each line with half intensity. Further quantization error was introduced by scanning normal to the original scan lines to avoid moiré patterns. Thus information is quantized along the original scan lines instead of taking advantage of the continuous nature of the data. Unfortunately, practical limitations have forced quantization at distances slightly larger than the system resolution, causing a further loss.

In addition to these degradations, which are essentially losses of resolution, a distortion is experienced due to the finite spacing of the scanning lines. The original scanning process at the satellite itself converts a two-dimensional earth image into a one-dimensional signal that is capable of being reconstructed into a replica of the original image. In the rescan process, particularly in a system that is exaggerating detail contrast, the interline spaces seriously distort the microscopic image of a small area, even though they have a negligible effect on the macroscopic view of the entire image. The problem is further complicated by various degrees of nonuniform focus and line density throughout the image.

Solutions to the two general problems outlined are somewhat in conflict. For example, the aperture problem could be helped by using a mosaic of photocells at a density appreciably greater than the picture-element density on the image. In this way, the aperture of each photocell would be very small, and no picture detail would be lost. This operation, however, would greatly enhance the distortion because of the dark spaces between scanning lines. The operation involving choosing the blackest element in a small area would almost always result in selection of the interline spacing.

For these reasons it is very important to operate from the original tape signal and avoid both the degradations and distortions. In addition, a magnetic-tape input system is representative of that implementation for a real-time operational environment, namely, processing directly from the taped signal.



**PLANK PAGE**

## VIII A POSSIBLE IMPLEMENTATION OF AN OPERATIONAL SYSTEM

In describing an on-line bandwidth reduction system, the following assumptions will be made concerning the system's input and output data. First, it will be derived from a Nimbus tape. This data will consist of a serial train of the video signals from the horizontal lines of the Nimbus TV pictures. Horizontal and vertical sync signals will be included as separate inputs to the system. The clock track from the Nimbus tape will also be made available as a separate input.

The system output will consist of a continuous video signal representing a serial train of the horizontal lines of a processed Nimbus picture. Horizontal and vertical sync signals will be superimposed on the video output signal. (A separate clock track will not be necessary on the output, as will be pointed out later.)

The foremost problem in specifying an on-line bandwidth reduction system stems from the way in which the bandwidth reduction is accomplished. As was described previously, the implementation of the bandwidth reduction algorithm is a parallel operation. A  $5 \times 5$  array of elements from a Nimbus picture are combined, in parallel, generating a single picture element to replace the array of elements in the processed picture. The problem, mentioned above, comes about when one attempts to gather a  $5 \times 5$  array of picture elements from the video signal as they are read off the Nimbus picture tape.

It becomes immediately obvious that the video signal must be stored until five lines of the picture can be accessed and processed in parallel. Solutions to the video storage problem could take two forms, an analog storage or a digital store.

An analog storage system would be very complex, possibly involving the synchronizing of a magnetic drum system to the reading of the Nimbus tape or the synchronizing of some other analog storage system to the Nimbus tape system. The problems encountered in the mechanization of

such systems render them less feasible for this application than digital storage systems, even though the digital systems require the conversions, in both directions, of analog and digital information.

A suggested mechanization of a bandwidth reduction system might appear as shown in block diagram of Fig. 39. This system has three functional areas or subsystems--the input subsystem, buffering subsystem, and output subsystem. The overall system will accept Nimbus picture information, in analog form from the Nimbus picture tape. The input subsystem will digitize the pictures by continuously sampling the analog signal from the tape and converting each sample into a binary number or binary picture element.

The serial train of binary picture elements generated will be transferred to the buffering subsystem. They will be stored here until sufficient picture information is available, in parallel, to allow picture processing to begin. The buffering of the picture elements will be done using a core memory, providing random-access capability. Once enough of a picture has been stored in memory, the picture elements will be addressed in a sequence satisfying the requirements of the bandwidth reduction algorithm.

As the picture elements are accessed from memory, they will be transferred into the output subsystem. The picture processing will be carried on in this subsystem. It will group picture elements, converting them back into analog form, and combine the analog signals, according to the bandwidth algorithm, into a continuous video signal. The video signal from the output subsystem will represent the processed Nimbus pictures.

As shown in Fig. 39, the four inputs from the Nimbus tape system enter the input subsystems. The video signal enters an analog-to-digital converter. This converter continuously tracks the video signal. Its output is strobed into the A-D buffer at a rate producing 800 digital picture elements per horizontal line of the Nimbus pictures.

The timing track, horizontal sync, and picture sync from the tape system are used in the input system's control logic. There, the timing

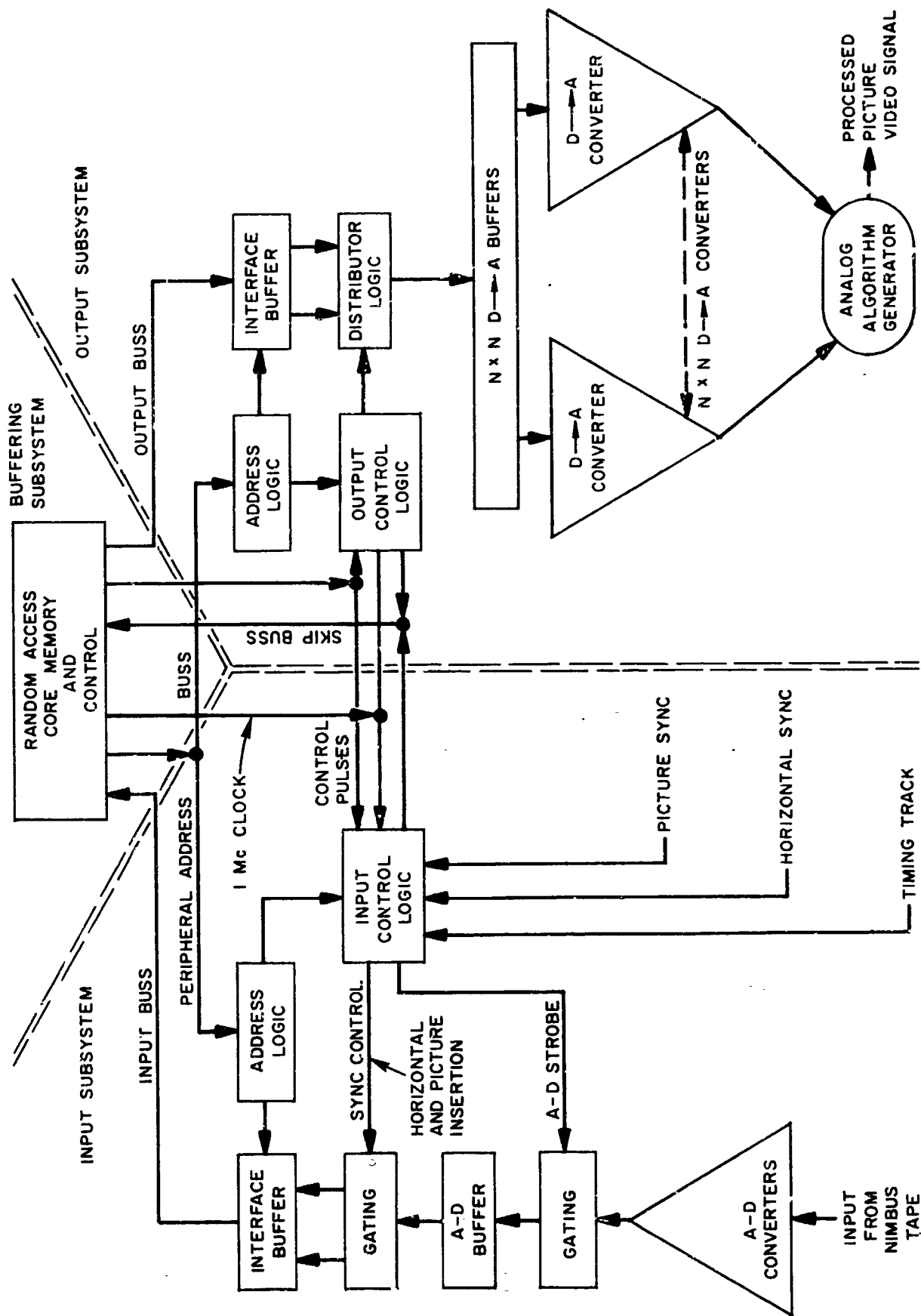


FIG. 39 ON-LINE BANDWIDTH-REDUCTION SYSTEM

signal is used to produce the strobe signal for controlling the sampling of the A-D converter output.

The picture and horizontal sync signals are used to synchronize the input subsystem and also to cause it to generate unique characters, identifying horizontal and picture sync. These characters are introduced into the digital picture data. The buffering subsystem will consist of the random access core memory, mentioned above, and a buffer control unit. Word transfers from the input subsystem are controlled by the buffer control unit. When a word is available, the buffer control unit will address the input subsystem and provide the control signals necessary to execute the word transfer and also signal the input subsystem at the finish of the transfer.

Other functions provided by the buffer control logic will include

- (1) The addressing of the memory during input,
- (2) Recognizing sync characters in the input data,
- (3) Determining when enough picture data has been stored before initiating the picture processing,
- (4) Initiating the picture processing, and
- (5) Addressing memory during the accessing of picture elements in the correct sequence for transfer to the output subsystem.

When the buffer control logic detects a picture sync character in the input data, it starts keeping track of the amount of picture information it has in memory for that particular picture. When enough data has been stored to allow picture processing to start, the buffer control signals the output subsystem to begin processing.

Once set into operation, the output subsystem will determine the picture processing rate. This rate will be constant eliminating the picture distortions due to the variations in the tape speeds in the Nimbus satellite and ground stations, and removing the need for a clock track accompanying the video signal. In order to allow variations in the input data rate while holding the output rate constant, the picture processing is not initiated until more picture information has been stored in memory than the minimum necessary. This allows the input data rate to decrease

somewhat during the picture processing. To allow for the possibility of the input data rate going over its average rate, additional memory space will be provided to prevent memory overflow. The rate at which the output subsystem will process the Nimbus pictures will be the average rate at which pictures can be read from the tape.

Once the output subsystem has been set into operation, it will request picture information from the buffering subsystem. The buffering subsystem will address the memory in such a way as to provide the output subsystem with picture elements which, when grouped, constitute the  $5 \times 5$  array required by the bandwidth-reduction algorithm. These picture elements will be presented to the interface buffer (between the buffering and output subsystems) one word at a time, accompanied by the addressing and control signals necessary to execute the word transfer.

The output subsystem will distribute the picture elements to the digital-to-analog converters. The outputs of the D-to-A converters will be combined in the analog algorithm generator producing the processed picture video signal.

**Appendix A**  
**NOISE CONSIDERATIONS**

## Appendix A

### NOISE CONSIDERATIONS

In conventional bandwidth reduction by simple averaging (where the image is convolved with a large aperture), high-frequency noise is averaged out. Only low-frequency or broad area noise remains. The resulting signal-to-noise ratio is equal to the original signal-to-noise ratio in relatively broad areas. This situation is aggravated, however, by the nonlinear processing, which is used to maintain detail contrast. The nonlinear operations can create low-frequency noise from the high-frequency noise components, rather than simply averaging them to zero. For example, an analog OR circuit for extracting the maximum value of a matrix of elements can cause the entire large element to respond to a single noise spike anywhere within the matrix.

Fortunately, in the picture material studied here, this has not been a problem. The signal-to-noise ratio of both the TIROS and Nimbus pictures, with one exception, have been good enough so as to show no appreciable degradation due to processing. Were noise to be a problem, however, the processing algorithm would be altered so as to minimize the problem. One approach assumes that most fine-line features of interest will occupy at least two picture elements in a matrix rather than one. A logical operation can thus be performed to extract the second largest (or smallest) signal in an area. This essentially requires that each feature, to be preserved, must occupy at least two elements. In general, the improvement in signal-to-noise performance would overshadow the losses in preservation of detail contrast. The specific method of providing analog logic to extract the second largest or smallest signal is described in Sec. VI-D-5.

The one processed picture containing appreciable amounts of noise is shown in Fig. 5(a). Unfortunately, this is a poor picture from many viewpoints, including grey-scale rendition and interference signals. The top part of the picture contains predominantly black spikes having



a unidirectional impulse noise characteristic. In the operations that involved extracting the blackest element, the deterioration is quite evident. The picture involving the whitest element, as would be expected, ignored the black spikes but reproduced the relatively less intense white components of the noise. Adding this signal to the blackest signal attenuated the black noise spikes. The nonlinear operations on the high-frequency noise components are thus generating relatively broad area, low-frequency noise. Desired information in the original scene is being obliterated. Unfortunately, time did not permit reproducing this picture using the second blackest rather than the blackest element. This would have materially aided all of the aforementioned processing operations. This improvement, however, is present in the picture, which enhances lines (Fig. 5d, Line Structure). In this algorithm, adjacent signals forming diagonal, vertical or horizontal lines are logically combined. Single black spikes are ignored unless they line up in the predetermined fashion and excite two or three photodiodes in a row. The improved noise performance in this picture over the one selecting the blackest element is indicative of the improved noise performance that can be expected by looking for more complex features within the scanning aperture. The final decision on the algorithm will depend upon the anticipated noise environment. In any case, the system discussed has a great deal of flexibility to cope with relatively noisy and noise-free environments.

The above discussion pertains to the effects of electrical noise. When the processing is accomplished by re-scanning a photograph, as has been done here, additional noise components are introduced. The primary source of this noise is the dark spaces between scanning lines, which do not contain useful information. Any attempt at rescanning the photograph of the monitor by following scanning lines is completely futile and simply leads to undesirable moiré patterns. Scanning normal to the original scanning lines eliminates moiré problems but introduces the interline noise component. This is a particularly bad problem on TIROS pictures and somewhat less of a problem on Nimbus pictures. In particular, the periodic failure of the system to "see" relatively

small white features can be attributed to a small black interline area predominating (since it departs more from the average, in a particular area, than the white feature). It is for these reasons that superior performance can be anticipated using a tape system where this interline source of noise will be eliminated.

Appendix B  
ANALOG LOGIC

## Appendix B

### ANALOG LOGIC

The implementation of the algorithms discussed in this report was accomplished by analyzing the original photograph with an array of photo-transistors. The outputs of these, representing the intensity of an array of incremental areas, were combined using various linear and nonlinear analog logical operations. These circuits thus provided the means for implementing the simulation of the algorithm using the pictures themselves as a storage device. However, these circuits also appear to be the most reasonable choice for a real-time implementation operating directly from the tape signals. Digital devices, such as core memories and buffers, would be used for the storage requirements of the system. The actual logical operations on the array of stored elements appear to be much more straightforward when done with analog logic than by computer processing. Thus, the desired stored elements would be decoded with D to A converters and applied to the same type of circuitry used with the photograph simulation work.

The signal levels at the point where the processing is performed was established with full black at +5 v and full white at -5 v. The averaging operation as shown in Fig. B-1 simply adds resistively the nine outputs. The operation to select the blackest or most positive element consists of an or circuit shown in Fig. B-2, where the output is taken from the common cathode terminals of the diodes. The circuit selecting the whitest or most negative element, shown in Fig. B-3, is identical to that of the blackest with all voltage polarities and diodes reversed. These circuits formed the basis for all of the early processing work. They are linearly combined by using difference amplifiers to provide one output proportional to the difference between the blackest and the average and another proportional to the difference between the whitest and the average. These are each added to the average in controlled amounts to form a signal  $O = A + k_1(B - A) + k_2(W - A)$ .

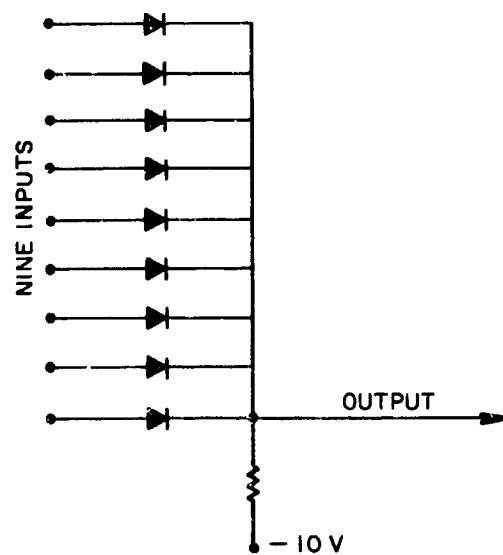


FIG. B-2 CIRCUIT FOR SELECTING  
BLACKEST ELEMENT

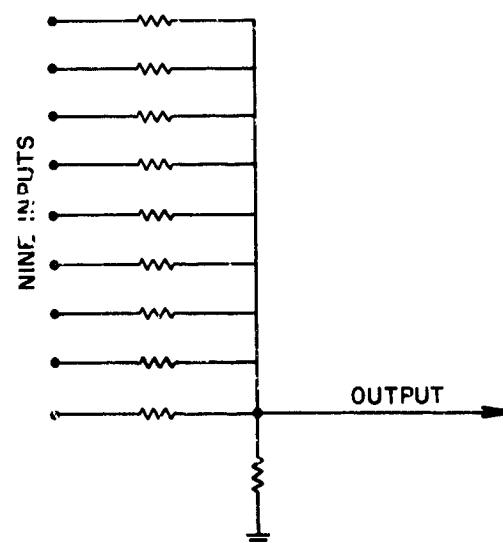


FIG. B-1 CIRCUIT FOR AVERAGING

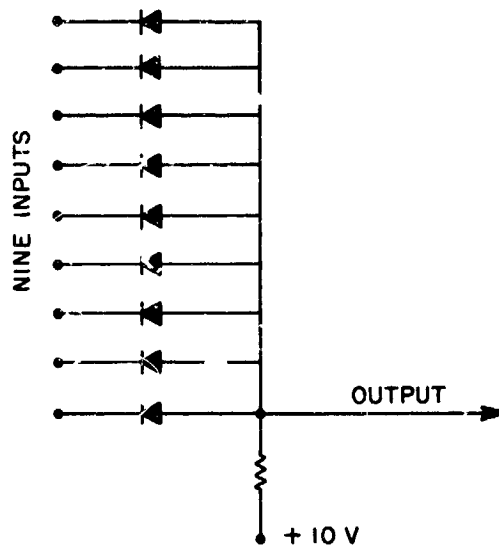


FIG. B-3 CIRCUIT FOR SELECTING  
WHITEST ELEMENT

Since  $k_1$  and  $k_2$  are controllable, the amount of detail contrast enhancement of black or white features can be adjusted.

In noisy situations, as was previously discussed, the selection of the second blackest or whitest element in a matrix of nine elements is desired. This was implemented by the method shown in Fig. B-4. The nine elements were divided into nine different groups of eight elements each. Each of these groups was applied to an analog OR circuit to extract its largest (or smallest) element. One of the nine groups of eight each will not contain the blackest element while eight of them will. An additional nine diode AND circuit is then used on the output of the nine groups to select the smallest (or largest) group. This will then correspond to the second blackest or whitest since the largest (or smallest) one has been eliminated. This operation uses 81 diodes, 72 for the nine OR circuits and nine for the final AND circuit. The digital implementation of this operation appears quite complex so that, in a real-time system, it would presumably be accomplished by using a D-to-A converter on the stored data and applying the resultant analog signals to this circuit.



Another algorithm of interest was the extraction of straight-line features occurring within the  $3 \times 3$  matrix. Eight possible lines can occur which cross three photocells including three vertical, three horizontal and two diagonal. In addition, four diagonal lines can occur that will cross two photocells in each of the corners. The circuit for finding the intensity of the blackest line within the matrix is shown in Fig. B-5. Eight 3-diode AND circuits and four 2-diode AND circuits are used for finding the whitest (most negative) voltage in each line group. Thus, the output of each group will be black only when every member of the line group is black. The resultant twelve outputs of each of the groups are then combined in an OR circuit to find the most positive or blackest group. Thus, the output will be black if any black line exists within the matrix. This signal is combined with the average in a difference amplifier as was done for the circuits which extracted the blackest and whitest signals. Although a system for extracting white lines was not constructed, it would be identical with all voltage polarities and diodes reversed.

In the course of the project, it was found necessary to avoid the reproduction of features within the aperture that were part of larger features external to the aperture. This is accomplished by comparing the photocells on the inner boundary of the aperture to a set of peripheral photocells on the border of the aperture. For the case of finding the blackest or most positive element, a peripheral photocell is compared with its neighbor on the inner boundary. If it is more positive, then the inner photocell is presumably seeing a "tail" of a larger feature that should not be preserved. The output of the inner photocell is thus rendered highly negative to ensure that it will not participate in the selection of the darkest element. The circuits for accomplishing this in the extraction of the blackest and whitest elements are shown in Fig. B-6 and B-7. In the case of extracting the blackest element, the inner photocell signal is connected to point A on Fig. B-6 which is the emitter of a PNP transistor. The neighboring peripheral photocell drives point B and therefore the base of that same transistor through an emitter follower. If A is more positive (black) than B, the inner element is preserved, since the transistor



1	2	3
4	5	6
7	8	9

NINE INPUTS

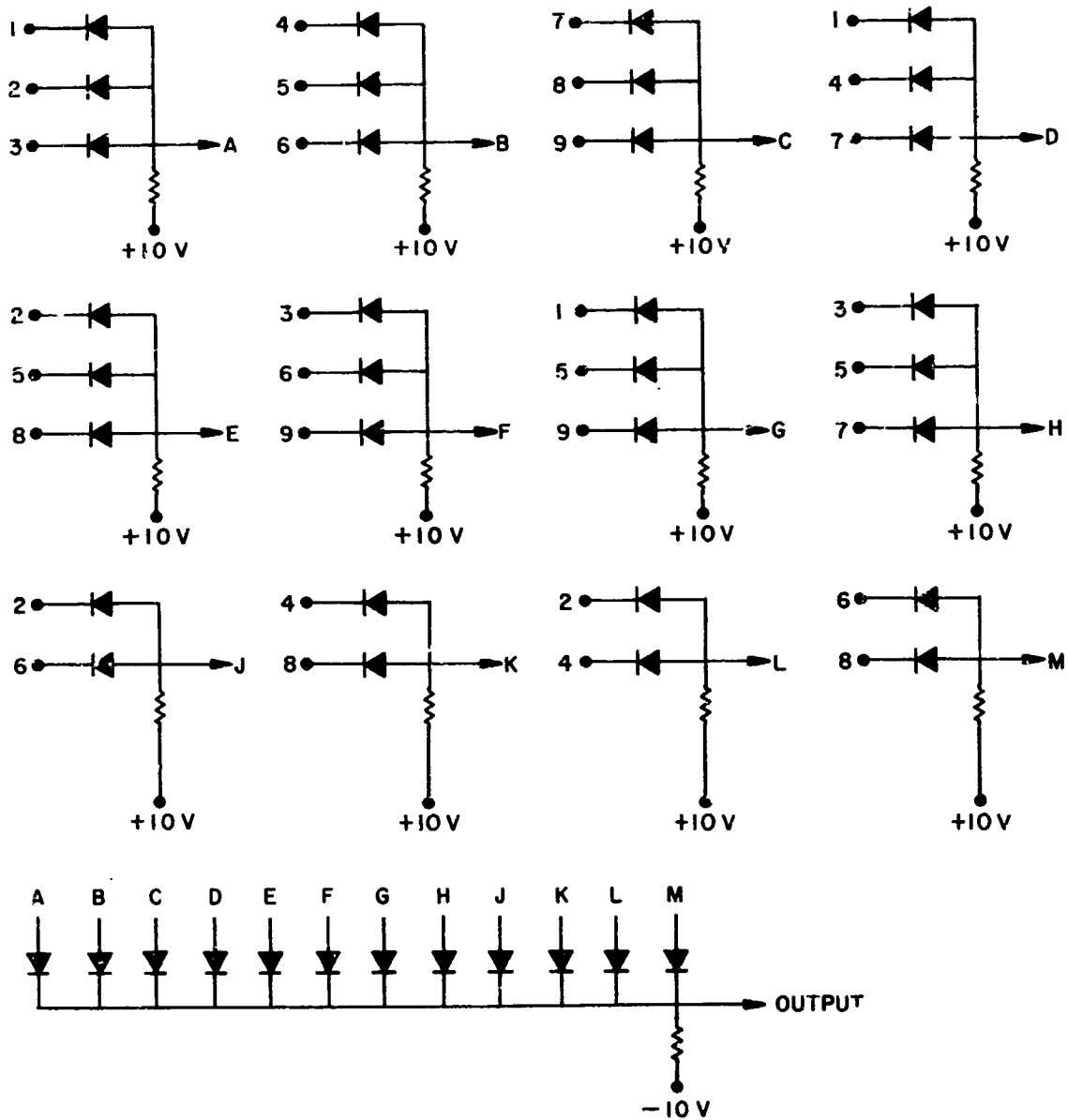


FIG. B-5 CIRCUIT FOR SELECTING BLACKEST LINE

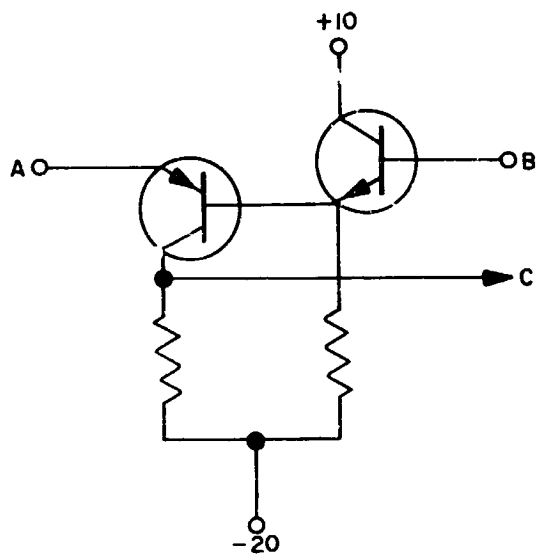


FIG. B-6 NONLINEAR COMPARISON  
CIRCUIT FOR BLACK

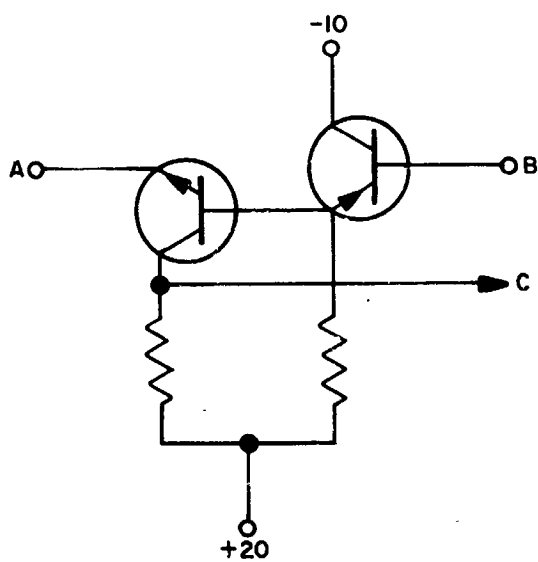


FIG. B-7 NONLINEAR COMPARISON  
CIRCUIT FOR WHITE

readily saturates, cutting off the emitter follower with the output at C identical to that of A. If the photocell signal from the outer element B is more positive than that of , the emitter follower causes the first transistor to cut off, driving the collector voltage C to -20 v, which is far below the level of the whitest signal encountered. Thus, that particular output will never appear in the output of the OR circuit that follows. In the case of corners, each inner boundary photocell has two peripheral neighbors, one above and one on the side. These two are first combined in an OR circuit to find the blackest or most positive. The output of this OR circuit is then compared with the inner corner photocell signal in the same manner as has been described. As shown in Fig. B-7, the system for extracting the whitest element is similar with voltage polarities and diodes reversed, and NPN transistors replacing PNP transistors. Selection of blackest and whitest with peripheral correction is shown in Fig. B-8.

Some thought was given to the preferred system for combining the blackest and whitest signals to ensure that small white detail in dark areas and small dark detail in white areas would be preserved. A linear combination has the effect of watering down the result. A more successful method is to compare each of the signals with the average, and choose the one which differs most from the average. This is accomplished by the circuit of Fig. B-9. The blackest signal is connected to the emitter of a PNP transistor and the whitest signal is connected to the emitter of an NPN transistor. Each base is connected to the average signal through equal resistors. The collectors are tied together and connected to the average through a relatively large resistor. If the blackest differs from the average by somewhat more than the whitest does, the NPN transistor will draw somewhat more current and saturate. This ensures that the common collector output signal will be identical to that of the blackest signal. The large size of the collector load ensures that only slight differences are required for saturation to take place. If both differ by identical amounts, the output will follow the average, as it should.

INPUT MATRIX

1	2	3	4	5
6	7	8	9	10
11	12	13	14	15
16	17	18	19	20
21	22	23	24	25

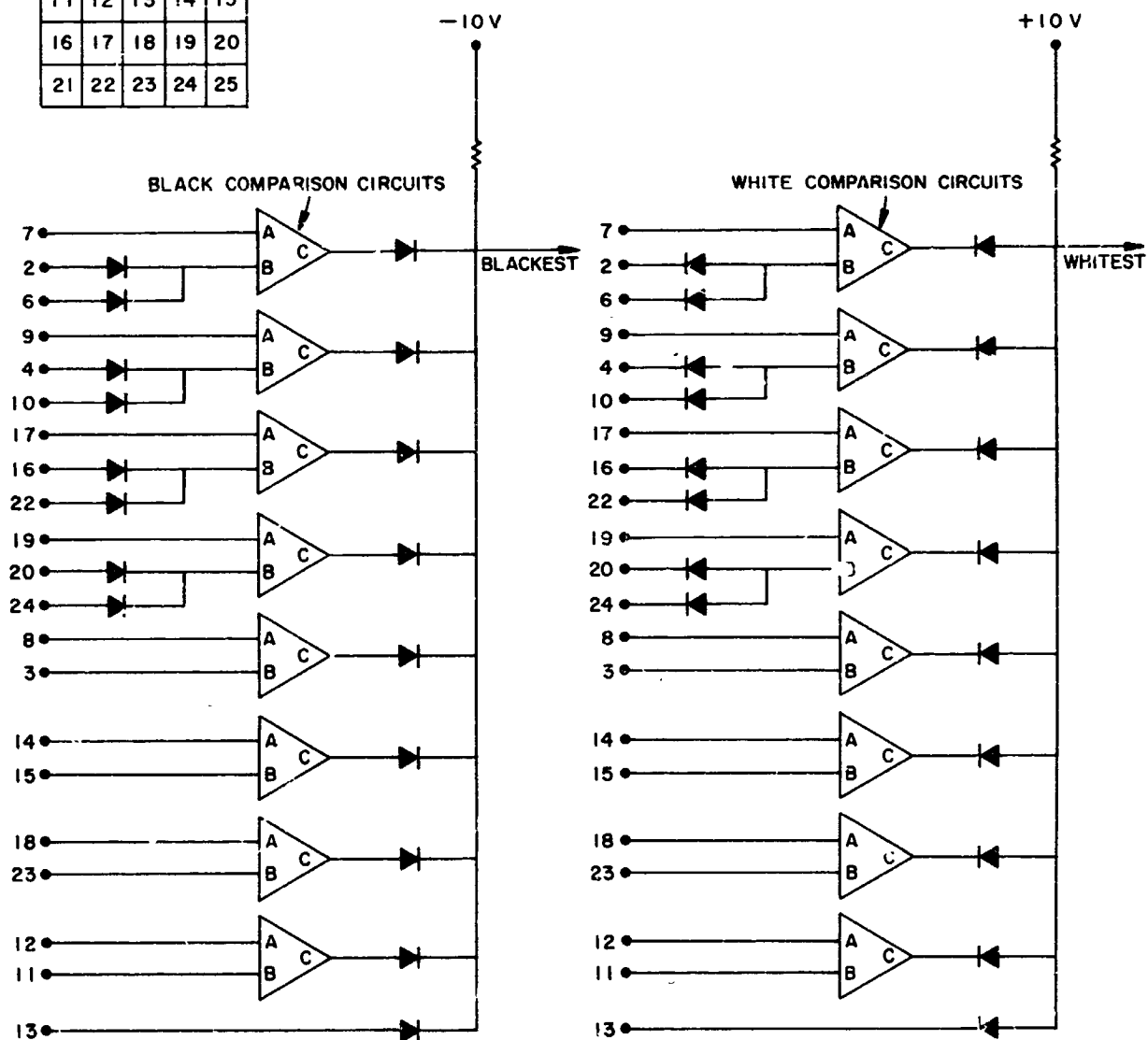


FIG. B-8 CIRCUITS FOR SELECTION OF PERIPHERALLY-CORRECTED BLACK AND WHITE SIGNALS

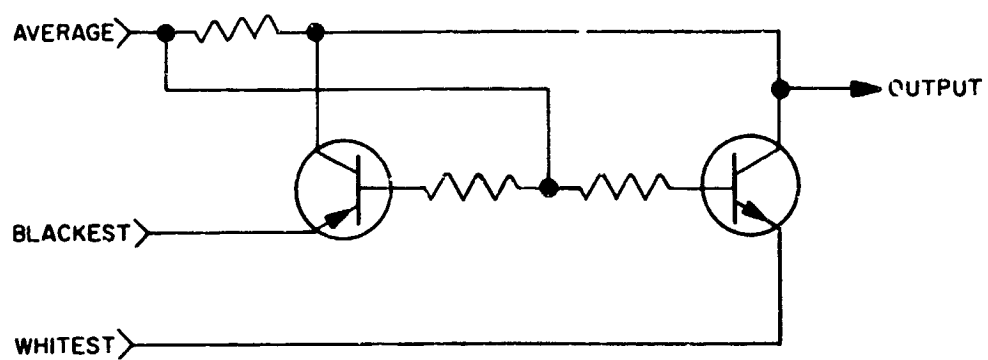


FIG. B-9 BLACK-WHITE COMBINING CIRCUIT

Appendix C  
COMPARISON WITH OTHER BANDWIDTH COMPRESSION SYSTEMS

**BLANK PAGE**

## Appendix C

### COMPARISON WITH OTHER BANDWIDTH COMPRESSION SYSTEMS

The study has been limited to constant-velocity scanning systems, as contrasted to a number of bandwidth compression methods, which use variable-velocity scanning systems. Variable-velocity systems, which include run-length coding, synthetic highs, and velocity modulation systems, depend upon picture statistics for the compression of data. Pictures containing large areas of relatively constant intensity are transmitted relatively rapidly, while pictures with many high-spatial-frequency components are transmitted relatively slowly. Thus the transmission time is a function of picture content.

The processing of picture signals for a run-length coding operation requires a digitizing operation. This operation increases the bandwidth by the number of defined bits per element. Compression systems, based on picture statistics, generally reduce the average total number of elements to approximately that of the original analog signal. Thus these systems generally do not achieve bandwidth compression of the original analog signal, as does the system described here. A direct comparison, however, is difficult, since the digitized signal can tolerate more noise than the analog signal. The analog signal is made noise immune by increasing the communication bandwidth through various PCM or FM techniques. This, of course, can make the communications bandwidth of the modulated analog signal comparable to that of the digital signal. Despite the obvious difficulties of comparison, a few general statements can be made. In a relatively noise-free, band-limited environment--such as a microwave link--where bandwidth is very expensive, there appears little justification for digitizing the signal and paying the relatively high cost of the increased bandwidth. Only in those cases where the cumulative degradation of a large number of repeater stations can be overcome by the regeneration capability of a digital signal, does digitizing appear warranted. In relatively



noise-free cases, the reduction in analog bandwidth by the methods described here result in a direct economic advantage, whereas the digitizing operations followed by run-length coding techniques provide little or no economic advantage over the original analog signal. In noisy environments, however, the analog signal must be encoded in some manner in the modulation process so as to provide an output signal-to-noise ratio greater than that existing in the communication link. Frequency modulation systems have the interesting characteristic of providing an output signal-to-noise ratio inversely proportional to modulation frequency. Thus the signal-to-noise ratio, or accuracy of rendition, is greater at lower frequencies. This characteristic appears to be especially significant in video presentation where greater accuracy of rendition is provided for relatively broad area information where it is needed. Transition of high-frequency detail information is reproduced with less accuracy, but this can presumably be tolerated. Thus, even relatively narrow-band FM system, with their large number of redundant sidebands for lower-frequency information, can compete favorably with digital systems. It is presumably this line of reasoning that led to the choice of analog FM for the TV transmission from communication satellites.

Digital systems have the additional problem, when used for video signals, of providing undesired contouring unless a relatively large number of bits per element are used. This problem, however, may be primarily an aesthetic one and may not seriously degrade the ability to interpret cloud photographs. In any case, many systems exist for minimizing the contouring problem while using a relatively small number of bits.

The most significant difference between the asynchronous signal coding schemes and the synchronous analog processing systems lies in the nature of the terminal equipment. Synchronous or constant velocity systems can use straightforward mechanical facsimile scanners that have relatively high inertia. These systems are low cost, reliable, and produce copy at a uniform rate. The particular time when any picture

from any orbit will be available can be predicted in advance. The processed analog signal can be sent over existing communication links to existing terminal equipment where the picture is reproduced.

The encoded digital signal, however, can only be processed by special purpose, low-inertia electronic scanners that are relatively expensive. The nonuniformity of the scan puts difficult requirements on linearity and intensity to produce a continuous picture without undesirable structure. Once the picture is reproduced at a receiving station, no method exists for retransmitting it at the reduced bandwidth. A rescan will require the original bandwidth, while a retransmission of the encoded signal will require the specialized low-inertia reproducing equipment at every receiving point. Thus, the signal is not capable of rebroadcast to many points that have simple facsimile equipment.

**BLANK PAGE**

## REFERENCES

- Bundgaard, R. C., "Billow Clouds and Deformation Exhaust Trails from Aircraft," Proceedings of the Toronto Met. Conf. 1963, Royal Meteorological Society, p. 182-187 (1954).
- Conover, J. H., "Lee Wave Clouds Photographed from an Aircraft and a Satellite," Environmental Research Papers No. 11, Meteorology Laboratory Project 6698, Office of Aerospace Research, USAF (1964).
- Conover, J. H., "Cloud Interpretation from Satellite Altitudes," Supplement 1 to Research Note 8, AFCRL 62-680, Suppl. 1, Office of Aerospace Research, USAF (May 1963).
- Conover, J. H., "The Identification and Significance of Orographically Induced Clouds Observed by TIROS Satellite," J. Meteor. 3, pp. 226-234 (1964).
- Doos, B. R., "A Theoretical Analysis of Lee Wave Clouds Observed by TIROS I," Tellus 14, No. 3, pp. 301-309 (1962).
- Dzhordzhie, V. A. and O. A. Lyapina, "Cyclone over the Caspian Sea Photographed from an Artificial Satellite," NASA Report No. N64-32784.
- Fritz, S. and C. V. Lindsay, "Lee Wave Clouds Photographed over the Appalachians by TIROS V and VI," Soaring, pp. 14-17 (March 1964).
- Hanson, D. M., "The Use of Meteorological Satellite Data in Analysis and Forecasting," Tech. Note 13, U.S. Weather Bureau, Office of Forecast Development (1963).
- Johnson, D. S., W. F. Hall, and C. L. Bristol, "Nimbus Data in Operational Meteorology," Astronautics and Aerospace Engineering, pp. 52-56 (April 1963).
- Kuettner, J., "The Band Structure of the Atmosphere," Tellus, 11, No. 3, pp. 267-294 (1959).
- Malrus, J. S., "Cloud Patterns over Tropical Oceans," Science, 141, No. 3583, pp. 767-777 (1963).
- Nordberg, W. and P. Press, "The Nimbus I Meteorological Satellite," Bull. Amer. Meteorological Soc., pp. 684-687 (1964).
- Schaefer, V. J. and W. E. Hubert, "A Case Study of Jet Stream Clouds," Tellus 7, No. 3, pp. 301-307 (1955).
- Sverdrup, H. V., Oceanography for Meteorologists, p. 201 (Prentice-Hall, Inc., New York, 1942).
- Tang, Wen, "Vortex Cloud Studies," Final Report, U.S. Weather Bureau Contract Cwb-10316, p. 32 (1963).
- Tang, Wen, E. M. Brooks and B. F. Watson, "Theoretical and Observational Studies of Vortex Cloud Patterns," Final Report, U.S. Wea. Bu., Cwb-10626, p. 5 (1964).

REFERENCES (Concluded)

- U.S. Weather Bureau, "Picture of the Month," Monthly Weather Review, 92, No. 2, p. 76 (1964).
- Wiegman, E. J., R. G. Hadfield, and S. M. Serebreny, "Atlas of Cloud Vortex Patterns Observed in Satellite Photographs," Final Report, U.S. Weather Bureau Contract Cwb-10627, Meteorological Satellite Laboratory (1964).
- Widger, W. K., Jr., et al., "Practical Interpretation of Meteorological Satellite Data," Final Report, AF Cambridge Research Laboratories Contract AF 19(628)-2471, Office of Aerospace Research (1964).